2019

Expedition 376 Preliminary Report: Brothers Arc Flux

Cornel E.J De Ronde
GNS Science

Susan E. Humphris
Woods Hole Oceanographic Institution

Tobias W. Höfig
Texas A&M University

Philipp A. Brandl
Geomar Helmholtz Centre For Ocean Research

Lanlan Cai
Xiamen University

See next page for additional authors

Expedition 376 Preliminary Report: Brothers Arc Flux

Abstract
Volcanic arcs are the surface expression of magmatic systems that result from the subduction of mostly oceanic lithosphere at convergent plate boundaries. Arcs with a submarine component include intraoceanic arcs and island arcs that span almost 22,000 km on Earth's surface, the vast majority of which are located in the Pacific region. Hydrothermal systems hosted by submarine arc volcanoes commonly contain a large component of magmatic fluid. This magmatic-hydrothermal signature, coupled with the shallow water depths of arc volcanoes and their high volatile contents, strongly influences the chemistry of the fluids and resulting mineralization and likely has important consequences for the biota associated with these systems. The high metal contents and very acidic fluids in these hydrothermal systems are thought to be important analogs to numerous porphyry copper and epithermal gold deposits mined today on land ...

Keywords
arc, brothers, 376, expedition, report:, preliminary, flux

Publication Details
De Ronde, C. E.J., Humphris, S. E., Höfig, T. W., Brandl, P. A., Cai, L., Cai, Y., Tontini, F. Caratori., Deans, J. R., Farough, A., Jamieson, J. W., Kolandaivelu, K. P., Kutovaya, A., Labonté, J. m., Martin, A. J., Massiot, C., McDermott, J. M., McIntosh, I. M., Nozaki, T., Pellizari, V. H., Reyes, A. G., Roberts, S., Rouxel, O., Schlicht, L. E.M., Seo, J. Hun., Straub, S. M., Strehlow, K., Takai, K., Tanner, D., Tepley, F. J. & Zhang, C. (2019). Expedition 376 Preliminary Report: Brothers Arc Flux. International Ocean Discovery Program.

Authors
Cornel E.J De Ronde, Susan E. Humphris, Tobias W. Höfig, Philipp A. Brandl, Lanlan Cai, Yuanfeng Cai, Fabio Caratori Tontini, Jeremy R. Deans, Aida Farough, John W. Jamieson, Kannikha P. Kolandaivelu, Anna Kutovaya, Jessica M. Labonté, Andrew J. Martin, Cécile Massiot, Jill M. McDermott, Iona M. McIntosh, Tatsuo Nozaki, Vivian H. Pellizari, Agnes G. Reyes, Stephen Roberts, Olivier Rouxel, Lucy E.M Schlicht, Jung Hun Seo, Susanne M. Straub, Karen Strehlow, Ken Takai, Dominique Tanner, Frank J. Tepley, and Chao Zhang

International Ocean Discovery Program Expedition 376 Preliminary Report

Brothers Arc Flux

5 May–5 July 2018

Cornel E.J. de Ronde, Susan E. Humphris, Tobias W. Höfig, and the Expedition 376 Scientists

IODP
INTERNATIONAL OCEAN DISCOVERY PROGRAM

Publisher's notes

Core samples and the wider set of data from the science program covered in this report are under moratorium and accessible only to Science Party members until 5 July 2019.

This publication was prepared by the *JOIDES Resolution* Science Operator (JRSO) at Texas A&M University (TAMU) as an account of work performed under the International Ocean Discovery Program (IODP). Funding for IODP is provided by the following international partners:

National Science Foundation (NSF), United States
Ministry of Education, Culture, Sports, Science and Technology (MEXT), Japan
European Consortium for Ocean Research Drilling (ECORD)
Ministry of Science and Technology (MOST), People's Republic of China
Korea Institute of Geoscience and Mineral Resources (KIGAM)
Australia-New Zealand IODP Consortium (ANZIC)
Ministry of Earth Sciences (MoES), India
Coordination for Improvement of Higher Education Personnel (CAPES), Brazil

Portions of this work may have been published in whole or in part in other IODP documents or publications.

Disclaimer

Any opinions, findings, and conclusions or recommendations expressed in this publication are those of the author(s) and do not necessarily reflect the views of the participating agencies, TAMU, or Texas A&M Research Foundation.

Copyright

Citation

de Ronde, C.E.J., Humphris, S.E., Höfig, T.W., and the Expedition 376 Scientists, 2019. *Expedition 376 Preliminary Report: Brothers Arc Flux*. International Ocean Discovery Program. https://doi.org/10.14379/iodp.pr.376.2019

ISSN
World Wide Web: 2372-9562

Expedition 376 participants

Expedition 376 scientists

Cornel E.J. de Ronde
Co-Chief Scientist
Marine Geoscience
GNS Science
New Zealand
cornel.deronde@gns.cri.nz

Susan E. Humphris
Co-Chief Scientist
Department of Geology and Geophysics
Woods Hole Oceanographic Institution
USA
shumphris@whoi.edu

Tobias W. Höfig
Expedition Project Manager/Staff Scientist
International Ocean Discovery Program
Texas A&M University
USA
hoefig@iodp.tamu.edu

Philipp A. Brandl
Igneous Petrologist
Dynamics of the Ocean Floor
GEOMAR Helmholtz Centre for Ocean Research Kiel
Germany
pbrandl@geomar.de

Lanlan Cai
Microbiologist
State Key Laboratory of Marine Environmental Science
Xiamen University (Xiang'an campus)
China
lanlancai@xmu.edu.cn

Yuanfeng Cai
Alteration Mineralogist
School of Earth Sciences and Engineering
Nanjing University
China
caiyf@nju.edu.cn

Fabio Caratori Tontini
Paleomagnetist
Marine Geoscience
GNS Science
New Zealand
f.caratori.tontini@gns.cri.nz

Jeremy R. Deans
Structural Geologist
Department of Geography and Geology
University of Southern Mississippi
USA
jeremy.deans@usm.edu

Aida Farough
Physical Properties Specialist/Petrophysics
Department of Geology
Kansas State University
USA
afarough@ksu.edu

John W. Jamieson
Alteration Mineralogist
Department of Earth Sciences
Memorial University of Newfoundland
Canada
jjamieson@mun.ca

Kannikha P. Kolandaivelu
Physical Properties Specialist/Downhole Measurements
Department of Geosciences
Virginia Polytechnic Institute and State University
USA
kannikha@vt.edu

Anna Kutovaya
Organic Geochemist
Institute of Geology and Geochemistry of Petroleum and Coal
RWTH Aachen University
Germany
ann.kutovaya@gmail.com

Jessica M. Labonté
Microbiologist
Department of Marine Biology
Texas A&M University at Galveston
USA
labontej@tamug.edu

Andrew J. Martin
Alteration Mineralogist
School of Earth and Ocean Sciences
Cardiff University
United Kingdom
martinaj4@cardiff.ac.uk

Cécile Massiot
Physical Properties Specialist/Downhole Measurements
Department of Geothermal Sciences
GNS Science
New Zealand
c.massiot@gns.cri.nz

Jill M. McDermott
Fluid Geochemist
Department of Earth and Environmental Sciences
Lehigh University
USA
jill.mcdermott@lehigh.edu

Iona M. McIntosh
Physical Properties Specialist/Petrophysics
Department for Solid Earth Geochemistry
Japan Agency for Marine-Earth Science & Technology (JAMSTEC)
Japan
i.m.mcintosh@jamstec.go.jp

Tatsuo Nozaki
Sulfide Petrologist
Research and Development Center for Submarine Resources
Japan Agency for Marine-Earth Science & Technology (JAMSTEC)
Japan
nozaki@jamstec.go.jp

Vivian H. Pellizari
Microbiologist
Instituto Oceanográfico
Universidade de São Paulo
Brazil
vivianp@usp.br

Agnes G. Reyes
Physical Properties Specialist/Downhole Measurements
Marine Geoscience
GNS Science
New Zealand
a.reyes@gns.cri.nz

Stephen Roberts
Alteration Mineralogist
School of Ocean and Earth Science, National Oceanography Centre Southampton
University of Southampton
United Kingdom
steve.roberts@noc.soton.ac.uk

Olivier Rouxel
Inorganic Geochemist
Department of Oceanography/SOEST
University of Hawaii at Manoa
USA
orouxel@hawaii.edu

Lucy E.M. Schlicht
Metamorphic Petrologist
Department of Geosciences
University of Bremen
Germany
lucy.schlicht@uni-bremen.de

Jung Hun Seo
Volcanologist
Department of Energy and Resource Engineering
Inha University
Republic of Korea
seo@inha.ac.kr

Susanne M. Straub
Volcanologist
Lamont-Doherty Earth Observatory
Columbia University
USA
smstraub@ldeo.columbia.edu

Karen Strehlow
Sedimentologist
Dynamics of the Ocean Floor
GEOMAR Helmholtz Centre for Ocean Research Kiel
Germany
kstrehlow@geomar.de

Ken Takai
Microbiologist
Department of Subsurface Geobiological Analysis and Research (D-SUGAR)
Japan Agency for Marine-Earth Science and Technology (JAMSTEC)
Japan
kent@jamstec.go.jp

Dominique Tanner
Igneous Petrologist
School of Earth and Environmental Sciences
University of Wollongong
Australia
dtanner@uow.edu.au

Frank J. Tepley III
Igneous Petrologist
College of Earth, Ocean, and Atmospheric Sciences
Oregon State University
USA
ftepley@coas.oregonstate.edu

Chao Zhang
Alteration Mineralogist
Institute of Mineralogy
Leibniz University of Hannover
Germany
c.zhang@mineralogie.uni-hannover.de

Education and outreach

Peregrin (Perry) A. Hyde
Education/Outreach Officer
Museum of New Zealand Te Papa Tongarewa
New Zealand
perry_hyde@hotmail.com

Tammy J. Orilio
Education/Outreach Officer
Stoneman Douglas High School
USA
tammyorilio@gmail.com

Operational and technical staff

Siem Offshore AS officials

Terry Skinner
Master of the Drilling Vessel

Sam McLelland
Drilling Supervisor

JRSO shipboard personnel and technical representatives

Alexis Armstrong
X-Ray Laboratory

Heather Barnes
Assistant Laboratory Officer

Inva Braha
Curatorial Specialist

Michael Cannon
Marine Computer Specialist

Etienne Claassen
Marine Instrumentation Specialist

William Crawford
Senior Imaging Specialist

Douglas Cummings
Publications Specialist

David Fackler
Applications Developer

Dean Ferrell
Engineer

Seth Frank
Thin Section Laboratory

Sheryl Frazier
Physical Properties Laboratory

Edwin Garrett
Paleomagnetism Laboratory

Jon Howell
Application Developer

Jurie Kotze
Marine Instrumentation Specialist

Jan Jurie Kotze
Marine Laboratory Specialist (temporary)

Zenon Mateo
Underway Geophysics Laboratory

Stephen Midgley
Operations Superintendent

William Mills
Laboratory Officer

Erik Moortgat
Chemistry Laboratory

Vincent Percuoco
Chemistry Laboratory

Cameron Ramsey
Core Laboratory

Jose Saenz, Jr.
Engineer

Mackenzie Schoemann
Marine Laboratory Specialist (temporary)

Kerry Swain
Logging Engineer

Steven Thomas
Marine Computer Specialist

CDEX consulting engineers

Yuichi Shimmoto
Engineer

Yasuyuki Yamazaki
Engineer

Abstract

Volcanic arcs are the surface expression of magmatic systems that result from the subduction of mostly oceanic lithosphere at convergent plate boundaries. Arcs with a submarine component include intraoceanic arcs and island arcs that span almost 22,000 km on Earth's surface, the vast majority of which are located in the Pacific region. Hydrothermal systems hosted by submarine arc volcanoes commonly contain a large component of magmatic fluid. This magmatic-hydrothermal signature, coupled with the shallow water depths of arc volcanoes and their high volatile contents, strongly influences the chemistry of the fluids and resulting mineralization and likely has important consequences for the biota associated with these systems. The high metal contents and very acidic fluids in these hydrothermal systems are thought to be important analogs to numerous porphyry copper and epithermal gold deposits mined today on land.

During International Ocean Discovery Program (IODP) Expedition 376 (5 May–5 July 2018), a series of five sites was drilled on Brothers volcano in the Kermadec arc. The expedition was designed to provide the missing link (i.e., the third dimension) in our understanding of hydrothermal activity and mineral deposit formation at submarine arc volcanoes and the relationship between the discharge of magmatic fluids and the deep biosphere. Brothers volcano hosts two active and distinct hydrothermal systems: one seawater-influenced and the other affected by magmatic fluids (largely gases). A total of 222.4 m of volcaniclastics and lavas was recovered from the five sites drilled, which include Sites U1527 and U1530 in the Northwest (NW) Caldera seawater-influenced hydrothermal field; Sites U1528 and U1531 in the magmatic fluid-influenced hydrothermal fields of the Upper and Lower Cones, respectively; and Site U1529, located in a magnetic low that marks the West (W) Caldera upflow zone on the caldera floor. Downhole logging and borehole fluid sampling were completed at two sites, and two tests of a prototype turbine-driven coring system (designed by the Center for Deep Earth Exploration [CDEX] at Japan Agency for Marine-Earth Science and Technology [JAMSTEC]) for drilling and coring hard rocks were conducted.

Core recovered from all five sites consists of dacitic volcaniclastics and lava flows with only limited chemical variability relative to the overall range in composition of dacites in the Kermadec arc. Pervasive alteration with complex and variable mineral assemblages attest to a highly dynamic hydrothermal system. The upper parts of several drill holes at the NW Caldera hydrothermal field are characterized by secondary mineral assemblages of goethite + opal-A + zeolites that result from low-temperature (<150°C) reaction of rock with seawater. At depth, NW Caldera Site U1527 exhibits a higher temperature (~250°C) secondary mineral assemblage dominated by chlorite + quartz + illite + pyrite. An older mineral assemblage dominated by diaspore + quartz + pyrophyllite + rutile at the bottom of Hole U1530A is indicative of acidic fluids with temperatures of ~230°–320°C. By contrast, the alteration assemblage at Site U1528 on the Upper Cone is dominated by illite + natroalunite + pyrophyllite + quartz + opal-CT + pyrite, which attests to high-temperature reaction of rocks with acid-sulfate fluids derived from the disproportionation of magmatic SO_2. These intensely altered rocks exhibit extreme depletion of major cation oxides, such as MgO, K_2O, CaO, MnO, and Na_2O. Furthermore, very acidic (as low as pH 1.8), relatively hot (≤247°C) fluids collected at depths of 160, 279, and 313 meters below seafloor (mbsf) in Hole U1528D have chemical compositions indicative of magmatic gas input. In addition, preliminary fluid inclusion data provide evidence for involvement of two distinct fluids: phase-separated (modified) seawater and an ~360°C hypersaline brine, altering the volcanic rock and potentially transporting metals in the system.

The material and data recovered during Expedition 376 provide new stratigraphic, lithologic, and geochemical constraints on the development and evolution of Brothers volcano and its hydrothermal systems. Insights into the consequences of the different types of fluid-rock reactions for the microbiological ecosystem elucidated by drilling at Brothers await shore-based studies.

Introduction

Magmatic systems that result from subduction of mainly oceanic lithosphere at convergent plate boundaries are manifested by volcanic arcs at the surface. Those arcs that contain a submarine component include intraoceanic arcs and island arcs, spanning almost 22,000 km on Earth's surface, the vast majority of which are located in the Pacific region (de Ronde et al., 2003). It is estimated that all intraoceanic arcs combined may contribute hydrothermal emissions equal to ~10% of that from mid-ocean ridges (MORs) (Baker et al., 2008).

Hydrothermal activity associated with these submarine arc volcanoes is commonly dominated by the discharge of magmatic volatiles in contrast to MOR systems that are governed by seawater circulation through basaltic oceanic crust. Submarine arc magmatic-hydrothermal systems are driven by crystallization of magmas produced by mantle melting fluxed by volatiles released from the subducting slab. These magmas are enriched by an order of magnitude in volatiles compared with MOR basalts (e.g., Wallace, 2005; Plank et al., 2013). Degassing of these arc magmas gives rise to extraordinary phenomena, such as the discharge of liquid CO_2 (Lupton et al., 2006) and the formation of liquid "lakes" of sulfur on the seafloor (de Ronde et al., 2015). Although intraoceanic arcs are some of the most hostile environments for life because of the exceptionally high concentrations of toxic metals and metalloids in very acidic, gas-rich, and high-temperature fluids, diverse animal and microbial communities are commonly observed (e.g., Clark and O'Shea, 2001; Takai et al., 2009).

The Kermadec segment of the Kermadec-Tonga intraoceanic arc (Figure **F1**) is host to ~32 large volcanoes, 80% of which are hydrothermally active, making it the most active arc in the world. The magmatic-hydrothermal signatures, including high concentrations of sulfur and carbon species gases and high iron contents, coupled with the shallow depths of venting (~1800–120 meters below sea level [mbsl]) of these volcanoes, heavily influence the chemistry of the discharging fluids and the minerals that precipitate from these fluids and have important consequences for the biota associated with these systems. Given the high metal contents and very acidic fluids, these hydrothermal systems are also considered to serve as important submarine analogs to many of the porphyry copper and epithermal gold deposits exploited on land today.

Brothers volcano on the Kermadec arc is such a system and has been the focus of a continuing series of studies. An International Ocean Discovery Program (IODP) workshop (Lisbon, November 2012: **http://www.ecord.org/science/magellanplus**) identified Brothers volcano as the top candidate worldwide for arc volcano drilling. Hence, Expedition 376 was designed to provide the missing link (i.e., the third dimension) in our understanding of mineral de-

posit formation along arcs, the subseafloor architecture of these volcanoes and their related permeability, and the relationship between the discharge of magmatic fluids and the deep biosphere.

Geological setting

The Kermadec-Tonga arc northeast of New Zealand (Figure **F1**) is one of the longest contiguous intraoceanic arcs in the world. More than 60 volcanoes of varying size occur along the arc—the vast majority of which are submarine—with more than half occurring in the Kermadec sector (de Ronde et al., 2003, 2007). Volcanic rocks along the Kermadec arc range in composition from basalt to rhyodacite. Trace element and isotopic data indicate significant magma source heterogeneity both along and across the arc as a result of variable subduction of continent-derived sediments, pelagic sediments, and oceanic crust and/or interaction with continental crust (e.g., Gamble and Wright, 1995; Gamble et al., 1996; Haase et al., 2002; Timm et al., 2012, 2013, 2014).

Brothers volcano (Figure **F2**) is one of three caldera volcanoes included in 13 major volcanic edifices that form the active Kermadec volcanic arc front between 37°S and 34°50′S (Wright, 1997; Wright and Gamble, 1999). Brothers volcano is part of a ~35 km long and 15 km wide predominantly silicic volcanic complex that is dissected by basement fractures and associated dike-controlled ridges that are 1–1.5 km wide and rise 400–500 m above the seafloor. These structures strike predominantly 55° to 65°, although a conjugate set of faults is observed subparallel to the elongated Brothers edifice and caldera (Figure **F2**). These orientations are consistent with Havre Trough rifting (e.g., Wright et al., 1996; Deltiel et al., 2002; Ruellen et al., 2003) and indicate first-order extensional tectonic control on Brothers volcano. The base of Brothers volcano rises from a water depth of ~2200 m to a continuous caldera rim at 1540 m, although locally the northwestern rim (or Upper Caldera wall) shoals to 1320 m. The caldera floor has a basal diameter of 3–3.5 km, reaches a water depth of 1850 m, and is surrounded by 290–530 m high walls. An elongate northeast–southwest postcollapse cone (1.5–2 km wide × 350 m high), the Upper Cone, occurs within the caldera, and a satellite cone appears (Lower Cone) on its northeastern flank (Figures **F3A**, **F3B**). The Upper Cone in part coalesces with the southern caldera wall and shoals to 1220 mbsl (de Ronde et al., 2005).

Brothers volcano represents a window into the complicated hydrothermal systems found at submarine arc volcanoes, which display a range of geological and structural settings and vent fluid chemistry, as well as animals and microbes as yet undiscovered at any other site on the seafloor. Six hydrothermal fields have been identified in or on the walls of the caldera at Brothers volcano (Figures **F2**, **F4**). Five of these fields are presently active (the Upper Caldera, NW Caldera, W Caldera, Upper Cone, and Lower Cone sites), whereas the Southeast (SE) Caldera site is currently inactive, or at least it does not contribute to vent plumes measured above the seafloor (Baker et al., 2012). Extensive autonomous underwater vehicle (AUV) mapping of the caldera (de Ronde et al., 2012; Embley et al., 2012) has shown that these hydrothermal fields, with the exception of the Lower Cone site, are closely correlated to areas of magnetic "lows" that are consistent with zones of hydrothermal upflow (Figure **F5**) (Caratori Tontini et al., 2012a, 2012b; Gruen et al., 2012).

The five active fields exhibit two different types of hydrothermal activity. Type I hydrothermal systems are characterized by high-temperature (≤320°C) venting of relatively gas-poor, moderately acidic fluids at the W, NW, and Upper Caldera sites, where Cu-Au–rich sulfide chimneys are common. Type II hydrothermal fields are characterized by lower temperature (≤120°C) venting of gassy, very low pH (to 1.9) fluids at the summits of the Upper and Lower Cone sites, where native sulfur chimneys and extensive iron oxyhydroxide crusts occur (de Ronde et al., 2005; 2011). Time-series studies of hydrothermal plumes above the four most active sites (i.e., Upper Caldera, NW Caldera, and the Upper and Lower Cone sites) show that the cone sites expelled fluids of widely differing compositions between 1999 and 2018, with large variations in dissolved H_2S, particulate Cu, dissolved Fe, and Fe/Mn values (Humphris et al., 2018). By contrast, the composition of chronic plumes above the NW Caldera site (the Upper Caldera site was discovered only in 2017), although chemically distinct from the other hydrothermal vent sites, have not changed over the same interval (de Ronde et al., 2005; Humphris et al., 2018).

In 2005, Neptune Minerals, Inc. drilled a number of shallow holes (to depths of 14.8 mbsf) at Brothers volcano. Sixteen holes were drilled on the slopes of the NW Caldera wall, and a single hole was drilled inside the crater atop the Upper Cone. The uppermost material of many of these holes consisted of dark brown ooze locally containing glass sand and grit. This material was commonly underlain by a zone of ~1 m thickness containing pieces of sulfide chimney, glass grit, Fe-Si-Mn oxyhydroxides, and mixtures thereof. Typically underlying this zone were variably hydrothermally altered volcanic rocks ranging from volcanic silt and sand to volcanic glass, gravel, breccia, and more massive volcanic rock (dacite). Alteration colors ranged from pale gray to pale green, and stockwork veins locally cut the rocks. The one core drilled inside the pit crater atop the Upper Cone intersected volcanic breccia, gravels, and rocks together with native sulfur down to 10 meters below seafloor (mbsf).

Microbial community development patterns associated with the two types of hydrothermal activity at Brothers volcano have been explored using limited (four) samples collected from the seafloor (Stott et al., 2008; Takai et al., 2009). Microbial community compositions obtained from chimneys at the NW Caldera site are characterized by an abundance of slightly thermophilic and hyperthermophilic chemolithoautotrophs (Takai et al., 2009), as observed in typical high-temperature hydrothermal vent environments of MORs and back-arc basin systems (Nakamura and Takai, 2014). By contrast, microbial communities from the Lower Cone exhibit a diversity of bacterial lineages, with potential psychrophilic and thermophilic sulfur- and iron-oxidizing chemolithotrophs (Stott et al., 2008) like those found in the magmatic volatile–rich hydrothermal environments of submarine arc volcanoes (Nakamura and Takai, 2014). These intrafield differences in microbial community composition and function are thought to be associated with the different hydrothermal fluid compositions in the two types of hydrothermal systems. In particular, the highly variable volatile species concentrations induced by phase separation, the variable mixing ratios of hydrothermal and seawater inputs, and the concomitant precipitation of mineral phases are considered crucial factors in the control of chemosynthetic microbial community development (Takai and Nakamura, 2011; Nakamura and Takai, 2014). The two distinct hydrothermal microbial ecosystems occurring together within a caldera, showing a clear niche segregation in response to both physical and chemical differences in the hydrothermal fluids, is currently globally unique (Flores et al., 2012; Nakamura and Takai, 2014).

Modeling of the subseafloor hydrology at Brothers volcano has suggested that subseafloor phase separation, inferred from measured temperatures and calculated end-member vent fluid chemical

and isotopic compositions, can be achieved only by the primary input of saline magmatic fluids at depth (de Ronde et al., 2011; Gruen et al., 2012, 2014). In addition, the vent systems appear to evolve over short time periods, as expulsion of magmatic heat and volatiles occurs within the first few hundred years of magma emplacement in the form of low-salinity vapor-rich fluid, while magmatically derived salt is temporarily trapped in the crust. This retained salt is then periodically expelled from the system by later convection of low- to high-temperature hydrothermal fluid of seawater origin (Gruen et al., 2014). This model has important implications for the distribution of metals in the hydrothermal mineralization. Sulfide-complexed metals (e.g., Au) will preferentially ascend during the early vapor-dominated fluid discharge, whereas chloride-complexed metals (e.g., Cu, Pb, and Zn) will be retained in the dense magmatic brine, thus potentially forming layers of metal sulfides with distinct zonation at depth (Gruen et al., 2014).

Scientific objectives

The four primary scientific objectives outlined in the Expedition 376 *Scientific Prospectus* (de Ronde et al., 2017) were to (1) characterize the subvolcano, magma chamber–derived volatile phase to test model-based predictions that this is either a single-phase gas or two-phase brine-vapor, (2) determine the subseafloor distribution of base and precious metals and metalloids and the reactions that have taken place along pathways to the seafloor, (3) quantify the mechanisms and extent of fluid-rock interaction and consequences for mass transfer of metals and metalloids into the ocean and the role of magmatically derived carbon and sulfur species in mediating these fluxes, and (4) assess the diversity, extent, and metabolic pathways of microbial life in an extreme, metal-toxic, and acidic volcanic environment. The drill sites represent discharge zones of geochemically distinct fluids that are variably affected by magmatic volatile input, allowing us to directly address the consequences of magma degassing on metal transport to the seafloor and its effect on the functioning of microbial communities.

To meet these objectives, a strategy involving two independent drilling efforts was developed to recover cores from both shallow (<200 m) and deep (~200–800 m) intervals. Cores with good recovery are required from the shallowest intervals (tens of meters depth) to examine aspects of hydrogeology, permeability, fluid flow, and seawater entrainment as well as their effects on microbial community development and habitability. We will acquire these cores by deploying the MeBo seafloor drill rig (Freudenthal and Wefer, 2007) from the R/V *Sonne* at a time yet to be planned (Bach, Haase, Wefer, and de Ronde, co-PIs). This scheduled shallow drilling allowed Expedition 376 to bypass coring in the shallowest parts of the holes when necessary and strategically prepare the holes for the casing required for deep coring. The operational plan for Expedition 376 was to drill, core, and log three sites—one on the northwest rim of the caldera, one on the western side of the caldera floor, and one atop the Upper Cone—to provide access to critical zones dominated by magma degassing and high-temperature hydrothermal circulation over depth ranges considered crucial in the development of multiphase mineralizing systems.

Site summaries

Site U1527

Background and objectives

Site U1527 (proposed Site NWC-1A) is located on the rim of the northwest caldera wall of Brothers volcano at a water depth of 1464 m (Figure **F6**). Drilling targeted what was thought to be either the margin of an older modified-seawater hydrothermal upflow zone or a recharge zone to the currently active discharge areas several hundred meters away from either side of the drill site. A key objective of Expedition 376 was to quantify the mechanisms and extent of fluid-rock interaction and the consequences for mass transfer of metals into the ocean in both seawater-dominated and magmatic fluid-dominated hydrothermal systems within the caldera of Brothers volcano. Hence, the main objective of Site U1527 was to drill through the margin of the inferred upflow zone of a modified-seawater system.

Operations

We conducted operations in three holes at Site U1527. Hole U1527A is located at 34°51.6528′S, 179°3.2397′E at a water depth of 1464.2 m. We used the rotary core barrel (RCB) system in Hole U1527A to core from the seafloor to 101.4 mbsf. Recovery was poor (1.27 m; 1.3%). The downhole conditions encountered in Hole U1527A determined the preparations for running a reentry system. In Hole U1527B, located at 34°51.6519′S, 179°3.2526′E at a water depth of 1464.2 m, 10.75 inch casing was drilled-in to 95.5 mbsf, and final penetration of the drilling assembly was 105.5 mbsf. Upon release from the casing, the reentry system hung up on the underreamer arms, which failed to retract, and the entire assembly was recovered to the surface.

Hole U1527C is located at 34°51.6625′S, 179°3.2534′E at a water depth of 1464.1 m. After installing 95.5 m of casing, we RCB cored continuously from 99.9 to 238.0 mbsf and recovered 25.9 m (19%) of material. We had extremely poor to no recovery in unconsolidated volcanic deposits until a formation change at 187 mbsf, when average recovery increased to 49% for the rest of coring in cemented volcaniclastic rocks. Unstable hole conditions forced abandonment of Hole U1527C and, once again, the reentry system was unintentionally retrieved because of clogging of the hydraulic release tool (HRT) and upper casing sub. A total of 249.5 h, or 10.4 days, were recorded while at Site U1527.

Principal results

Igneous rocks cored at Site U1527 were divided into two units (Figure **F7**). Igneous Unit 1 was recovered in Hole U1527A (29.10–67.81 mbsf) and Hole U1527C (108.40–176.16 mbsf). It consists of plagioclase-clinopyroxene phyric and Fe-Ti oxide–bearing black dacite lava with glassy trachytic groundmass and spatially associated fresh scoria and pumice lapilli.

Igneous Unit 2 was recovered in Hole U1527C (185.20–234.38 mbsf). The contact between Units 1 and 2 was not recovered. Igneous Unit 2 consists of progressively hydrothermally altered lapilli-tuffs, tuff-breccias, and lapillistone and is divided into four subunits (2a–2d) based on changes in modal composition of clasts, matrix-

to-clast ratio, and color. Igneous Subunit 2a (185.20–185.44 mbsf) is a lapilli-tuff, consisting of fresh dacitic clasts surrounded by a brown, fine-grained matrix that probably represents altered tuff. Igneous Subunit 2b (185.44–220.98 mbsf) is composed of matrix-supported monomict and polymict lapilli-tuffs, lapillistones, and tuff-breccias. Igneous Subunit 2c (220.98–226.49 mbsf) is made up of clast-supported polymict lapillistones, whereas Igneous Subunit 2d (228.40–234.38 mbsf) is composed of both altered matrix-supported and clast-supported tuff-breccias and lapilli-tuffs.

Igneous Unit 2 rocks contain various clasts of volcanic origin: (1) fresh to slightly altered dacite in Subunit 2a; (2) volumetrically significant greenish gray altered volcanic clasts in Subunits 2b, 2c, and 2d; (3) fine-grained, dark green altered clasts in Subunit 2b; and (4) various types of rare dark gray volcanic clasts in Subunits 2b, 2c, and 2d. The matrix of the volcaniclastic rocks and the groundmass within volcanic clasts in Igneous Unit 2 appear very similar to the trachytic groundmass of the dacite clasts in igneous Unit 1, but they are increasingly replaced by secondary chlorite, clays, and quartz with depth. All clasts contain varying amounts of plagioclase, clinopyroxene, and Fe-Ti oxides, strongly resembling the primary phenocryst assemblage of the dacite lavas of Igneous Unit 1. Although the degree of alteration increases downhole, as indicated by the increasing degree of silicification, plagioclase crystals are only slightly altered, whereas clinopyroxene is altered significantly or disappears, and Fe-Ti oxides alter to sulfides.

Three distinct types of alteration were observed in core material recovered from Site U1527 (Figure **F8**). Alteration Type I (0–185.44 mbsf) occurs in intervals of fresh to slightly altered volcanic rocks and is characterized by low-temperature alteration mineral assemblages (Figure **F9**). This alteration type is divided into distinct Subtype Ia and Subtype Ib. Alteration Subtype Ia (0–185.20 mbsf) consists of unaltered to slightly altered vesicular dacitic lava characterized by formation of zeolite in vesicles and the occurrence of palagonite, iron oxyhydroxide, and trace pyrite partly replacing volcanic glass. Alteration Subtype Ib (185.20–185.44 mbsf) solely pertains to the volcaniclastic rocks of Igneous Subunit 2a, which are slightly to moderately altered. The clasts exhibit only trace alteration and retain primary plagioclase and clinopyroxene phenocrysts, but the degree of alteration in the matrix increases compared to alteration Subtype Ia. The alteration material in the matrix consists of iron oxyhydroxide and illite with minor zeolite, smectite, magnetite, and pyrite.

Alteration Type II (185.72–234.38 mbsf) is characterized by more extensive alteration of most primary minerals, with the clasts and matrix of the volcaniclastic rocks being replaced by clay minerals, silica, and pyrite (Figure **F9**). This alteration type is also divided into two subtypes. Alteration Subtype IIa (185.72–234.38 mbsf; intercalated with Subtype IIb and Type III) features a pervasive green-gray chlorite-smectite mineral assemblage with increasing amounts of cryptocrystalline/amorphous silica, infilling pore spaces, and increasing abundance of disseminated pyrite with depth. Moderate to intense alteration occurs in both clasts and matrix of the primary volcaniclastic rocks and increases in degree downhole. Alteration Subtype IIb (186.40–208.06 mbsf; intercalated with Subtype IIa) is characterized by several centimeter- to meter-scale zones of yellow-brown alteration, overprinting greenish Alteration Subtype IIa. The overprinting boundary is sharp. Iron oxyhydroxide and occasionally oxidized pyrite give this alteration type its characteristic yellow-brown color. Throughout both the green and yellow-brown altered intervals, clasts display a range of degrees of alteration and resorption from slightly altered clasts with primary igneous textures and sharp boundaries to intensely altered clasts with diffuse boundaries to the surrounding matrix.

Alteration Type III (220.98–226.49 mbsf) represents a more heterogeneous alteration type that is intercalated with Alteration Subtype IIa. In this type of alteration, both clasts and matrix are pervasively altered (Figure **F9**). The matrix contains dark gray silica and chlorite, disseminated pyrite (as much as 3 vol%), and magnetite. Vugs are partially filled with clay minerals and silica.

Unaltered volcanic rocks from Hole U1527A and the shallower sections of Hole U1527C (Igneous Unit 1) represent dacites that are compositionally similar to those previously reported from Brothers volcano (e.g., Haase et al., 2006; Wright and Gamble, 1999; Timm et al., 2012). Most of the pervasively altered volcaniclastic rocks recovered from Hole U1527C (Igneous Unit 2) share the incompatible element composition (i.e., Zr/Y and Zr/TiO_2) of overlying Igneous Unit 1 from the same hole. This commonality suggests a common parental magma, despite petrographic differences.

Geochemical analyses of the highly altered, variously colored volcaniclastic rocks demonstrate the mobility of alkali elements during high- and low-temperature hydrothermal alteration of the rock (Figure **F10**). Analyses of K_2O, Rb, Ba, MgO, and SiO_2 contents define a complex history of hydrothermal overprinting marked by multiple alteration stages. Alteration Type III displays significant enrichment in total sulfur content (up to 1.9 wt%). Geochemical changes recorded in Hole U1527C are consistent with petrographic observations, including the formation of pyrite and replacement of groundmass and matrix by clay in deeper, more altered volcaniclastic rocks.

Organic carbon comprises the bulk of measured total carbon concentrations. Detectable only from 185–205 mbsf in Hole U1527C, this organic carbon may originate from seawater-derived fluid circulation and/or microbial biomass. Headspace analysis of gases evolved from Hole U1527C hard rock samples indicates higher than ambient H_2 contents that may have been produced by mechanochemical sampling artifacts such as generation during RCB drilling and/or crushing rock samples prior to headspace sampling.

Site U1527 is characterized by moderately to steeply dipping alteration boundaries, fractures, and faults in addition to shallowly dipping shears and relatively few veins. Alteration boundaries are sharp and range in dip from 0° to 74° (average and median = 48°) and demarcate the transition from Alteration Subtypes IIa to IIb. Fractures also dip moderately to steeply, ranging from 37° to 90° (average = 68°). The density of veins and fractures is low but increases slightly downhole. Fractures almost always have a brown/orange alteration halo overprinting all other types of alteration, indicating late formation of fractures. The presence of brown/orange alteration along fractures and defining Alteration Subtype IIb may indicate the ingress of seawater through late-forming fractures. Faults were observed only in Hole U1527C and dip steeply, ranging from 45° to 83° (average = 66°), and are most abundant in Igneous Subunit 2c. All faults are discrete centimeter-scale zones with a normal sense of shear. Shallowly dipping shears are defined by elongate ribbons of white clays that may represent flattened and altered volcanic clasts. White ribbons wrapped around larger volcanic clasts may indicate some crystal-plastic deformation. The shallowly dipping shears (average = 22°) are overprinted by higher-angle brittle faults. The overall lack of veins and indications of late fracturing suggest that alteration is not structurally controlled and may instead be due to pervasive flow.

The two igneous units from Site U1527 have different natural remanent magnetization (NRM) intensities before demagnetization; samples from Igneous Unit 1 show more intense NRM (>0.5 A/m) than those from Igneous Unit 2. However, the direction of magnetization is consistent in both units, with an average inclination of –59°, which is very close to the inclination of a geomagnetic axial dipole (GAD) of –60° at the latitude of Brothers volcano. This consistent GAD inclination suggests a coherent young age for these rocks, most certainly from the current normal polarity Brunhes geomagnetic epoch. Igneous Unit 1 also has significantly larger magnetic coercivities than Igneous Unit 2. Thermal demagnetization experiments from Igneous Unit 2 show a more complex pattern compared to similar experiments from Igneous Unit 1, but coherently indicate magnetite or titanomagnetite as the main magnetic mineral in both igneous units. In addition, susceptibility measurements and isothermal remanence magnetization (IRM) experiments suggest comparable magnetite content in both units, with a slight decrease in Igneous Subunits 2c and 2d.

The fresh dacitic volcanics of Igneous Unit 1 show an inverse correlation between porosity and bulk density, but no such correlation is observed between *P*-wave velocity and bulk density or *P*-wave velocity and porosity. Variably altered volcaniclastic rocks in Igneous Unit 2 display an inverse correlation between porosity and bulk density and between porosity and *P*-wave velocity. Mean bulk density (2.2 g/cm^3), porosity (30%), and *P*-wave velocity (3330 m/s) generally show small variations throughout Igneous Unit 2 and do not appear to be affected by transitions between alteration types. Alteration Subtypes IIa and IIb are clearly identifiable in reflectance colorimetry data. *P*-wave velocity sharply increases at the boundary between Igneous Subunits 2b and 2c (velocities of ~4000 and 4200 m/s on section halves and discrete samples, respectively), followed by a downhole decrease in *P*-wave velocity to the bottom of Igneous Subunit 2c. In Igneous Subunit 2C, this variation in *P*-wave velocity is reflected in a similar trend in bulk density and matching inverse variation in porosity, which appears to be associated with deformation and shear in this unit.

Magnetic susceptibility measured on whole-round and section-half cores is consistent with discrete measurements. Magnetic susceptibility in Igneous Subunits 2a and 2b is overall higher than that in Igneous Subunits 2c and 2d. Thermal conductivity values range from 1.09 to 2.35 W/(m·K) (average = 1.72 W/[m·K]); Igneous Unit 2 has higher values than Igneous Unit 1. Thermal conductivity in Igneous Unit 2 varies over smaller scales, reflecting changes in type and distribution of alteration minerals. Thermal conductivity values are lower where alteration is dominated by the presence of water-rich clay minerals (e.g., low of 1.53 W/[m·K] in Igneous Subunit 2b at ~203.40 mbsf), whereas the highest value of thermal conductivity is observed along with increases in pyrite, silica, and magnetite concentrations in Igneous Subunit 2c. Hence, thermal conductivity data reflect the heterogeneity of mineral compositions and alteration assemblages throughout the core.

Five whole-round samples (each 9–19 cm long) collected from hydrothermally altered, relatively hard materials in Hole U1527C (Table **T1**) were processed and preserved as subsamples for shore-based biological investigations that will include quantification of microbial and viral biomass, molecular analysis of the microbial communities from extracted DNA and RNA, estimation of microbial metabolic activity and viral production, and cultivation of subseafloor microbial components. Quantification of the contamination tracer perfluoromethyldecalin (PFMD) was conducted for the drilling fluid and the exterior and interior parts of whole-round samples. PFMD was routinely detected, although barely above detection levels, suggesting that penetration of drilling fluids to the interior of whole-round samples was minimal.

Site U1528

Background and objectives

Site U1528 (proposed Site UC-1A) is located inside a small (~40 m diameter at the top; ~25 m diameter at the bottom) pit crater at the summit of the Upper Cone of Brothers volcano at a water depth of 1228 m (Figure **F6**). The primary objective at this site was to drill into the upflow zone of the Type II hydrothermal system that is strongly influenced by magmatic degassing. In this area, discharge of relatively gas-rich, very acidic fluids has resulted in advanced argillic alteration. Site U1528 addresses important Expedition 376 objectives related to the role of magmatically influenced hydrothermal fluids in transporting metals to the seafloor and provides a comparison of fluid-rock reactions with the Type I seawater-dominated hydrothermal system drilled at Sites U1527 and U1530.

Operations

We conducted operations in four holes at Site U1528. Hole U1528A is located at 34°52.9177′S, 179°4.1070′E at a water depth of 1228.4 m. We used the RCB system to core from the seafloor to 84.4 mbsf and recovered 17.1 m (20%). The downhole conditions encountered in Hole U1528A dictated the need to deploy a reentry system to achieve our objectives.

Hole U1528B is located 10 m south of Hole U1528A at 34°52.9222′S, 179°4.1077′E at a water depth of 1229.4 m. Here, we drilled-in 10.75 inch casing to 24.3 mbsf, with the drilling assembly penetrating to 25.6 mbsf. We had trouble extracting the drilling assembly from the reentry system, which ultimately took several hours. Because of drilling-induced suspension of sediment in the seawater, visibility was limited and we could see only the top of the reentry funnel, observed to be at a water depth of 1224.8 m, consistent with it being properly set on the seafloor. After two separate, unsuccessful attempts to reenter Hole U1528B with both the RCB coring system and the CDEX turbine-driven coring system (TDCS), we suspended operations. Further visual observations showed the reentry system was sitting at a slight angle, preventing the drill string from passing through the throat of the reentry funnel.

Our next objective was to perform the first offshore test of the TDCS. In Hole U1528C, located at 34°52.9215′S, 179°4.1128′E at a water depth of 1229.1 m, we drilled without coring using the TDCS to 22 mbsf, then cored to 53.5 mbsf, recovering 3.6 m (12%). Further advancement was prevented by a broken core barrel that remained in the TDCS bottom-hole assembly (BHA), forcing abandonment of Hole U1528C.

In Hole U1528D, located at 34°52.9219′S, 179°4.1164′E in the very limited flat central area of the pit crater and at a water depth of 1228.1 m, we drilled-in 13.875 inch casing to 59.4 mbsf, with the drilling assembly penetrating to 61.3 mbsf. We then RCB cored to 359.3 mbsf and recovered 87.2 m (29%) under good hole conditions. After the bit reached 40 h of rotation time, whereupon it would normally be changed before continuing to core, we instead decided to take downhole temperature measurements and obtain borehole fluid samples in the open hole through the existing bit.

The Elevated Borehole Temperature Sensor (ETBS) tool was deployed first and recorded a maximum temperature of 35°C at 357 mbsf, being 2 m above the drilled bottom of the hole. The subsequent deployment of the 1000-mL Kuster Flow-Through Sampler (FTS) tool ended with its failure under compression in the open

hole. We then made an unsuccessful attempt to recover the tool with a fishing tool BHA equipped with boot-type junk baskets. Reentry into Hole U1528D was complicated by a plume emanating from the reentry funnel. We next deployed a logging BHA, lowered the backup 600-mL Kuster FTS tool on the core line, and successfully recovered a fluid sample from 279 mbsf. A subsequent ETBS downhole temperature measurement at the same depth recorded a maximum temperature of 212°C, confirming that the flasked wireline high-temperature triple combo (HTTC) logging tool string (natural gamma ray, lithodensity, and temperature tools) could be deployed. We successfully performed two upward logging passes from 323 mbsf. Another deployment of the Kuster FTS tool then recovered a second borehole fluid sample from 313 mbsf; subsequent deployment of the ETBS tool recorded a maximum temperature of 165°C. Next, we drilled down with a tricone bit BHA to clean out the hole to 356 mbsf—the depth of the top of the lost Kuster FTS tool.

A concave mill bit, along with two boot-type junk baskets, was then deployed to attempt to remove the remaining parts of the lost Kuster FTS tool. After reentering Hole U1528D for the sixth time—despite very poor visibility around the reentry funnel—we advanced the mill bit to the bottom of the hole at 359.3 mbsf. Upon recovery, there was no evidence of the Kuster FTS tool in the boot baskets. The next fishing attempt used the reverse-circulation junk basket (RCJB) assembled in conjunction with the boot-type junk baskets. After the seventh reentry of Hole U1528D, we worked the RCJB BHA back to bottom (359.3 mbsf), where we circulated 25 barrels of high-viscosity mud for ~15 min while working the RCJB up and down. When the end of the drill string cleared the rig floor, the discovery that the lowermost 172.8 m was missing ended Hole U1528D operations. The drill string failed in a piece of 5 inch pipe above the BHA. The recovered broken piece showed significant damage directly attributable to the corrosive downhole environment.

After completion of coring operations at Site U1531, we returned to Hole U1528D (about 3 weeks later) to conduct a series of alternating downhole temperature measurements using both the ETBS tool and Petrospec spool-in thermocouple memory tool (TCMT) as well as two Kuster FTS deployments that resulted in recovering a borehole fluid sample from 160 mbsf. Two successful temperature measurement runs recorded maximum values of 198°C (ETBS) and 156°C (TCMT) at 160 mbsf. Site U1528 operations concluded with successful recovery of the failed Hole U1528B reentry system at the end of Expedition 376. A total of 592.8 h, or 24.7 days, were spent at Site U1528.

Principal results

Rocks cored at Site U1528 are divided into three igneous units (Figure **F11**). Igneous Unit 1, recovered in Hole U1528A (0–6.03 mbsf) and Hole U1528C (26.50–31.41 mbsf), consists of polymict lapilli tephra made up of subangular to subrounded volcanic clasts that have experienced varying degrees of alteration. Igneous Unit 2, recovered in Hole U1528A (16.30–83.57 mbsf), Hole U1528C (35.50–46.00 mbsf), and Hole U1528D (61.30–269.30 mbsf), is divided into three subunits based on internal rock fabric and the presence of primary minerals. Subunits 2a and 2c are composed of sequences of altered lapillistone and lapilli-tuff, with subordinate intervals of altered tuff and tuff-breccia. Clasts are volcanic in origin and altered to differing degrees; the matrix consists of secondary mineral assemblages. Identification of original lithologies becomes increasingly difficult with depth (especially in Subunit 2c). More coherent, massive dacitic lavas, affected by a lesser degree of alteration, occur between 152.90 and 160.17 mbsf and make up Subunit 2b. Igneous Unit 3, recovered exclusively in Hole U1528D (162.50–269.03 mbsf), consists of altered dacite lava with some relatively unaltered intervals.

The dacitic pyroclastic rocks and lavas at Site U1528 are pervasively altered, yet still show distinct similarities in petrography and whole-rock geochemistry to fresh volcanics encountered in each Igneous Unit 1 at Sites U1527, U1529, and U1531 and to published descriptions and geochemical results for unaltered dacite recovered from elsewhere at Brothers volcano (e.g., Haase et al., 2006; Wright and Gamble, 1999; Timm et al., 2012). Even though intervals with (partially) fresh phenocrysts are rare, primary igneous textures, such as vesicles, and the crystal shapes of plagioclase and (rarely) pyroxene phenocrysts and microlites—now infilled and replaced by secondary minerals—can be recognized in most samples. Petrography and the abundance of elements that are less affected by alteration suggest that the Site U1528 protolith was dacitic tephra and lava similar to those previously encountered at Brothers volcano.

Four distinct alteration types are observed in core material recovered from Site U1528 (Figure **F12**). Alteration Type I (0–35.76 mbsf), classified as slightly altered, occurs in unconsolidated gravels. The dominant alteration mineral assemblage consists of smectite with minor pyrite, opal-CT, natroalunite, pyrophyllite, and native sulfur. Two distinct volcanic clast colors are observed: dark gray clasts, which contain more smectite and light gray clasts. Native sulfur occurs in crystalline-tabular (orthorhombic) and globular grain morphologies.

Alteration Type II (classified as highly altered) occurs in several intervals throughout Site U1528 (e.g., 148.1–150.5 mbsf) and is characterized by an alteration mineral assemblage of illite, smectite, opal-CT, quartz, pyrite, and anhydrite. Alteration is typically blue-gray in color, manifested by brecciation, and exhibits relict perlitic texture (Figure **F13**). Plagioclase phenocrysts are variably pseudomorphed by alunite and anhydrite, whereas pyroxene is pseudomorphed by anhydrite, smectite, and pyrite. The latter is abundant (average = 1–5 vol%) and occurs not only in pyroxene pseudomorphs but also as subhedral to euhedral disseminated grains and in discrete veins associated with anhydrite. Primary titanomagnetite is rimmed and shows progressive replacement by pyrite that exhibits skeletal texture and contains abundant anhydrite inclusions.

Alteration Type III, classified as highly to intensely altered, is intercalated with Alteration Type II (e.g., 239.3–268.1 mbsf), and the boundary between these alteration types can be either gradational or sharp. Alteration Type III is represented by pervasively altered white-gray volcaniclastic rocks (Figure **F13**). A mineral assemblage of natroalunite, pyrophyllite, and rutile, with lesser quartz, opal-CT, smectite, pyrite, and anhydrite, characterizes Alteration Type III. Alunite, pyrophyllite, and silica are more abundant in the matrix, whereas smectite is enriched in clast material. Plagioclase and pyroxene are completely pseudomorphed by alunite, anhydrite, and pyrite. Late-stage anhydrite-pyrite veins commonly cut pseudomorphed plagioclase crystals. Titanomagnetite is almost completely replaced with leucoxene and pyrite. Vugs are infilled with anhydrite and minor pyrite, native sulfur, alunite, and silica. In addition, fine-grained pyrite is finely disseminated throughout matrix and clasts.

Alteration Type IV is defined by discrete to diffuse white veins that cut and postdate Alteration Types II and III. Alteration Type IV is first observed at 77.2 mbsf and occurs until the cored bottom of Hole U1528D, at 355.1 mbsf. This alteration type is characterized by

an alteration assemblage of natroalunite, anhydrite, rutile, quartz, opal-CT, native sulfur, and pyrophyllite (Figure **F13**). Mineralogically, Alteration Type IV is distinguished from Alteration Types II and III by higher abundances of native sulfur, silica, and rutile. This alteration type occurs as discrete white veins and distinct alteration halos typically <1 cm but occasionally as wide as 4 cm, commonly with a vuggy texture, overprinting previous alteration and often preserving earlier alteration textures. Pyrite is generally absent or oxidized to iron oxyhydroxides within the halos, and native sulfur is the major mineral phase infilling vugs.

Fluid inclusions in the most recent vug and vein crystals of anhydrite, quartz, natroalunite, and gypsum indicate that the hydrothermal system at Site U1528 is highly dynamic. Two dominant fluid types are variably involved in fluid-rock interactions (Figure **F14**): a buoyant, hot (220–360°C), sulfur-rich, and acidic hypersaline brine (NaCl >30 wt%) and a hot, modified seawater. A massive influx of seawater (NaCl = 3.2 wt%) locally overwhelmed the hypersaline brine along fractures or pervasively diffused into the hot formation, where it is heated to temperatures of 55–360°C. Fluid inclusion salinities both higher and lower than seawater compositions, or the hypersaline brine, plot on the NaCl saturation curve and are attributed to depressurization in the formation caused by sudden fracturing events, resulting in phase separation ("boiling"). This process gives rise to a more saline, higher density fluid for both hypersaline brine and seawater and, at the same time, forms a low-density vapor phase that condenses through cooling to a low-salinity aqueous solution under subcritical conditions (Figure **F14**).

Structures that occur across Holes U1528A, U1528C, and U1528D include volcanic fabrics, alteration veins, and fractures. Volcanic fabrics are best observed in Holes U1528A and U1528D and are defined by vesicles and plagioclase microlites (primary and altered) and, to a lesser extent, phenocrysts. Volcanic fabrics have two forms, those in volcanic clasts and those in coherent lavas. Volcanic fabrics within clasts can be weak to strong, but each clast has a distinct orientation, suggesting brecciation after fabric formation. Fabrics over continuous intervals (i.e., lavas) have a similar orientation and tend to dip >45°. Peaks in volcanic fabric intensity are observed in Igneous Subunit 2b and Unit 3 in Hole U1528D.

Alteration veins occur throughout Holes U1528A and U1528D across all igneous units and alteration types. Veins are most commonly filled by anhydrite, pyrite, silica, and native sulfur. Veins are typically uniform but can be vuggy; some have halos. The presence of halos is the basis for Alteration Type IV. Vein density peaks between 100 and 190 mbsf, coincident with a peak in native sulfur and vuggy veins and a deviation in borehole temperature. Vein dip varies from horizontal to vertical, with an average of ~60° in both holes. The distribution of dips downhole is variable: a few zones have a large range in dip (e.g., 0°–90°) and other zones have dips >45°. Vein thickness ranges from 0.05 to 1 cm and averages ~0.2 cm. Vein thickness is variable downhole, but it appears to increase in intervals with a large range of vein dip, and thicker veins tend to have steeper dips.

Fractures were observed in all three holes, but their abundance is limited. Fractures in Hole U1528C are irregular and lined with native sulfur. Native sulfur is more abundant where the fractures are irregular. In Hole U1528D, fractures are typically clustered in the uppermost 175 m of the hole and have steeper dips (i.e., >60°). Fracture density has three peaks; the one near 290 mbsf coincides with a deviation in borehole temperature and a large range in vein dip.

Considering that Y is relatively mobile under hydrothermal conditions in contrast to Zr, the Y/Zr value of altered volcaniclastics is used as a tracer for the extent of alteration. Two main intervals are characterized by lower Y/Zr values (i.e., relative to unaltered dacite from Brothers volcano): (1) 46–95.5 mbsf in Igneous Subunit 2a, dominated by Alteration Type III, and (2) 240–325 mbsf overlapping Igneous Subunit 2c and Unit 3, as well as associated alternating Alteration Types II and III. Variable extents of depletion in alkalis (K, Rb, and Na), Mg, Ca, and Fe, as well as strong enrichment in total sulfur (as much as 15 wt%) occur throughout the hole (Figure **F15**). Based on average compositions of discrete intervals throughout the entire 360 m section at Hole U1528D, we estimate that >75% of both Mn and Mg have been lost due to hydrothermal alteration. Other significantly depleted elements include Na, K, and Rb (>50% loss of each element) as well as Ca and P (>30% loss of each element). Total S concentrations vary between 2.1 and 15.1 wt%, due to the formation of S-dominated secondary minerals (e.g., alunite, native S, pyrite, and anhydrite), although anhydrite appears to represent a minor component of the total S inventory. Iron appears to be strongly depleted in late-stage Alteration Type IV, suggesting that pH, fO_2, and fS_2 conditions changed substantially from Alteration Types II/III, leading to extensive loss of Fe in possibly SO_4-rich but H_2S-poor hydrothermal fluids. Similar to Site U1527, organic carbon comprises the bulk of measured total carbon concentrations but remains very low, yielding an average of ~250 µg/g at Site U1528.

One sample of interstitial water (376-U1528C-7N-1, 140–150 cm) recovered from 45.9 mbsf has a low pH value of 4.1, consistent with the presence of acidic magmatic fluids. Nearby equimolar enrichments in Ca and SO_4 suggest that dissolution of anhydrite at low temperatures may be occurring in the pore waters.

Three borehole fluid samples were collected from Hole U1528D using the Kuster FTS tool at ~279 and ~313 mbsf and then 23 days later at 160 mbsf. Maximum estimated temperatures of 212° and 247°C for the first two samples and 140°C for the later sample were determined by downhole logging. The fluids have nearly identical Cl, Br, and Mg contents and Na concentrations all lower than seawater. Highly elevated ΣSO_4 and very acidic pH values (as low as 1.8) are characteristic of acid-sulfate fluid. This fluid may either represent unaltered seawater mixing with the vapor phase of a phase-separated, seawater-derived parent fluid ($Cl_{fluid} < Cl_{seawater}$), direct input from a low-salinity magmatic volatile-derived fluid, and/or a mixture of fluids derived from both origins. Elevated Si and K contents in the fluids are due to the likely dissolution of Si- and K-bearing minerals in the presence of highly acidic fluids.

Gas headspace components including H_2, CO_2, and acid-volatile S are elevated over ambient atmospheric levels. These gas anomalies may derive from subseafloor hydrothermal input of volatile-rich fluids that share similar chemical properties with the seafloor hydrothermal fluids discharging at the Upper and Lower Cone sites.

Eighty-three archive-half sections were measured for NRM and underwent alternating field (AF) demagnetization experiments using the cryogenic magnetometer. The sections show generally low NRM intensities where the largest pieces have primary magnetization components, after AF steps of 20 mT, with negative inclinations suggesting normal polarities. AF and thermal demagnetization experiments on 82 discrete samples from Igneous Units 2 and 3 were also carried out. The drilling-induced overprint is generally removed after 20 mT AF demagnetization on the discrete samples, leaving, in most cases, a stable primary magnetization. The two ig-

neous units have very low NRM intensities in agreement with the observations from the cryogenic magnetometer. Both units show a consistent direction of magnetization with average inclination compatible with the inclination of a GAD of −55°, the present-day latitude of Brothers volcano. This consistent GAD inclination suggests a coherent young age for these rocks, most certainly during the current normal polarity Brunhes geomagnetic epoch. Thermal demagnetization experiments from these units show a complex pattern, suggesting irreversible transformation of magnetic minerals during heating to >400°C; this transformation is confirmed by changes in the magnetic susceptibilities measured with the Agico Kappabridge susceptibility meter before and after heating. In addition, IRM experiments suggest that these rocks contain minerals with large magnetic coercivities, such as titanohematite, in addition to titanomagnetite.

Physical properties measurements for Igneous Unit 1 (Alteration Type I) are consistent with the ranges expected for fresh unconsolidated dacitic volcaniclastics. In Igneous Units 2 and 3, more complex variations in physical properties associated with igneous unit and/or alteration type are observed. For example, magnetic susceptibility values are generally higher in intervals of Alteration Type II than Type III (Figure **F12**), which may be explained by the observed partial replacement of titanomagnetite by rutile and pyrite in the relatively more altered rocks of Alteration Type III. Downhole measurements also indicate an association between Alteration Type II and increases in natural gamma radiation (NGR) attributed to ^{40}K; however, this association could not be confirmed by NGR measurements in the laboratory due to the fragmented core material that was recovered. The relatively high ^{40}K NGR signal identified in a core from Alteration Type II (Section 376-U1528D-48R-1) is consistent with this observation.

The boundary between Igneous Units 2 and 3 is clearly defined by changes in grain density, bulk density, porosity, *P*-wave velocity, and thermal conductivity as well as by an increase in magnetic susceptibility associated with the concurrent transition from Alteration Type III to Type II. By contrast, boundaries between igneous subunits within Igneous Unit 2 are clearly defined by variations in physical properties. An interval of relatively lower bulk density and *P*-wave velocity and higher porosity is observed between ~145 and ~220 mbsf, but it is not associated with a defined igneous subunit or alteration type boundary. Instead, this interval corresponds to the depth at which H_2S gas was smelled during core splitting, and its boundaries correspond to a borehole temperature anomaly and increased fracture densities, vein thicknesses, and range of vein dip.

A series of downhole measurements was conducted and borehole fluid was sampled at the end of Hole U1528D coring operations. Three runs of the ETBS memory tool were completed in Hole U1258D. The first deployment, made prior to logging to help determine which logging tools could be deployed, measured an average temperature of 33°C at 357 mbsf. After we collected borehole fluid samples using the Kuster FTS tool at 279 and 313 mbsf, two other temperature measurements were made at these same depths, recording temperatures of 212°C and 165°C, respectively, with the latter affected by circulation of cold seawater in the borehole prior to the measurement.

A high-temperature flasked wireline logging string consisting of lithodensity, NGR, and logging head temperature tools was run to 332 mbsf in Hole U1528D. Variations in the total natural gamma ray measurements are mostly related to peaks in potassium, generally correlated to Alteration Type II, which is rich in illite. Overall, the downhole density log correlates well with bulk density measured on the core samples and shows different trends that are generally correlated with igneous units and subunits: (1) from 65 to 145 mbsf (Igneous Subunit 2a), density gradually decreases downhole; (2) from 145 to 250 mbsf, there is a sharp decrease in density (between 140 and 155 mbsf; Igneous Subunit 2b) followed by a gradual increase with depth (Igneous Subunit 2c); and (3) from 250 to 330 mbsf, the density is very variable (Igneous Unit 3). Downhole caliper measurements revealed three zones of washouts where the borehole diameter exceeded 33.0 cm and reached up to 43.2 cm (17 inches): 149–162, 195–210, and 297–324 mbsf. The median diameter was determined at 28.5 cm (11.2 inches), only slightly exceeding the drill bit diameter of 25.1 cm (9.875 inches). Two bridges were encountered on top (292 mbsf) and at the bottom (323 mbsf) of the deepest washout interval while lowering the logging tool string.

The three temperature profiles acquired during wireline logging suggest a convective temperature regime with small temperature increases at ~100 and 150 mbsf and larger increases at ~275 and 295 mbsf. A temperature reversal (i.e., a decrease in temperature with depth) was observed at ~250–260 mbsf. Over the 2.5 h of logging, the temperature increased by about 8°C in the isothermal zones and by 24.5°C between 270 and 310 mbsf, reaching 247°C. This increase suggests that the downhole temperatures had not yet reached equilibrium. The temperature anomalies at ~150 and ~295 mbsf are accompanied by increases in borehole diameter, peaks in potassium, the first instance of sulfur odor emanating from the cores, native sulfur observed in veins, high fracture density with varied fracture dips, crosscutting fractures, and increased vein density. These zones are interpreted to be structurally controlled permeable intervals.

A total of 3, 1, and 13 whole-round samples (3–16 cm long) were collected from Holes U1528A, U1528C, and U1528D, respectively, for microbiological analyses (Table **T1**). Lithologies sampled represented the various igneous units recovered. Samples were processed for shore-based DNA and RNA analyses, cell and viral counting, and viral and microbial activity measurements. All samples were analyzed onboard for adenosine triphosphate (ATP) concentration; two samples gave positive values. The other samples contained compounds that inhibited the enzyme luciferase used for the ATP test. Nutrient addition bioassays with inorganic nitrogen and phosphorus, or organic carbon, were initiated to determine the nutritional constraints on biomass in this environment. PFMD was used for contamination testing. PFMD was usually detected on the outside of uncleaned cores and, on rare occasions, was above detection levels on the cleaned outside of cores. However, it was usually below detection on the inside of cores, indicating that penetration of drilling fluid to the interior of whole-round drill cores (where we collected samples) is unlikely.

Site U1529

Background and objectives

Site U1529 (proposed Site WC-1A) is located on the western side of the caldera floor of Brothers volcano at a water depth of 1765 m (Figure **F6**). The primary objective for this site was to drill a second hole (the first was at Site U1527) into the margin of the upflow zone of a hydrothermal system dominated by modified seawater-derived fluids. This site was planned to penetrate deeper into the hydrothermal system and obtain a record of the recent eruptive history in the caldera.

Operations

We conducted operations in two holes at Site U1529. Hole U1529A is located at 34°52.5161′S, 179°3.5139′E at a water depth of

1735.0 m. We used the RCB system to core from the seafloor to 12.0 mbsf, with poor recovery of 1.86 m (16%). The downhole conditions encountered in Hole U1529A were extremely difficult because of the unconsolidated volcaniclastic material, which caused high torque and tight hole conditions that ended drilling of this hole. In Hole U1529B, located at 34°52.5217′S, 179°3.5207′E at a water depth of 1733.0 m, RCB coring under similar difficult hole conditions penetrated to only 34.4 mbsf, with very poor recovery of 0.6 m (1.7%). After observing a tight hole, we attempted to work the drill string back to ~15 mbsf but lost circulation because the bit and jets were plugged off with volcaniclastic material. This loss of circulation resulted in abandonment of Hole U1529B. An 8.2 m long ghost core was recovered from the core barrel that was in place while working the drill string out of the hole. A total of 44.0 h, or 1.8 days, were recorded while at Site U1529.

Principal results

A single igneous unit was recovered in Hole U1529A (0–2.52 mbsf) and in Hole U1529B (0–24.82 mbsf). Igneous Unit 1 consists of decimeter-thick, alternating intervals of fresh, black plagioclase-pyroxene phyric dacite lavas and unconsolidated, black monomict lapilli tephra (Figure **F16**). The contacts between the lavas and the tephra were not recovered. The moderately vesicular (~10 vol%) lava was recovered as individual pieces 0.5–6 cm in length. The lava has a hypohyaline texture with groundmass rich in flow-aligned plagioclase microlites and shows fine fracture networks indicative of incipient breakup. The lapilli tephra consists of fine-ash- to medium-lapilli-sized angular to subangular fragments of dacite lavas, as well as fragments of plagioclase and pyroxene crystals. The finest grain size fraction contains 85 vol% of angular vitric ash, resembling the larger lapilli clasts and fragments of dacite lava recovered at Site U1527.

The ghost core from Hole U1529B, which contains material from anywhere between 0 and 34.4 mbsf, similarly consists of unconsolidated fresh, black volcanic lapilli-ash ranging in size from ash to medium lapilli. Maximum clast sizes are very large pebbles. Ash- and lapilli-sized clasts are subangular and angular with a vesicularity and mineral assemblage (plagioclase-clinopyroxene phenocrysts and glomerocrysts) consistent with the lapilli tephra, being a mixture of Igneous Unit 1 volcanic rocks.

The volcanic rocks of Igneous Unit 1 appear fresh to slightly altered. Alteration Type I is the only alteration type recognized at this site and occurs within the lapilli tephra and coarser fragments of dacitic lava. The alteration type is defined by the presence of minor smectite and iron oxyhydroxide replacing phenocrysts and groundmass and lining some vesicles. A few individual clasts in Igneous Unit 1 are more strongly altered and contain microcrystalline silica, iron oxyhydroxide, and a green clay mineral.

Unaltered to slightly altered clasts and lapilli from Igneous Unit 1 are typical dacites, with SiO_2 ranging from 62.3–65.4 wt% and $Na_2O + K_2O$ varying from 6.61–7.07 wt%. These dacites are similar in major element composition to fresh dacites from Site U1527 and consistent with the small compositional range previously reported for dacites at Brothers volcano (e.g., Haase et al., 2006; Wright and Gamble, 1999; Timm et al., 2012).

The uppermost sample (0.06 mbsf) from Hole U1529A and two samples from the ghost core have lower values of total carbon (<200 µg/g) compared to the other five samples from this hole, for which total carbon ranges from 221 to 344 µg/g. Total sulfur concentrations are less than 220 µg/g, consistent with total sulfur abundances previously reported from Brothers volcano. Total nitrogen and total inorganic carbon are below the limit of detection in all Site U1529 samples.

At Site U1529, no meaningful structural measurements could be made because no pieces of oriented core were recovered. Some pieces of dacite have a network of microfractures, but there are no faults or alteration veins present. In both Holes U1529A and U1529B, the main structure observed is a shape-preferred orientation defined macroscopically by vesicles and microscopically by vesicles, phenocrysts, and microlites.

No paleomagnetic measurements were performed on the samples from Site U1529 because of the absence of any oriented core pieces. Moreover, the low recovery and the fragmented nature of the clasts and volcaniclastic sediments made the cores mostly unsuitable for continuous physical properties measurements on whole-round and section-half cores. However, NGR measurements for Hole U1529A recorded values of ~13 cps (1.9 mbsf), and section-half multisensor logger point data indicated magnetic susceptibilities as high as ~2250×10^{-5} IU (15.14 mbsf).

A total of five discrete samples from Hole U1529A and three samples from Hole U1529B, including cut clasts and volcaniclastics, were analyzed for moisture and density. Bulk density values range from 1.92 to 2.37 g/cm^3, whereas grain density has a range of 2.43 to 2.50 g/cm^3. Porosity varies from 6–38 vol% and is inversely correlated with bulk density. Three measurements of *P*-wave velocity made in the *x*-direction on coherent clasts in section halves of Hole U1529A vary from ~3500 to 4500 m/s. No thermal conductivity measurements were made because of the limited recovery and fragmented nature of the material.

No samples were collected from Site U1529 for microbiological analyses because of the nature of the material recovered.

Site U1530

Background and objectives

Site U1530 (proposed Site NWC-3A) is located on a narrow bench on the NW Caldera site of Brothers volcano at a water depth of 1595 m (Figure **F6**). The primary objective at this site was to drill through the lower part of the Type I hydrothermal system. Site U1530 is located ~400 m east of Site U1527 on a ~30 m long by ~10 m wide bench toward the upper part of the NW Caldera wall. It is situated structurally above a known prominent metal-rich stockwork zone. The operations plan at Site U1530 was to penetrate ~450 m through the upper stockwork and then into deeper portions of the inferred hydrothermal upflow zone and continue through a thicker stratigraphic section of lavas in the caldera, hoping to intersect the footwall of the original caldera. Intersection of the stockwork was expected to provide the best opportunity to investigate the transport of metals through the Brothers hydrothermal system.

Operations

Operations were conducted in one hole at Site U1530. Hole U1530A is located at 34°51.6588′S, 179°3.4572′E at a water depth of 1594.9 m. We used the RCB system to core from the seafloor to 453.1 mbsf and recovered 76.8 m (17%). We encountered optimum downhole conditions throughout coring. After successfully penetrating to target depth, we decided to terminate coring in Hole U1530A to take advantage of the good hole conditions for downhole measurements and fluid sampling. Hence, we released the bit in the bottom of the hole by deploying the rotary shifting tool.

Our downhole measurement plan for Hole U1530A consisted of running (1) the ETBS tool, (2) the Kuster FTS tool, (3) the triple combination logging tool string ("triple combo"—natural gamma

ray, porosity, and density sondes, including magnetic susceptibility, resistivity, caliper, and logging head temperature), (4) the Formation MicroScanner (FMS)-Sonic logging tool string, and (5) the Petrospec spool-in TCMT. After recording a temperature of 40°C at the bottom of the hole (stationary measurement time of 15 min) with the ETBS, we lowered the Kuster FTS tool on the core line to a depth of ~433 mbsf but did not recover a fluid sample because the valves failed to close completely. We then raised the end of drill string to a logging depth of 67.1 mbsf, lowered the triple combo tool string into the hole, and performed a calibration pass and a full logging run from the fill at 442 mbsf to the seafloor. This run was followed by two logging passes with the FMS-Sonic tool string from 442 mbsf to just below the end of the pipe at 51.8 mbsf. We then lowered the end of the drill string to 416.2 mbsf and obtained a borehole fluid sample with the Kuster FTS. Finally, the third-party TCMT was deployed on the wireline and, with the temperature-sensitive TCMT data logger kept inside the drill string, the two thermocouple joints were lowered 8 m past the end of the drill pipe and held at 447 mbsf for 10 min. This first test of the newly designed high-temperature TCMT recorded a temperature of 20°C. This test completed our operations at Site U1530. A total of 184.0 h, or 7.7 days, were spent at Site U1530.

Principal results

Five igneous units were identified at Site U1530 (Figure **F17**). Igneous Unit 1 (0–26.62 mbsf) consists of clast-supported polymict lapillistone with occasional blocks and bombs. Clasts are volcanic in origin and reside in a matrix of altered, smaller volcanic fragments and secondary minerals. Igneous Unit 2 (30.70–59.62 mbsf) consists of a sequence of altered tuffaceous mudstone, siltstone, and sandstone, with one subordinate horizon of polymict lapillistone, and is divided into five subunits (2a–2e), based on color, grain size, and internal structures. Igneous Unit 2 displays various sedimentary textures including normal and reverse grading as well as horizontal, wavy, lenticular, and inclined bedding, indicating transport, depositional, and soft-sediment deformation events. Igneous Unit 3 (59.62–64.40 mbsf) consists of altered plagioclase phyric lava with pseudomorphs after glomerocrystic plagioclase. Igneous Unit 4 (64.40–218.21 mbsf) is a sequence of highly altered volcaniclastic rocks with discernible monomict and polymict lapillistone and monomict lapilli-tuff in the upper half that consists of altered volcanic clasts in a fine-grained, completely altered matrix. Significantly pronounced alteration hinders detailed classification in the lower half of Unit 4. Igneous Unit 5 (222.70–448.68 mbsf) consists of highly altered volcanic rocks with five discrete horizons of less altered plagioclase phyric lava containing pseudomorphs after glomerocrystic plagioclase.

Despite the pervasive alteration, the volcanic and volcaniclastic rocks retain residual volcanic textures and original compositions of alteration-resistant elements and ratios (Ti, Zr, Ti/Zr), suggesting that the protolith was a typical Brothers dacite. Similar to volcaniclastic rocks of Igneous Unit 2 of Hole U1527C, Hole U1530A rocks appear to have the same systematically lower Ti/Zr value (~27) compared to volcanic rocks of Sites U1528 and U1529, where the Ti/Zr value is ~36. Although this disparity is small compared to the overall range observed in Kermadec arc lavas (i.e., Ti/Zr as high as 220), it points toward slight genetic variability among the Brothers dacitic magma series.

Five distinct alteration types were identified based on alteration mineral assemblage in core material recovered from Hole U1530A (Figure **F18**). All alteration types occur at various intervals downhole, overprinting each other, and therefore cannot be assigned to certain depth intervals.

Alteration Type I, classified as highly to intensely altered, has an alteration mineral assemblage of opal-CT, smectite, pyrite, anhydrite, sphalerite, and barite, with minor quartz, chlorite, and illite (Figure **F19A**). A network of anhydrite-barite veins with fine- to medium-grained sphalerite cuts blue-gray lapillistone. The clasts are variably altered/silicified, and the contacts between clasts and matrix are distinct. Anhydrite is most abundant in veins and only rarely infills vugs within clasts. In one sample, an acicular mineral, most likely natroalunite, is observed microscopically cutting anhydrite-pyrite-silica veins but was not detected by X-ray diffraction (XRD) analysis.

Alteration Type II, classified as intensely altered, has a characteristic green-gray color and an alteration mineral assemblage of quartz, illite, and chlorite, with variable amounts of anhydrite, pyrite, and smectite (Figure **F19B**). Alteration Type II is associated with three distinct lithologies throughout the hole: tuffaceous fine-grained sediments, coherent lava, and pyroclastic rocks. The abundance of individual alteration minerals varies with lithology. For example, pyrite is more abundant in fine-grained sediments compared to pyroclastic rocks. The fine-grained tuffaceous sediment interval (Igneous Unit 2) is frequently cut by coarse-grained vuggy anhydrite veins. The altered lava unit exhibits a vuggy texture, the vugs filled with quartz, anhydrite, and minor pyrite. Chlorite and illite are intergrown with microcrystalline quartz, forming a homogeneous matrix. The upper volcaniclastic interval (Igneous Unit 1) is characterized by subangular clasts that are visually distinguishable from matrix material. Clasts are rich in chlorite and illite relative to the silica- and pyrite-rich matrix. Plagioclase is completely pseudomorphed by chlorite, quartz, and occasionally smectite.

Alteration Type III, classified as intensely altered, is characterized by an alteration mineral assemblage of quartz and illite, with minor smectite, anhydrite, and chlorite. It is divided into two Subtypes IIIa and IIIb based on relative abundances of anhydrite (enriched in Subtype IIIa) and chlorite (enriched in Subtype IIIb), respectively. Alteration Subtype IIIa is white-gray and consists of well-defined pyroclastic texture with soft illite-rich clasts within a silica- and pyrite-rich matrix (Figure **F19C**). Alteration Subtype IIIb is blue-gray, and both matrix and clasts are intensely silicified (Figure **F19D**). Pyrite occurs as a minor phase disseminated throughout. Iron oxyhydroxide is likely derived from pyrite oxidization. Magnetite is an accessory phase and is frequently partially resorbed and overprinted by pyrite.

Alteration Type IV, classified as intensely altered, is light gray and has a mineral assemblage of pyrophyllite, quartz, illite, and smectite, with minor pyrite and rutile (Figure **F19E**). Clasts are poorly defined and strongly resorbed. Pyrophyllite is patchy and intergrown with illite and disseminated fine-grained anhydrite and likely represents the core of relict clasts. Quartz is intergrown with illite and forms discrete veins associated with subhedral pyrite. Common leucoxene and minor rutile form <0.1 mm grains and are variably overprinted by pyrite.

Alteration Type V exhibits a buff color and occurs as two distinct subtextures: fine-grained homogeneous material and coarse-grained equigranular material with a mottled texture (Figure **F19F**). Both subtextures exhibit the same alteration mineral assemblage of diaspore, quartz, pyrophyllite, smectite, and rutile, with minor illite, pyrite, and anhydrite. Iron oxyhydroxide staining is well developed throughout this alteration type, and pyrite is absent in some samples. Vugs are abundant and commonly infilled with chalcedony and

anhydrite, with the latter filling the core of the vug. Anhydrite occurs in two distinct generations, coarse euhedral grains that infill vugs and veins and a fine-grained subhedral to euhedral form intergrown within the matrix. Rutile occurs in traces, mantled or overprinted by pyrite.

Unlike Hole U1528D, most veins in Hole U1530A are sealed with anhydrite + sulfides + quartz with only a few vugs partly filled by drusy quartz or anhydrite that may record the latest fluid compositions and temperatures. All fluid inclusions are two-phase and homogenize to the liquid phase at 209° to 390°C, except for one (at 406 mbsf) that exhibits critical point behavior at 345°C. The highest homogenization temperatures are measured in Alteration Types V (key minerals: pyrophyllite + diaspore) and II (key minerals: illite + chlorite). By contrast, the lowest median temperature of 255°C was determined at 291 mbsf. The salinities of fluid inclusions plot into two separate regions: at or near seawater compositions and as a hypersaline brine at or along the NaCl saturation curve (Figure **F20**). Only Alteration Types II and V can be associated with hypersaline brines. The fluid inclusion data are consistent with three different fluids being responsible for the alteration assemblages: a pervasive fluid of modified-seawater composition that has been heated to ~390°C, a fluid that has condensed from NaCl vapor within the supercritical region, and a hypersaline brine with temperatures of 288° to 390°C (Figure **F20**).

Structures in Hole U1530A consist of volcanic fabrics, alteration veins, fractures, and sedimentary boundaries. Sedimentary boundaries, defined by changes in grain size and/or texture, are all subhorizontal (<10°). Volcanic fabrics are in two forms: within volcanic clasts or within coherent lava. In both forms, the fabric is defined by vesicles and plagioclase microlites. Volcanic fabrics within volcanic clasts can be weak to strong but do not share a common orientation across clasts. This type of fabric is observed in the top half of Hole U1530A in lapilli tuffs defining Igneous Units 1 and 4. Moderate to strong volcanic fabrics that occur over decimeters define Igneous Units 3 and 5, which consist of lavas. Volcanic fabrics within the lavas tend to be moderate to steep, with dips >45°.

Alteration veins occur throughout the hole and are typically filled with anhydrite, silica, and/or pyrite. Vein density is variable downhole, with the highest density related to the presence of network veins, typically filled with pyrite or silica. The largest abundance in network veins is at the very top of the hole, from 0 to 25 mbsf. Discrete veins are most abundant at ~70 and ~270 mbsf. These depths also correspond to a large range in vein dip (0°–90°), an increase in vein thickness and, at ~270 mbsf, a deviation in borehole temperature. These depth intervals are also related to changes in igneous rock type between sedimentary and lavas above lapilli tuffs at ~70 mbsf and a change from lapilli tuff to lava at ~270 mbsf. The presence of sedimentary and volcanic rocks, large range in vein dip and thickness, and a deviation in borehole temperature may indicate the presence of lateral flow zones related to permeability contrasts. Fractures are less abundant compared to veins but are more common than at any other site. Fractures have a large range in dip and are more frequent at ~55 and ~255 mbsf, coincident with zones of more abundant veins. Slickenlines were identified from ~190 to 290 mbsf and typically have steep rake and a normal sense of shear.

All hard rock samples from Site U1530 have been affected by various degrees of hydrothermal alteration. Altered volcaniclastic materials and lavas show strong geochemical changes for a large range of elements, with major loss of Mn, Ca, and Na (Figure **F21**). The observed downhole variations of major oxide and trace elements are much more pronounced at Site U1530 compared with Site U1527, including the extensive loss of Na_2O relative to unaltered dacites recovered at Sites U1527 and U1529. Other alkali elements, such as potassium (K_2O) and rubidium (Rb), as well as the alkaline-earth metals (Mg, Ca, Sr, and Ba), show both depletions and enrichments relative to fresh dacites. The strongest geochemical shifts in Hole U1530A occur between 189 and 191 mbsf, with a decrease in K_2O, Rb, Ba, Y, and Cu concentrations, which corresponds to the transition to Alteration Type V, (i.e., the first appearance of pyrophyllite and decreasing abundance of illite). Alteration Types IV and V in Igneous Unit 5 form two important end-members and display the strongest depletions in Mg, Ba, Sr, Fe, Cu, and Zn. The reverse pattern is seen in Alteration Type I in Igneous Unit 1, suggesting that some of the loss of elements observed at the bottom of the hole may be, in part, balanced by a gain of these elements in the upper part of the hole. Depletions in Ca are associated with higher Sr concentrations and the identification of anhydrite by XRD, suggesting that the abundance of Ca is mainly controlled by the occurrence of anhydrite. Principally hosted in barite, Ba at Site U1530 ranges from trace levels of ~20 µg/g in Alteration Types IV and V to very high abundances of ≤ 3.4 wt% in Alteration Type I. A pronounced correlation is observed between total S and Fe concentrations throughout Hole U1530A, suggesting that pyrite represents the primary host of sulfur in the rock (predominantly in Igneous Units 1, 2, and 4). Significant enrichments in Zn (≤5.2 wt%), Cu (≤1760 µg/g), As (≤660 µg/g), Pb (≤100 µg/g), and Mo (≤560 µg/g) were also recorded in pyrite-rich intervals, consistent with high-temperature hydrothermal fluid contributions.

Total carbon (TC) abundances in the majority of Hole U1530A samples are <200 µg/g and are overall lower than TC abundances at Sites U1527, U1528, and U1529. An average total sulfur (TS) concentration at Site U1530 of 5.1 wt% is similar to the 5.9 wt% average at Site U1528. In contrast to Site U1528, however, TS concentrations decrease with depth from ~11 wt% to ~3.5 wt% on average.

Headspace dissolved gases, including H_2, CO, CH_4, C_2H_6, CO_2, and H_2S, were analyzed from several intervals of the recovered cores in Hole U1530A. As reported at Sites U1527, U1528, and U1529, headspace dissolved C_2H_6 concentrations were below detection limit (<0.03 µM) for all depths of Hole U1530A. Five intervals with elevated H_2, CH_4, CO_2, and acid-volatile sulfide (AVS) concentrations were detected. Maximum pore-fluid AVS and ΣCO_2 concentrations of 1.6 and 37 mM, respectively, are similar in concentration to those previously determined by de Ronde et al. (2011) for actively venting chimneys of the NW Caldera vent field and may originate from fluids rich in magmatic volatiles.

A fluid sample was collected with the Kuster FTS tool at 435 mbsf. The in situ fluid temperature was estimated to be <38°C based on downhole temperature logging. The borehole fluid sample is slightly acidic relative to seawater, with a pH of 6.8, and is characterized by the same major and minor species composition (i.e., dissolved Na, K, Ca, Sr, Mg, Cl, Br, and SO_4) as drilling fluid (surface seawater) within analytical error. Dissolved ΣH_2S is below detection. The abundances of several metal species are highly elevated above seawater values and are likely derived from contamination by the steel bit and drill string or the Kuster FTS itself.

NRM of 81 archive-half sections from Hole U1530A was measured using the cryogenic superconducting rock magnetometer. The overprint magnetization from drilling and coring was reduced by using the inline AF demagnetizer. Detailed measurements of anisotropy of magnetic susceptibility (AMS), AF and thermal demagnetization, and IRM experiments on 65 discrete oriented samples were also conducted (four from Igneous Unit 1, five from

Igneous Unit 2, two from Igneous Unit 3, twenty-four from Igneous Unit 4, and thirty from Igneous Unit 5). Magnetic directions for discrete samples show relatively shallow inclinations compared with Sites U1527 and U1528. In particular, three samples from Igneous Unit 2 (Cores 376-U1530A-10R to 11R; 50–55 mbsf) show consistent positive inclinations, confirmed by corresponding pieces measured in the cryogenic magnetometer. The NRM intensities and magnetic susceptibilities also highlight relative differences between the various igneous units. For example, Igneous Unit 1 is characterized by low NRM intensities, low coercivities, and erratic thermal demagnetization curves. Igneous Units 2 and 4 are characterized by very low NRM intensities with complex AF and thermal demagnetization curves, but larger coercivities. Igneous Units 3 and 5 show low NRM intensities, low-to-medium magnetic coercivities, and relatively simple AF and thermal demagnetization curves, with a minor overprint from drilling. Igneous Units 1, 2, and 4 also show increases of NRM intensity after heating to temperatures >400°C, suggesting irreversible transformation of the original magnetic minerals during heating.

Variations of physical properties at Site U1530 show good correlations with defined igneous units and subunits but correlate less well with transitions in alteration types. Igneous Unit 1, which corresponds to Alteration Type I, contains the peak values for magnetic susceptibility and NGR at the site. NGR peaks are also recorded by downhole measurements with the hostile environment natural gamma ray sonde (HNGS) and are an order-of-magnitude higher than those recorded at the other Brothers drill sites, attributed to radioactive U isotopes in the sulfide and barite veins observed at this depth.

Transitions between and within igneous units and subunits are clearly defined by variations in bulk density, porosity, and *P*-wave velocity. These data do not show strong correlation with structural features such as fractures or alteration veins. Observed variations in magnetic susceptibility and thermal conductivity do not correspond clearly to the observed abundance or distribution of particular minerals, but there is a large increase in magnetic susceptibility from Igneous Unit 4 to 5.

Overall, physical properties data define two intervals of markedly different characteristics: ~30 to ~35 mbsf in Igneous Unit 2 and ~75 to ~85 mbsf in Igneous Unit 4. These intervals are characterized by high grain density, low bulk density, and high porosity. They also correspond to increased concentrations of Fe_2O_3, S, trace metals, and metalloids and are located directly beneath intervals characterized by increased fracture density and wide ranges in dip angles of alteration veins. These intervals may therefore be important for understanding the past fluid-rock interactions and flow pathways of the hydrothermal system at Site U1530.

Multiple borehole temperature measurements obtained over the downhole logging period indicate that the hole warmed from ~35° to 94°C at ~430 mbsf during the first 5 h after stopping circulation and then cooled to 37°C during the subsequent 10 h. The temperature profile shows a gradual increase in temperature with depth, indicative of a largely conductive-dominated regime in the borehole, and also displays a "concave up" shape suggestive of recharge into the formation. Thermal anomalies in the temperature profiles observed between 255 and 295 mbsf may indicate a permeable flow zone. This interval is also characterized by the highest number of veins with a large range in vein dip and a higher abundance of fractures, suggesting structural control for this permeable zone. Downhole caliper measurements show an overall comparatively large borehole diameter partially exceeding the measurable 43.2 cm (17 inches), with a minimum of 24.0 cm (9.5 inches) and a median of 41.1 cm (16.2 inches). Downhole natural gamma ray measurements revealed high uranium content between 23 and 35 mbsf, correlating well with high values measured on the recovered core and most likely related to barite that was identified by XRD analysis. High potassium values correspond to Alteration Types II and III, both of which contain abundant illite. Downhole density and porosity measurements are in good agreement with discrete core measurements. The interval between 70 and 85 mbsf in Igneous Unit 4 and Alteration Type IIIa has low bulk density and high porosity from both discrete and downhole measurements as well as low resistivity.

A total of 18 whole-round samples (5–11 cm long) were collected from Hole U1530A for microbiological analysis (Table **T1**). Samples were processed for shore-based DNA and RNA analyses, cell and viral counting, and viral and microbial activity measurements. PFMD was used for contamination testing and was usually detected on the outside of uncleaned cores and, on rare occasions, was above detection levels on the cleaned outside of cores. However, concentrations of PFMD in drilling fluid samples were much lower than the expected 500 ppb values. Based on the results, the decision was made to increase the PFMD tracer pumping rate by a factor of 10 at the next drill site (U1531) and to collect drilling fluid from every core.

Site U1531

Background and objectives

Site U1531 (proposed alternate Site LC-1A) is located on the saddle between the Lower and Upper Cones of Brothers volcano at 34°52.7767′S, 179°04.2241′E at a water depth of 1355 m (Figure **F6**). This site likely sits between the margins of the upflow zones of both the Upper and Lower Cones because there is no detectable magnetic low in this area. The Lower Cone hydrothermal vent field includes vents that discharge the most Fe- and Mg-rich fluids sampled at Brothers volcano to date, although there is no evidence for venting at the saddle. The main objective of Site U1531 was to drill and core to ~300 mbsf to sample the various volcanic cycles that comprise the Lower Cone as well as to intersect the upflow zone of metal-rich fluids.

Operations

We implemented operations in five holes at Site U1531. Holes U1531A, U1531B, and U1531E were drilled on the saddle stretching between the Lower and Upper Cone of Brothers volcano. Holes U1531C and U1531D were established on the summit of the Lower Cone. Hole U1531A is located at 34°52.7767′S, 179°4.2241′E at a water depth of 1354.9 m. In this hole, we conducted RCB coring from the seafloor to 15 mbsf, with poor recovery of 1.0 m (7%). Further advancement was impossible due to very poor hole conditions that led to a stuck drill string several times. In Hole U1531B, located at 34°52.7721′S, 179°4.2111′E at a water depth of 1351.9 m, RCB coring penetrated from the seafloor to 26 mbsf and recovered 4.0 m (15%). However, poor hole conditions in blocky/fragmented lava deposits prevented us from further deepening the hole. We then offset the vessel ~110 m northeastward to the summit of the Lower Cone to Hole U1531C at 34°52.7239′S, 179°4.2586′E at a water depth of 1306.9 m. Here, we RCB cored from the seafloor to 28.4 mbsf and recovered 2.3 m (8%), with tight hole conditions throughout coring. We thus abandoned Hole U1531C at 28.4 mbsf.

We then decided to deploy a reentry system with a short, 16 m long casing string to establish a stable hole for reaching deeper cor-

ing and logging objectives. We drilled in casing in Hole U1531D at 34°52.7228′S, 179°4.2606′E at a water depth of 1306.9 m at the summit of the Lower Cone. After the pilot bit drilled to the target depth of 19 mbsf, we released the reentry system from the drilling assembly (mud motor, underreamer, and drill bit), but we were unable to pull the drilling assembly clear of the casing string, as the underreamer arms did not completely retract. After several hours of attempting to free the reentry system, we started pulling the drill string and attached reentry system out of the hole and back to the vessel. While we were retrieving the casing-reentry system assembly, it unfortunately dropped off in sight of the moonpool, with our position above the bottom part of Lower Cone slope in its transition to the surrounding southeastern caldera floor.

We then moved back to the saddle between the Lower and Upper Cone and made up another drilling assembly to drill-in 16 m of casing in Hole U1531E, which is located at 34°52.7591′S, 179°4.2344′E at a water depth of 1355.0 m. We drilled-in the casing to 17.9 mbsf. We then conducted another test of the CDEX TDCS, which washed down (drilled without coring) to 17.9 mbsf to start coring in Hole U1531E. We could not advance any deeper, as the TDCS core barrel got stuck in the BHA and could not be retrieved. After the TDCS test, we RCB cored from 17.9 to 39.6 mbsf and recovered only 0.8 m (4%). At this point, the blower motor in the top drive failed. We decided not to repair it at this time due to our remaining scientific priorities and the approaching end of the expedition. Our final operation at Site U1531 consisted of a downhole temperature measurement with the ETBS memory tool. It recorded a maximum temperature of ~5°C at 20 mbsf. A total of 264.25 h, or 11.01 days, were spent at Site U1531.

Principal results

At Site U1531, one igneous unit was observed in Holes U1531A (0–1.14 mbsf), U1531B (0–21.97 mbsf), U1531C (0–23.75 mbsf), and U1531E (17.90–34.95 mbsf). Several cores were also recovered during hole cleaning ("ghost cores"; Cores 376-U1531E-2G to 4G). Igneous Unit 1 consists of unaltered to slightly altered plagioclase-pyroxene phyric dacite lava intercalated with unconsolidated ash, ash with lapilli, and lapilli tephra with ash. The moderately to highly vesicular dacite lava contains glomerocrysts and phenocrysts of plagioclase, ortho- and clinopyroxene, and Fe-Ti oxides in cryptocrystalline and hypocrystalline groundmass. Volcaniclastic material is mainly composed of unaltered vitric clasts and crystals, likely fragments of the dacite lava, and subordinate lithic components. The composition of the dacitic lavas and pyroclastic rocks from Site U1531 is typical for those of the youngest dacitic magmas erupted at Brothers volcano.

Based on the alteration mineral assemblage, one alteration type was identified at Site U1531. This Alteration Type I, classified as slightly altered, has an alteration mineral assemblage of smectite, iron oxyhydroxide, zeolite, pyrite, and rarely native sulfur. Alteration occurs as infilling and lining of vesicles as well as smectite replacing the glassy matrix.

Site U1531 has a structural record of volcanic eruptions and brittle deformation in all holes, yielding volcanic fabrics and fractures, respectively. Volcanic fabric intensity ranges from isotropic to strong, with the majority of intervals having a strong fabric and isotropic intervals being present in only three intervals. Fabrics are defined by elongated vesicles, plagioclase microlites, and to a lesser extent plagioclase phenocrysts and glomerocrysts. Vesicles have aspect ratios between 5 and 15. Hole U1531C is the only hole where fabric orientation was able to be measured with dips that range from moderate to steep. A few pieces in Hole U1531C have lineations defined by vesicles; all plunges are subparallel to the dip. Several core pieces from all holes have microfractures delineated by the growth of halite and gypsum in the core description laboratory after pieces were cut and dried. Discrete fractures are best preserved in Hole U1531C. Fractures range from shallow to steep and are typically marked by secondary minerals such as native sulfur or iron oxyhydroxide.

Unaltered to slightly altered lavas and tephra from Igneous Unit 1 represent typical dacites, with 62.3–65.0 wt% SiO_2 and Na_2O + K_2O contents ranging from 6.5–6.9 wt%. They are essentially similar in major and trace element composition to fresh dacites from Site U1529 and Hole U1527A (Igneous Unit 1 at those sites) and confirm the low compositional range previously reported for dacites at Brothers volcano. TC and sulfur concentrations are generally low (<250 and <300 µg/g, respectively) except in one sample with TC ≈ 1900 µg/g. Low total sulfur is consistent with previously reported data for dacitic glass in Brothers volcano, suggesting minimal influence of magmatic volatile input in the selected samples. However, the detection of relatively high concentrations of H_2 and acid-volatile sulfides in some intervals is consistent with discharging magmatic gases through the volcanic pile.

Only three core sections recovered from Site U1531 (i.e., Hole U1531C) had oriented pieces that could be measured in the cryogenic superconducting rock magnetometer. In addition, we selected five discrete samples from the working-half core sections for detailed measurements of AMS, AF, and thermal demagnetization, as well as IRM experiments. As expected from fresh dacites, NRM intensities are large. Magnetic directions from these samples have inclinations of ~–60°, suggesting a very young age for the primary magnetization component. The shape of the thermal demagnetization curve indicates that these samples contain pure magnetite and titanomagnetite with variable Ti content.

Physical properties measurements made on limited fragmented core recovered from Holes U1531A, U1531B, U1531C, and U1531E are consistent with the range of expected values for fresh dacitic lavas and tephras and are similar to those for fresh volcaniclastic material from Igneous Unit 1 at corresponding Sites U1527 to U1529. There is no clear difference in physical properties between material recovered from the summit of the Lower Cone and material recovered from the saddle, although interpretation is significantly limited by the low recovery, fragmented nature of the core, and limited number of oriented pieces.

The ETBS memory tool was deployed in Hole U1531E after about 24 h without circulation. It recorded a maximum temperature of 5.2°C at 20 mbsf, which is similar to the bottom seawater temperature.

One whole-round sample of moderately vesicular dacite lava was collected from Hole U1531C for microbiological analysis (Table **T1**). Sample aliquots were taken and preserved for shore-based DNA and RNA analyses, as well as prokaryotic and viral counting and activity measurements.

Preliminary scientific assessment

Expedition 376 was designed to provide the missing link (i.e., the third dimension) in our understanding of hydrothermal activity and mineral deposit formation at submarine arc volcanoes and the relationship between the discharge of magmatic fluids and the deep biosphere. The drill sites are located in areas considered to be hydrothermal upflow zones of geochemically distinct fluids that are

variably affected by magmatic volatile input, allowing us to directly address the consequences of magma degassing for metal transport to the seafloor and its effect on the functioning of microbial communities.

Expedition 376 completed five sites: two (Sites U1527 and U1530) within the NW Caldera seawater-dominated hydrothermal field, two (Sites U1528 and U1531) within the Upper and Lower Cone magmatic fluid-influenced hydrothermal fields, and one (Site U1529) in a magnetic low that delineates the W Caldera upflow zone. Although three of these sites were original primary sites and one (Site U1531) an original alternate site, Site U1530 was added during the expedition. This addition was needed because we encountered much thicker than expected loose, unconsolidated volcanic gravels, sands, and ash-like material that caused significant drilling difficulties early in the expedition, particularly for Site U1529 on the caldera floor, where Hole U1529B collapsed after only ~34 m of penetration. Hence, we sought and obtained approval to move an alternate caldera floor site to a new location on a bench on the NW Caldera wall (Site U1530) to minimize the likelihood of an overburden of unconsolidated volcaniclastic material.

Expedition 376 used rotary coring for most sites, but it also tested a prototype TDCS developed by Japanese Agency for Marine-Earth Science and Technology (JAMSTEC) in Holes U1528C and U1531E. Drilling was extremely successful, coring 1244 m and recovering 222.4 m of core—almost four times that of ODP Leg 158 (TAG hydrothermal field, Mid-Atlantic Ridge) (Herzig et al., 1998) and almost three times that of ODP Leg 193 (PACMANUS hydrothermal field, Eastern Manus Basin) (Barriga et al., 2007), representing the two previous endeavors with volcanic rock-hosted hydrothermal systems as drilling targets. Important to the success of Expedition 376 was the use of drill-in casing, which provided stability in the volcaniclastic deposits encountered in the upper part of some holes. Overall, the recovery averaged 18% for Expedition 376 (cf. 13% for ODP Leg 158 and 11% for ODP Leg 193), varying between 1% (U1527A) and 29% (U1528D), depending on the hole and lithologies encountered. Downhole measurements and borehole fluid sampling were conducted in Holes U1528D, U1530A, and U1531E. Given the low and variable recovery, the downhole logs from Sites U1528 and U1530 will be extremely helpful post-expedition in the interpretation of the rock record.

We expect that integration of the shipboard data with post-expedition shore-based analyses will result in significant progress toward addressing all four of the primary scientific objectives outlined in the Expedition 376 *Scientific Prospectus* (de Ronde et al., 2017), discussed below.

1. *Characterize the subvolcano, magma chamber–derived volatile phase in order to test model-based predictions that this is either a single-phase gas, or two-phase brine-vapor*

Hole U1528D penetrated 359.3 m through the center of the Upper Cone, beginning at the floor of a pit crater at its summit. Much of the core recovered from this hole smelled strongly of H_2S, and a mineral assemblage of illite + natroalunite + pyrophyllite + quartz + opal-CT + pyrite attests to acid-sulfate fluids derived from the disproportionation of magmatic gases, such as SO_2. Headspace gas analyses confirm relatively high levels of acid-volatile sulfide (as much as 20 mM near the bottom of the hole) and CO_2 (as much as 182 mM). The effects of strong acid on the host rock are also reflected in the geochemical data, which indicate extreme depletion of major elements, such as MgO, K_2O, and Na_2O. Furthermore, very acid (as low as pH 1.8), relatively hot (≤247°C) fluids collected by the Kuster FTS tool at depths of 160, 279, and 313 mbsf have compositions indicative of significant magmatic gas input. In addition, preliminary fluid inclusion results provide evidence for two dominant fluids having transgressed the Upper Cone: a hot (≤340°C) hydrothermal fluid of modified-seawater origin that appears to have undergone phase separation and a hot (≤360°C) hypersaline brine that may be transporting metals, given the observation of sulfide daughter crystals (together with halite) in some of the inclusions. The highest fluid inclusion homogenization temperatures are coincident with a high-temperature acidic alteration mineral assemblage of natroalunite + pyrophyllite + opal-CT, indicating ≥230°C (e.g., Reyes et al., 1990). These results clearly show brine-vapor conditions occurring within the Upper Cone site at Brothers volcano.

Hole U1531E penetrated 39.6 mbsf into the SW flank of the Lower Cone immediately east of the saddle between the lower flanks of the Upper and Lower Cones. Cores recovered from this hole are largely fresh lavas with only incipient low-temperature alteration, although native sulfur, coating the walls of small fractures, indicates limited interaction with magmatic volatiles and/or hydrothermal fluids. However, the observation of extensive diffuse venting of gassy, very acidic fluids emanating from and surrounding the summit of the Lower Cone (de Ronde et al., 2011) implies that magmatic degassing must be restricted to narrow upflow zones.

Further shore-based studies, including additional analyses of the borehole fluids and more extensive fluid inclusion studies, will help constrain the characteristics of the fluids within the Upper Cone hydrothermal system, allowing us to test models of the subsurface hydrologic regimes at Brothers volcano.

2. *Explore the subseafloor distribution of base and precious metals and metalloids as well as the reactions that have taken place along pathways to the seafloor*

Holes U1527C and U1530A are located in different parts of the NW Caldera hydrothermal vent field, the former on the western margin of the field atop the caldera rim and the latter on the caldera wall. Hole U1527C was drilled to 238 mbsf and penetrated variably altered volcaniclastic rocks and coherent lava of dacitic composition. The upper 185 m of Hole U1527C is dominated by a mineral assemblage of goethite + opal + mordenite, indicative of relatively low-temperature (<150°C) alteration. This assemblage is replaced downhole by chlorite + quartz + illite ± smectite, and the lower parts of the hole are characterized by an assemblage dominated by quartz + chlorite + pyrite ± illite. These assemblages indicate alteration temperatures >230°C. Pyrite is the predominant sulfide phase in Hole U1527C and is disseminated mainly in the deeper chlorite + illite-rich part of the core.

Hole U1530A was located proximal to a fault that exposes a stockwork zone, where several centimeter-thick, metal-rich veins form an anastomosing network within the altered host rock. Hole U1530A was drilled to 453 mbsf through a sequence of altered volcaniclastics with intercalated coherent lavas and an interval of altered volcanic sediments. The upper ~30 m of core has a mineral assemblage of opal-CT + smectite + chlorite + pyrite + barite + sphalerite, indicative of alteration temperatures of 100°–250°C. The occurrence of sphalerite and pyrite in close proximity to the sulfate minerals, along with the presence of a dense network of veins averaging 0.2 cm in thickness and enrichment in metals and metalloids (Zn, As, Cu, Mo, Se, and Pb), is consistent with the proximity of the hole to the exposed stockwork zone.

This assemblage is replaced downhole by quartz + illite + chlorite + anhydrite, pointing to alteration temperatures <275°C. More

acid (pH < 4) and hotter (250°–300°C) fluids are implied even further downhole with the appearance of pyrophyllite below ~190 mbsf, followed by a final assemblage of diaspore + quartz + pyrophyllite + rutile ± zunyite below ~225 mbsf. Two-phase fluid inclusions (with and without daughter halite crystals) associated with the pyrophyllite- and diaspore-rich alteration assemblages have homogenization temperatures of ~350°C to 390°C. Other inclusions are complex and contain various daughter minerals, including halite, sulfates, and other anisotropic minerals, with homogenization temperatures >320°C. Combined, the fluid inclusions are indicative of hypersaline brines like those seen in fluid inclusions at Upper Cone Site U1528. Pyrite is the main proxy for metals in the borehole and is distributed throughout the hole, though more so in the chlorite + illite-rich zones. The loss of K, Ba, Y, and Cu below ~190 mbsf and an increase in the magnitude of depletion below ~225 mbsf, corresponding to the appearance of pyrophyllite and diaspore, are also consistent with a downhole decrease in pH and increase in temperature (above ~250°C) of fluid-rock reaction. Later incursion and mixing of seawater and hydrothermal fluid that overprints earlier mineral assemblages resulting from reaction with more acidic fluids is reflected in the increased abundances of smectite, chlorite, and anhydrite in a later alteration event.

The large variations observed in the alteration mineral assemblages encountered at Sites U1527, U1528, and U1530 clearly attest to complex but distinct paragenetic sequences at both the NW Caldera and the Upper Cone hydrothermal fields. Interestingly, it appears that the currently seawater-dominated NW Caldera hydrothermal field may have undergone an earlier phase of reactions with acid-sulfate fluids, resulting in alteration assemblages resembling those observed in the Upper Cone. Further mineralogical, geochemical, and fluid inclusion shore-based studies will elucidate the reactions that take place along pathways to the seafloor as well as the distribution, transport, and fate of metals and metalloids within the hydrothermal systems of Brothers volcano.

3. *Quantify the mechanisms and extent of fluid-rock interaction, the consequences for mass transfer of metals and metalloids into the ocean, and the role of magmatically derived carbon and sulfur species in mediating these fluxes*

Fluid-rock reactions at Sites U1527, U1528, and U1530 have occurred under a range of conditions (i.e., temperature, pH, Eh, etc.), and hence quantifying mass transfer of elements into the ocean is difficult, particularly given the heterogeneous lithologies encountered at all sites. The mineral assemblage of quartz + illite + chlorite + anhydrite ± smectite in Holes U1527C and U1530A in the NW Caldera hydrothermal vent field clearly points to a complex exchange between a hydrothermal fluid of modified-seawater composition and the dacitic protolith, indicated by Mg and S enrichment as well as both depletion and enrichment in K and Rb, in addition to relatively subtle changes in other major elements (normalized to the composition of unaltered dacitic lava from Site U1527). These element exchanges are distinct from those observed in the mineral assemblage indicative of interaction with hot acidic fluids (i.e., denoted by the assemblage of pyrophyllite + diaspore + quartz + illite ± rutile) seen deeper in Hole U1530A, which show strong depletions in K, Mg, Ca, Na, and Fe contents.

In contrast, at the Upper Cone site, alteration and elemental exchange are affected by magmatic volatile-driven reactions. Magmatic gases (high concentrations of H_2, ΣCO_2, and dissolved H_2S were measured in headspace gas analyses) condense in seawater with disproportionation reactions involving SO_2 and H_2S buffering the hydrothermal fluid compositions, resulting in rocks of the Upper Cone being strongly leached by acids. The leaching leads to depletion of many major elements, including Mg, K, Rb, Na, Fe, Ca, and Mn, and enrichment in S (note that the loss of Fe may be related to interaction with a later-stage, sulfate-rich fluid). Fluid inclusion data from depth in Hole U1528D suggest that most metals are likely still at depth, given the highly saline (33 wt% equiv. NaCl) brines, with noticeable sulfide daughter minerals included. Active venting at the Upper and Lower Cone sites is testament to the flux of CO_2, sulfur, and iron in particular into the overlying water column (de Ronde et al., 2011).

Shore-based analyses will focus on more detailed geochemical, isotopic, and fluid inclusion studies to decipher the conditions of alteration, the sources of elements, and the elemental exchanges that accompany fluid-rock reactions.

4. *Assess the diversity, extent, and metabolic pathways of microbial life in an extreme, metal-toxic, and acidic volcanic environment*

The overarching objectives for microbiological studies for Expedition 376 focus on determining the biomass, activity, and community structure of subsurface microbial and viral communities using an array of molecular microbiological applications. Whole-round samples collected for microbiological studies were subsampled for shore-based analyses to explore the limits of microbial life and characterize the microbial diversity (including Bacteria, Archaea, and viruses) using cultivation-based and cultivation-independent molecular biological approaches.

Relatively few shipboard analyses were performed because most measurements require postexpedition studies in shore-based laboratories. First, detection of ATP was attempted on board to identify signs of bacterial life in the rock samples. However, detection was not successful in most cases due to denaturation of the luciferase enzyme by compounds found within the retrieved material. Second, tracers were pumped into the drill string prior and during core recovery. Systematic sampling of the cored material and drilling fluids indicated that the interiors of the whole-round samples for microbiology are suitable for shore-based analyses.

Postexpedition analyses will include an array of techniques: (1) total cell counts to quantify microbial biomass, (2) DNA analysis of small-subunit (SSU) ribosomal gene amplicon sequencing to address community structure, (3) metagenomics analysis to reconstruct the metabolic potential and identify entire genomes from microbial populations in the samples, (4) RNA determination using metatranscriptomics to establish potential community activity (i.e., the genes that are most highly expressed in a given microbial environment), (5) characterization of the viral diversity using polymerase chain reaction and metagenomic approaches to identify the role of viruses in the ecosystem, (6) metabolic activity measurements of microbial communities using stable isotope-labeled or radioactive isotope-labeled tracers to identify what kinds of major energy and carbon metabolisms are present, and (7) enrichment of specific groups of organisms to identify the unique physiological properties of the organisms.

Operations

Auckland port call

Expedition 376 started with the first line ashore at the Freyberg Wharf B in Auckland, New Zealand, at 0652 h on 5 May 2018, marking the end of Expedition 375 (Hikurangi Subduction Margin). Activities on the first day of port call included boarding the Expedi-

tion 376 Co-Chief Scientists, *JOIDES Resolution* Science Operator (JRSO) staff, and Center for Deep Earth Exploration (CDEX) engineering staff. The JRSO staff conducted the crossover with their Expedition 375 counterparts. Initial loading of incoming freight began while Expedition 375 core and sample shipments were offloaded.

On 6 May, Expedition 376 (Brothers Arc Flux) scientists boarded the vessel, moved their luggage into their cabins, received an introduction regarding information technology, were given an initial safety orientation, and then were introduced to life on board and the science laboratories. Loading and discharge of freight continued throughout the day. The freight activity included loading 83 joints of casing (10.75 inch and 13.375 inch), 40 joints of 5.5 inch drill pipe, and 88.5 metric tons of sepiolite.

On 7 May, the scientists and JRSO technical staff were introduced to each other, and the Co-Chief Scientists initiated the expedition with a presentation on the expedition science objectives. This presentation was followed by a second talk addressing the science work plan presented by the IODP Expedition Project Manager. In the afternoon, the Captain introduced key staff to the science party and gave an orientation on ship safety. All science groups then started learning their onboard laboratory tasks, including setting up applicable instruments, assisted by JRSO staff.

On 8 May, all loading of supplies and hardware as well as public relations activities were completed. In the evening, the ship shifted to Wynyard Wharf for fueling, with the first line ashore at 1930 h. Fueling was completed at 0400 h on 9 May.

Transit to Site U1527

At 0758 h on 9 May 2018, the pilot arrived on board, and the vessel departed Wynyard Wharf with the last line away at 0821 h. Our departure was assisted by one harbor tug, and we thereafter proceeded to the pilot station, where the pilot departed the vessel at 0924 h. We then began our transit through the Hauraki Gulf to Site U1527 at Brothers volcano. In the afternoon of 9 May, the Captain held the first fire and safety drill. During the transit, the Co-Chief Scientists met with key members of the IODP JRSO staff and ship's crew to review the coring and logging plan for the expedition.

Site U1527

The original plan for Site U1527 (proposed Site NWC-1A) was to drill two holes. The first, a pilot hole, was designated to core to ~50 m with the RCB system. The second hole was to drill-in a reentry system to a depth determined based on the pilot hole. The reentry system was supposed to allow for 405 m of penetration at Site U1527. Actual operations proved different from the plan, leading to drilling of three holes. Hole U1527A was RCB cored to 101.4 mbsf. Hole U1527B was RCB drilled to 105.5 mbsf, with 95.5 m long casing installed, but could not be reentered due to the reentry system being inadvertently retracted. Hole U1527C was cased to 95.5 mbsf and reentered with continuous RCB coring from 99 to 238 mbsf. All cores, penetration depths, and core recovery are displayed in Table **T2**.

Hole U1527A

After completion of the 24 h transit from Auckland (246 nmi at 10.6 kt), we arrived at Site U1527 at 0800 h on 10 May 2018. We picked up a new RCB coring bit with a mechanical bit release, assembled the RCB BHA, verified the correct space-out of the core barrel, and lowered it to the seafloor. We deployed nonmagnetic core barrels throughout coring at Site U1527. The subsea camera system, along with the advanced piston corer temperature tool (APCT-3) temperature shoe (for recording a water column temperature profile), was lowered to the seafloor to conduct a survey, and the seafloor site marker left in 2017 by a remotely operated vehicle (ROV) was quickly located. After tagging six potential hole locations to verify the water depth, the subsea camera system was retrieved and the acoustic beacon deployed. We then spudded Hole U1527A at a water depth of 1464.2 m at 2240 h on 10 May. Tracer material PFMD was pumped continuously while drilling. Maximum downhole temperatures were recorded by temperature strips contained in a housing tool attached to the RCB core barrel head.

Cores 376-U1527A-1R to 15R penetrated the seafloor to a final depth of 101.4 mbsf, with extremely poor recovery of only 1.27 m (1.3%) in unconsolidated volcanic deposits. The change to half-length advance (4.8 m) RCB coring from Cores 7R to 15R did not improve the recovery, with all but one core barrel recovered being empty. Coring was terminated when we determined that the hole conditions were worsening, leading to the decision that ~100 m of casing was all that could likely be installed and would be sufficient to prevent the hole from collapsing. A total of 51.3 h, or 2.1 days, were spent in Hole U1527A.

Hole U1527B

After completing Hole U1527A, the ship was offset 20 m east, and we started assembling a reentry system for installation in Hole U1527B to facilitate the deep coring and logging objectives at this site. We assembled a 95.5 m long, 10.75 inch casing string and a BHA consisting of a 9.875 inch tricone drill bit, an underreamer (set to 12.75 inch), a mud motor, two stands of drill collars, and 23 m of drill pipe. The preassembled running stand with the HRT (casing running tool) was lowered to the moonpool and connected to the casing string. The reentry funnel was picked up, installed, and welded to the top casing joint, together with the hard rock landing frame.

At 1000 h on 13 May 2018, we opened the moonpool and started lowering the 95.5 m long casing string and drilling assembly to the seafloor. After deploying the subsea camera system at 1530 h, we spudded Hole U1527B at 1715 h at a water depth of 1464.2 m. After drilling-in the casing to ~92 mbsf, drilling slowed to a stop with high standpipe pressures. We then worked the reentry system and eventually landed it on the seafloor, completing drilling-in the casing when the bit reached 105.5 mbsf at 0030 h on 15 May. The HRT was activated to release the drill string from the casing. After recovering the subsea camera system and pulling the drill string back to the ship, we found the reentry system and casing were still attached to the drill string because the underreamer arms had not retracted. The reentry system was landed back in the moonpool, and the reentry funnel and hard rock landing frame were removed. After working the drill string, the underreamer was finally drawn up into the casing, and the HRT BHA was disassembled. When the end of the drill string cleared the rig floor at 1530 h on 15 May, we discovered that the 9.875 inch tricone bit was missing from the bit sub, which was damaged beyond repair. After examining the damaged components and the rig instrumentation data, we determined that the bit most likely failed at a depth of ~92 m. In total, 76.3 h, or 3.2 days, were spent in Hole U1527B.

Hole U1527C

We then offset the vessel 20 m south of Hole U1527B as we started making up a new reentry system for installation in Hole U1527C, utilizing the 95.5 m of casing already landed in the moonpool. A new 9.875 inch tricone bit and underreamer (set to 12.75

inch) were installed in the drilling assembly, which was shortened by ~5 m. The remainder of the BHA—two stands of drill collars and 23 m of drill pipe—were assembled, and the HRT stand was attached to the top of the casing string. The drilling assembly was lowered through the moonpool and bolted to the casing string. The reentry funnel was then reassembled in the moonpool. The assembled reentry funnel and the hard rock landing frame were welded to the casing.

At 0615 h on 16 May 2018, the reentry system and 95.5 m long casing string were lowered through the open moonpool doors to the seafloor. The subsea camera system was deployed at 0945 h to observe the reentry funnel while drilling-in the casing. Hole U1527C was spudded at 1130 h on 16 May. Drilling was completed at 0045 h on 17 May when the bit reached 99.9 mbsf. The HRT was activated through deployment of a go-devil tool, which freed the drill string from the casing. The drill string was raised so that the HRT was visible above the reentry funnel. After the underreamer was verified to have entered the casing, the remainder of the hole was displaced with heavy mud. The drill string was pulled out of the hole, and the bit reached the rig floor at 1150 h on 17 May. The BHA was disassembled, and the mud motor and underreamer were flushed with freshwater.

An RCB BHA was made up, including a new RCB bit, and at 1300 h, the drill string was lowered to the seafloor. We deployed the subsea camera system, located the reentry funnel immediately, and reentered Hole U1527C at 2014 h on 17 May after only 14 min of maneuvering. Upon recovery of the subsea camera system, the bit was washed down (i.e., drilling without coring) to 99.9 mbsf, and 30 barrels of mud sweep were pumped. We dropped a core barrel and began RCB coring from 99.9 mbsf. Cores 376-U1527C-2R to 20R penetrated to 238.0 mbsf and recovered 25.9 m of core (19%). The first nine of these cores took only 10 min each to cut but had no to extremely poor recovery (0 to 0.54 m), retrieving pebbles from unconsolidated volcanic deposits. While cutting Core 11R, we encountered a substantial formation change at ~187 mbsf, and core recovery improved to 29%. After Core 11R, we switched to half-length advances (4.8 m) and continued through Core 20R, recovering 54% on average. The change in formation was reflected in the lithology, intersecting a consolidated volcaniclastic rock. Regular mud sweeps were required to keep the hole clean, and a total of 425 barrels of high-viscosity mud were pumped during the coring.

While pulling up to make a connection after cutting Core 376-U1527C-20R at 0700 h on 19 May, we experienced high torque with the bit at 234 mbsf. Although circulation and rotation were maintained, we had problems picking up the drill string. After working the stuck pipe for 13.75 h, we were unable to work it past 125 mbsf (30 m below the end of the casing string). The decision was made to release the bit in the hope that we could then pull the drill string clear of the hole. We offset the vessel ~75 m to access a drill pipe connection at the rig floor to retrieve Core 20R and to release the bit in an attempt to free the drill string. The vessel was offset back to its original location while tension was maintained on the drill string and attempts to free the stuck pipe continued. Eventually, the drill string cleared the seafloor at 0155 h on 20 May, but overpull was observed at 0530 h. The reentry system was stuck to the drill string. The reentry system was secured in the moonpool, and the hard rock landing frame was removed from the system. Upon removal of the reentry funnel, we broke the flange connection and cleaned out cuttings made of lapilli-sized tephra that clogged the HRT latch sleeve and upper casing sub. The cuttings were collected and curated for sampling. After working the drill string up and down, it was freed from the reentry system and pulled back to the rig floor. The bit cleared the rig floor at 1725 h on 20 May, ending Hole U1527C. The total time spent in Hole U1527C was 122.0 h, or 5.1 days. While disassembling the remainder of the reentry system, including eight joints of 10.75 inch casing, the vessel moved to Site U1528 about 1 nmi away using the dynamic positioning system.

Site U1528

Our highest priority, Site U1528 (proposed Site UC-1A), consisted of four holes. The original plan was made for a two-hole operation: a pilot hole cored to ~50 m with the RCB system, followed by installation of a reentry system in a hole to a depth determined by lithological conditions encountered in the pilot hole. Penetration to a depth of 800 mbsf at Site U1528 was envisioned. All operations at Site U1528 were challenged by the fact that the space to operate was restricted to a small flat area of only ~25 m in diameter at the bottom of a steep-walled pit crater at the summit of the Upper Cone. Thus, we relied heavily on the subsea sonar system attached to the vibration isolated television (VIT) frame (i.e., the subsea camera system) throughout operations at Site U1528 for conducting seafloor surveys, drill-in casings, and reentries.

First, Hole U1528A was cored with the RCB as a pilot hole to a depth of 84.4 mbsf. Coring was terminated when we determined that the hole conditions were worsening and would likely result in a stuck drill string. Hole U1528B was drilled to 25.6 mbsf to install 24.3 m of casing but could not be reentered because the reentry system was tilted. Hole U1528C saw the very first offshore test of the CDEX TDCS, which drilled down to 22 mbsf and cored to a final depth of 53.5 mbsf. At that depth, the reduction gear section of the coring system failed, and the hole had to be terminated. In Hole U1528D, we drilled in a reentry system to 61.3 mbsf and installed 59.4 m of casing. Upon reentry, Hole U1528D was then RCB cored to 359.3 mbsf.

After completing 40 h and 10 min of coring with the RCB bit, coring was halted for borehole fluid sampling, temperature measurements, and logging. We ran our in-house ETBS tool three times to record downhole temperatures. Deployment of the ETBS alternated with three deployments of the Kuster FTS tool using two different devices: a primary 1000 mL and a spare 600 mL tool. Two runs with the latter tool recovered borehole fluid samples. The first Kuster FTS deployment using the primary tool was unsuccessful, as the tool failed in the hole and the vast majority of it was not retrieved. Downhole wireline logging was implemented after the second ETBS and Kuster FTS deployments. Given that the ETBS measured a maximum temperature of 212°C, we assembled the flasked HTTC wireline logging string consisting of the lithodensity, natural gamma ray, and logging head temperature tools. After two successful logging passes between the seafloor and fill at 332 mbsf, we deployed a drill bit to clean out Hole U1528D from 326 to 356 mbsf, the depth of the top of the Kuster FTS tool that was still in the bottom of the hole. To ensure that we could resume coring, we then deployed a milling bit and two boot-type junk baskets to remove the lost Kuster FTS tool in the bottom of the hole. The milling bit drilled down to the bottom of the hole at 359 mbsf, but the junk baskets did not retrieve any remnants of the Kuster FTS tool. We then deployed a reverse-circulation junk basket tool with twin boot-type baskets for another attempt at clearing the hole so we could continue coring. We worked the tool down to 359 mbsf and circulated high-viscosity mud sweeps. However, when the end of the drill

string arrived back on the rig floor, we discovered that the lowermost 172.8 m of the drill string was missing. The loss of part of the drill string ended any further attempt to resume coring in Hole U1528D.

After completion of coring at Site U1531, we returned to Hole U1528D 23 days later and successfully deployed the ETBS tool, Kuster FTS tool, and Petrospec spool-in TCMT. In addition, we also pulled the failed reentry system of Hole U1528B back to the surface at the very end of the Site U1528 operations. A total of 616.8 h, or 25.7 days, were recorded while at Site U1528.

Cores, penetration depths, and core recovery are listed in Table **T2**.

Hole U1528A

After pulling out of Hole U1527C at 1725 h on 20 May 2018, the vessel was moved ~1.1 nmi to Site U1528 (proposed Site UC-1A) in dynamic positioning (DP) mode. Once we were positioned over the site, we made up an RCB BHA for coring in Hole U1528A. While we were running the RCB BHA to the seafloor, we began a camera and sonar survey of the seafloor to identify four possible hole locations in the narrow confines of the Upper Cone pit crater, tagging the seafloor at each location to verify the water depth (1228.4 m).

After retrieving the subsea camera and sonar system (along with the APCT-3 temperature shoe that recorded temperatures throughout the water column) and reassembling the rig floor, we picked up the top drive, dropped a core barrel, and spudded Hole U1528A at 0825 h on 21 May. Cores 376-U1528A-1R to 15R penetrated from the seafloor to a final total depth of 84.4 mbsf (reached at 1430 h on 22 May) and recovered 22.2 m (26%). We switched to half-length advances (4.8 m) after Core 6R. We pumped high-viscosity mud sweeps during the coring to keep the hole clean, adding up to a total of 670 barrels of high-viscosity mud. A substantial change to a hard formation was observed at 12.7 mbsf. Once Core 15R was cut, we had to work a stuck drill string that was finally freed after 3 h. While we were pulling out of the hole, we had to work through poor hole conditions with high torque from 83 to 66 mbsf, likely due to unconsolidated volcanic debris from the uppermost ~13 m of the hole. The drill string finally cleared the seafloor at 1850 h on 22 May. We were finally able to retrieve Core 15R at 1945 h, ending Hole U1528A. All cores, penetration depths, core recovery, and time recovered on deck are displayed in Table **T2**. The time spent in Hole U1528A was 50.2 h, or 2.1 days.

Hole U1528B

After the drill string cleared the seafloor from Hole U1528A, we offset the vessel 10 m south to the surveyed location of Hole U1528B. Our initial objective for this hole was to determine the length of casing needed to stabilize the uppermost unconsolidated formation to enable deeper coring. At 2040 h on 22 May 2018, we started RCB drilling without coring, using a center bit in Hole U1528B. After reaching 13 mbsf and verifying the hard formation encountered in Hole U1528A, the drill string was pulled back to the surface, clearing the seafloor at 2100 h.

Once the drill bit returned to the rig floor, we started casing operations for Hole U1528B. After assembling 24.3 m of 10.75 inch casing, we lowered it to the moonpool and latched it to the mud skirt. We then made up the casing drilling stinger with a BHA consisting of an 8 inch mud motor, an underreamer set to 12.75 inch, and a 9.875 inch tricone drill bit, to drill-in the reentry system. Following a successful test of the mud motor and underreamer in the moonpool, the drilling assembly was run inside the casing and attached to the casing flange on the mud skirt with the HRT. After assembling the reentry funnel and welding it to the casing hanger, we shut down operations at 1500 h on 23 May due to inclement weather and spent the next 20 h waiting for the weather to improve enough so that we could safely deploy the reentry system, as well as precisely position Hole U1528B.

At 1100 h on 24 May, we picked up the reentry system and lowered it to the seafloor. With rough seas, it was very difficult to position the vessel over the intended coordinates. After reaching 13 mbsf, the casing was drilled-in to 25.6 mbsf and the drilling assembly released from the casing using the go-devil. Drilling-in the casing had caused disturbance of the seafloor and visibility was very poor, but the HRT inside the throat of the reentry funnel was visible. We had trouble extracting our drilling assembly from the reentry system. After working the drill string with varying pump strokes for several hours, we finally managed to retract it from the reentry system. We pulled the drill string out of the reentry system with the drilling assembly sliding through the casing with drag, clearing the top of the reentry funnel at 2330 h on 24 May. The subsea camera system was retrieved, and the inner drill pipe sleeve was removed so that the camera system could be deployed over the HRT to examine the reentry funnel and confirm its landing position. Visibility remained poor, but the very top of the reentry system was observed, although the seafloor was not visible. The top of the funnel was observed at 1224.7 m water depth, which seemed to verify that it was in the correct position. We then recovered the subsea camera system and pulled the drill string out of Hole U1528B.

Once the drilling assembly had reached the moonpool, the mud motor and underreamer were flushed with freshwater. The bit returned to the rig floor at 0450 h on 25 May. The return of the bit to the rig floor essentially ended operations in Hole U1528B, as two separate attempts at trying to reenter using both the TDCS (see Hole U1528C) and an RCB system failed because the reentry system had been damaged while landing the casing too close to the crater walls. The second unsuccessful attempt to reenter was made after completion of coring at Site U1529. The final operation of Expedition 376 saw another return to Hole U1528B at the end of the expedition to retrieve the failed reentry system. We reentered Hole U1528B at 0958 h on 3 July, latched into the mock hanger, and pulled the reentry system back to the surface on the same day. A total of 79.25 h, or 3.3 days, were recorded while in Hole U1528B.

Hole U1528C

After completing the installation of the reentry system and casing in Hole U1528B, our intention was to reenter the hole to start coring operations. For this purpose, we assembled the TDCS designed by CDEX to implement its very first offshore test. Once the TDCS BHA, including a polycrystalline diamond compact (PDC) bit, was assembled, we successfully tested the function of the TDCS core barrel on the rig floor to verify the operation of the equipment prior to beginning the pipe trip to bottom.

At 1800 h on 25 May 2018, we started lowering the TDCS BHA to the seafloor. We then deployed the subsea camera system and made a reentry attempt at 2245 h on 25 May. The PDC bit hung up in the reentry funnel throat, possibly due to the base of the reentry system not sitting flat on the seafloor. After we had made several unsuccessful attempts to reenter Hole U1528B, we offset the vessel to a preselected hole position, tagged the seafloor to verify the water depth, retrieved the subsea camera, and spudded Hole U1528C at 0230 h on 26 May. We advanced with a center bit installed to 22 mbsf, pulled it, and deployed a TDCS core barrel on a wireline.

Cores 376-U1528C-2N to 8N penetrated from 22.0 to 53.5 mbsf at full 4.5 m advancements and recovered 3.6 m (12%). We pumped 30 barrels of mud sweeps at several depths to keep the hole clean. When Core 8N was pulled, we observed that only the top one-third of the core barrel was recovered. The core barrel had parted in the reduction gear, so the lower core barrel remained in the BHA. We pulled the drill string out of the hole, with the bit clearing the seafloor at 2330 h on 26 May. The drill string was pulled to the surface, and the TDCS BHA was disassembled and the lower section of the core barrel was recovered from the BHA. The TDCS PDC bit cleared the rig floor at 0430 h on 27 May, ending Hole U1528C. While laying out the TDCS subs, the vessel moved to Site U1529 using the DP system (~1.0 nmi move). A total of 47.75 h, or 2.0 days, were recorded while on Hole U1528C.

Hole U1528D

Upon returning from Site U1529 to make another unsuccessful attempt of reentering Hole U1528B, we prepared the installation of casing in Hole U1528D. The preparation consisted of: (1) assembling a 9.5 inch mud motor, an underreamer (set to 16.5 inches), and a 12.25 inch tricone drilling bit to form the drilling assembly; (2) connecting five joints of 13.375 inch casing to form a 59.4 m long casing string; (3) installing and testing the drilling assembly; and (4) landing the casing running tool (HRT) in the moonpool and attaching it to the casing string. We then installed and welded the reentry funnel and hard rock frame. Although the reentry system was ready to be deployed at 0500 h on 30 May 2018, we had to wait for 7 h until the weather improved enough to start lowering the reentry funnel and casing to the seafloor.

Once the weather abated, we lowered the reentry system to the seafloor and then deployed the subsea camera and sonar system. We began drilling-in the casing into Hole U1528D at 1750 h on 30 May. We encountered firm formation between 13 and 15 mbsf. The casing running tool (HRT) prematurely released at 35.5 mbsf while we were pumping a mud sweep. We decided to continue drilling down, with the possibility that the casing would continue to settle into the hole following the bit. The bit eventually reached 50 mbsf. However, after observing that the casing was not following the bit, we attempted to move the casing with the underreamer arms to no avail for 2 h. We then continued drilling the 16.5 inch hole from 50 mbsf to the planned total depth of 61.3 mbsf, which was reached at 0640 h on 31 May. After reaming and circulating the hole clean, we pulled out of the hole while observing the reentry funnel. Hole U1528D appeared to be located in the flat central area of the pit crater, with the casing and funnel standing independently 23 m above the seafloor. We set back the top drive, recovered the subsea camera, and pulled the drill string out of the hole, with the bit clearing the rig floor at 1605 h on 31 May. Subsequent function tests of the mud motor and underreamer indicated that they were both working properly.

Our next objective was to reenter Hole U1528D to get the reentry funnel and casing to settle to the appropriate depth. For this purpose, we installed a 13.375 inch cup seal on top of the drilling assembly (54.4 m above the bit) to seal the inside of the casing while circulating. This installation was intended to clean the annulus between casing and surrounding formation to promote complete settling of the casing string into the hole. We deployed the subsea camera and sonar system, continued lowering the drill string to the seafloor, picked up the top drive, and reentered the funnel of Hole U1528D at 0110 h on 1 June. We lowered the drill string to position the cup seal inside the casing with the mud motor and underreamer below the casing shoe, pumped a 20-barrel mud sweep, and began attempting to circulate and work the drill string down. After 3 h, the casing began falling at 0534 h on 1 June, and the reentry system finally landed at the seafloor at 0602 h. After circulating the hole, we pulled the drill string out of the hole, set back the top drive, recovered the subsea camera, retrieved the drill string, disassembled the drilling assembly, and flushed the mud motor and underreamer.

We then made up the RCB BHA, lowered it to the seafloor, deployed the subsea camera and sonar system, and reentered Hole U1528D at 2035 h on 1 June. After installing the top drive and retrieving the subsea camera system, we lowered the bit through the casing and circulated ~7 m of soft debris out of the bottom of the hole with 30 barrels of high-viscosity mud. We started RCB coring from a depth of 61.3 mbsf at 2337 h on 1 June. Half-length (4.8 m advance) Cores 376-U1528D-2R to 63R penetrated from 61.3 to 359.3 m and recovered 87.2 m (29%). Hole conditions for the entire interval remained optimum, with 30 barrels of mud sweeps being pumped on each core to keep the hole clean. The only short interruption (1.5 h) of that coring period was caused by a failure of the hydraulic return line from the top drive (after cutting Core 50R).

After Core 376-U1528D-63R was cut, we stopped coring, as the bit had reached 40 h of rotating time and needed to be changed for us to continue coring deeper. Before recovering the drill string to change the bit and resume coring, we decided to measure the borehole temperature and obtain a borehole fluid sample. At 0500 h on 6 June, we started preparing the ETBS memory tool and the primary (1000 mL) Kuster FTS tool for deployment on the coring line. First, we lowered the ETBS attached to a core barrel and let the tool collect data for 15 min at the bottom of the hole; on recovery, it revealed an average temperature of 33°C. We then deployed the Kuster FTS tool with a core barrel to sample borehole fluid, but sometime during the sampling run the tool failed under compression. Only the top connector from the tool returned to the surface, leaving almost 3 m of tool behind. We then recovered the drill string, with the bit reaching the rig floor at 1450 h on 6 June.

A fishing tool BHA with a Gotco junk basket and two boot-type junk baskets was assembled to recover the Kuster FTS and lowered to the seafloor, followed by deployment of the subsea camera and sonar system for reentering Hole U1528D. Reentry was hampered by a plume emanating from the funnel, but we successfully reentered at 0235 h on 7 June. We then recovered the subsea camera system, picked up the top drive, and continued lowering the fishing tool assembly to the bottom of the hole. We started circulating at 335 mbsf and had to work the assembly through soft fill from 341 to 350 mbsf, which was circulated out with high-viscosity mud sweeps. At 350.0 mbsf, we encountered hard fill. After washing/drilling down, we tagged the final hole depth of 359.3 mbsf. The junk basket was worked up and down with rotation and cycling the mud pumps on and off. We started pulling the drill string out of the hole at 0945 h on 7 June, set back the top drive, and the drill string cleared the seafloor at 1140 h. The Gotco junk basket came back with all the fingers missing from the junk basket catchers. We emptied the boot baskets and saved the contents, consisting of rock debris and minor unidentifiable small pieces of metal. We then were confronted with 5 m ship heave and had to wait for the weather to improve for 8 h before starting to prepare for downhole measurements and borehole fluid sampling in Hole U1528D.

At 0330 h on 8 June, we made up a logging BHA and lowered it to the seafloor. We deployed the subsea camera system (along with the APCT-3 temperature shoe to monitor water column and bottom water temperatures), continued lowering the drill string, and

positioned the vessel for reentry. We maneuvered for more than 2 h in poor visibility, due to a hydrothermal plume emerging from the reentry funnel, but finally reentered Hole U1528D for the fourth time at 0950 h. We tagged hard fill at 303 mbsf. We then picked up the top drive and deployed the back-up (600 mL) Kuster FTS tool on the core line, successfully recovering a borehole fluid sample. The recovery was followed by lowering the ETBS, which measured a maximum temperature of 212°C. When the bit reached 323 mbsf, a high-viscosity mud sweep was circulated to clean the hole and the bit was raised to 50.6 mbsf—inside the 13.375 inch casing. The HTTC tool string consisting of the LEH-MT (Logging Equipment Head-Mud Temperature Tool), EDTC (Enhanced Digital Telemetry Cartridge), HNGS, and HLDS (Hostile-Environment Litho-Density Sonde) was assembled and lowered to 332 mbsf. Two upward logging passes were conducted, and the tools were back on the rig floor at 0210 h on 9 June. The logging tools were disassembled, cleaned, and secured.

We then lowered the drill string back down to the bottom of Hole U1528D in preparation for another Kuster FTS tool run and encountered hard fill at 330 mbsf. The top drive was picked up, and the end of the drill pipe was set at ~323 mbsf. We deployed the Kuster FTS tool and successfully recovered a borehole fluid sample from 313 mbsf. On breaking the drill string connection at the rig floor, we measured an H_2S concentration of 20 µg/g. The connection was made back up, and the drill pipe was circulated out to clear the drill string of H_2S. We then deployed the ETBS memory tool to 313 mbsf, which yielded a maximum temperature measurement of ~165°C (not equilibrated), following 15 min of stationary measurement. After recovering the ETBS tool, we started pulling the drill string out of the hole and set back the top drive; the logging BHA cleared the seafloor at 1200 h on 9 June, and the bit arrived on the rig floor at 1535 h.

We then assembled a new 9.875 inch tricone bit BHA to clean out Hole U1528D. We lowered the drill string and deployed the subsea camera and sonar system to aid in the reentry. We reentered Hole U1528D for the fifth time at 2110 h on 9 June. After the subsea camera was recovered, we picked up the top drive and lowered the bit to 326 mbsf, where hard fill was encountered. The bit was worked down to 356.0 mbsf, where we observed torque at the depth of the top of the Kuster FTS tool that was left in the bottom of the hole. After working the top of the tool remnants, two 30-barrel mud sweeps were pumped, and the hole was circulated out. The bit was raised to 291.2 mbsf and the top drive was set back. We continued to pull the drill string out of the hole, clearing the top of the reentry funnel at 0535 h on 10 June. The remainder of the drill string was pulled back to surface, and the bit cleared the rig floor at 0840 h. The bit and the float were inspected at the rig floor. The bit was intact, with slight markings indicating its interaction with the Kuster FTS remnants; however, the Baker float was severely damaged by heat and all rubber components were disintegrating.

We next assembled a milling bit and two boot-type junk baskets and lowered the drill string to the seafloor to attempt to clean the Kuster FTS tool from the hole. We reentered Hole U1528D for the sixth time at 1519 h on 10 June, lowered the bit to 356 mbsf, and started grinding up the Kuster FTS tool with the milling bit from 356 to 359 mbsf. No torque was observed during the milling. After reaching 359 mbsf, we worked the junk basket multiple times, circulated high-viscosity mud sweeps, and started pulling the drill string out of the hole. The milling bit cleared the rig floor at 0225 h on 11 June. The junk baskets contained rock debris but no remnants of the lost Kuster FTS tool.

We then assembled the reverse-circulation junk basket (RCJB) tool with twin boot-type baskets for a last attempt at clearing the hole. At 0415 h, we stopped operations due to storm-force winds and high seas. The next 31.75 h were spent waiting for the weather to improve enough to continue operations.

Once the weather had abated, we completed assembling the RCJB tool BHA, lowered it to the seafloor, and deployed the subsea camera and sonar system to assist in positioning the ship for reentry. We reentered Hole U1528D for the seventh time at 1714 h on 12 June. We continued lowering the drill string into the hole, retrieved the subsea camera, picked up the top drive, and washed down from 327 to 352.3 mbsf. At this depth, we tagged hard fill that led to high torque. We continued attempting to work the drill string back to the bottom of the hole, starting to divert the flow path on the RCJB at 2100 h. When we reached 359.3 mbsf, we pumped 25 barrels of high-viscosity mud sweep, worked the RCJB BHA down to the bottom of Hole U1528D, and circulated for 15 min in an attempt to recover any parts of the lost Kuster FTS tool. At 0030 h on 13 June, we started pulling the drill string out of the hole. The drill string cleared the seafloor at 0220 h. When the end of the drill string arrived back on the rig floor at 0405 h, we discovered that the lowermost 172.8 m of the drill string was missing; this loss ended Hole U1528D drilling operations. The drill string failed in a piece of 5 inch pipe above the BHA. Furthermore, the broken piece that was recovered showed significant damage from corrosion, likely due to the acid and high H_2S conditions encountered in the hole.

After conducting operations at Sites U1530 and U1531, we returned to Hole U1528D to perform downhole temperature measurements and fluid sampling, marking our final science operations of Expedition 376. At 1720 h on 1 July, we lowered the drill string to the floor of the pit crater and reentered Hole U1528D at 1805 h. We lowered the end of the drill string to 27.2 mbsf and started an alternating series of temperature measurements and two borehole fluid sampling attempts. These measurements consisted of: (1) the ETBS memory tool, which tagged the bottom of the hole at 195 mbsf and recorded a maximum temperature of 198°C at 160 mbsf, (2) the Kuster FTS tool, which successfully recovered borehole fluid at 160 mbsf, (3) the Petrospec spool-in TCMT, which flooded and did not obtain any data, (4) the Kuster FTS tool deployed at 160 mbsf again but returned empty to the ship due to the sample chamber valves failing to close, and (5) another deployment of the Petrospec TCMT to a depth of 160 mbsf, where it recorded 156°C. We then pulled the drill string out of the hole, and it cleared the seafloor at 0630 h on 2 July. Upon an ETBS memory tool deployment in Hole U1531E, we returned one last time to Hole U1528D in an attempt to perform another Kuster FTS tool run. We abandoned the attempt when we observed the Hole U1528D reentry funnel to be on its side on the seafloor, ending all operations in this hole. A total of 391.5 h, or 16.3 days, were recorded while in Hole U1528D.

Site U1529

The original plan for Site U1529 (proposed Site WC-1A) was to drill two holes. The first, pilot hole, was to core to ~50 m with the RCB system. The second hole was dedicated to drilling-in a reentry system to a depth determined by lithologies revealed by the pilot hole to enable 565 m of penetration at Site U1529. The actual operations consisted of RCB coring two pilot holes—Hole U1529A to 12.0 mbsf and Hole U1529B to 34.4 mbsf—both of which had to be

abandoned because of poor hole conditions. Cores, penetration depths, and core recovery are listed in Table **T2**.

Hole U1529A

After clearing the seafloor from Hole U1528C, the vessel moved slowly in DP mode from Site U1528 to Site U1529 while continuing to recover the drill string. The 0.7 nmi transit was done between two periods of operations at Site U1528. Once the bit cleared the rig floor at 0430 h on 27 May 2018, we made up the RCB BHA with a new CC-7 RCB coring bit. A perforated brass insert that contained fractured crystals wrapped in gold foil, supplied by the science party, was installed in the bit prior to assembly into the BHA. It was hoped that these crystals would trap borehole fluids (as fluid inclusions) while coring. The bit was then lowered to just above the seafloor, and the subsea camera system was installed and run down to conduct a survey at Site U1529. Prospective hole positions were located, and the seafloor was tagged to confirm the water depth. Upon recovery of the subsea camera system, Hole U1529A was spudded at 1610 h on 27 May 2018 at a water depth of 1735.0 m. RCB coring began with a 12 m core to allow us to make the first connection without clearing the seafloor. After Core 376-U1529A-1R penetrated the seafloor to a depth of 12 mbsf and recovered 1.86 m of core (15.5%), we measured high torque and had to work a tight hole from 12 mbsf back to the seafloor. We were unable to retrieve the core barrel, and the drill string had to be pulled out of the hole because of poor hole conditions related to unconsolidated volcanic material. Hole U1529A ended when the bit cleared the seafloor at 1925 h on 27 May 2018. The core barrel was retrieved, and another core barrel was dropped. A total of 15 h (0.6 d) were spent in Hole U1529A.

Hole U1529B

The vessel was offset 20 m east, and RCB coring in Hole U1529B started at a water depth of 1733.0 m at 2030 h on 27 May 2018. Cores 376-U1529B-1R to 3R penetrated from the seafloor to 34.4 mbsf, with extremely poor total recovery of 0.6 m (2%). We once again experienced a tight hole at the bottom depth and attempted to work the drill string back to ~15 m. We dropped a core barrel to improve circulation; however, circulation was lost when the bit was at 15 mbsf. We decided to abandon Hole U1529B because the drill bit and jets were plugged with debris and hole conditions were extremely unstable. We pulled the drill string out of the hole, and the bit cleared the seafloor at 1015 h on 28 May. The core barrel that was in place during the attempt to get back to the bottom of the hole was then retrieved (i.e., ghost Core 4G; 8.17 m of lapilli-sized tephra). After two unsuccessful attempts to establish an adequate pilot hole, coring operations at Site U1529 were abandoned. The drill string was pulled back to a water depth of 1116.5 m, and the vessel was moved in DP mode back to cased Hole U1528B where we arrived at 1530 h on 28 May. The total time spent in Hole U5129B was 29.0 h (1.2 d).

Site U1530

After the drill string cleared the seafloor from Hole U1528D at 0220 h on 13 June 2018, the vessel moved slowly in DP mode from Site U1528 to Site U1530 at the NW Caldera wall while we continued to recover the drill string. The transit was completed before the end of the drill string reached the rig floor (officially ending Site U1528).

The original plan for Site U1530 (proposed Site NWC-3A) was to drill two holes. The first, a pilot hole, was to core to ~50 m with the RCB system. The second hole was to install a reentry system to a depth determined by lithologies intersected by the pilot hole to allow 450 m of penetration. The actual operation involved RCB coring of only a single hole. Hole U1530A was RCB cored to the target depth of 453.1 mbsf without the need for installation of a reentry system. Coring was then terminated and the bit was dropped in the bottom of the hole. The ETBS tool and the Kuster FTS tool were deployed, followed by two wireline logging runs with both the triple combo and FMS-Sonic tool strings. At the conclusion of logging, we deployed the Kuster FTS tool for borehole fluid sampling again and tested the Petrospec TCMT to record borehole temperatures. Cores, penetration depths, and core recovery are listed in Table **T2**.

Hole U1530A

An RCB BHA was assembled with a new CC-7 bit, into which a perforated brass insert containing crystals to enable potential trapping of borehole fluids (supplied by the science party) had been installed.

The RCB bit was lowered to just above the seafloor and the subsea camera and sonar system were deployed. A subsea survey for Site U1530 was conducted and three prospective hole positions were located. Seafloor tags were performed with the bit to verify precise water depths of the seafloor at each hole position. The top drive was picked up while the subsea camera system was retrieved and secured at the surface. We then pumped a pig to clean out the inside of the new pieces of drill string. The PFMD tracer pump was turned on and slow circulating pressure was recorded.

RCB coring in Hole U1530A (water depth of 1594.4 m) began at 1900 h on 13 June with a 7.2 m mudline core to enable the first pipe connection to be made without clearing the seafloor. After a 9.7 m cored interval that recovered Core 376-U1530A-2R, the decision was made to switch to half-length (4.8 m) coring advances to maximize core recovery. Thirty barrels of high-viscosity mud sweep were pumped with every other core to keep the hole clean. Good hole conditions remained throughout coring. These conditions continued to a final depth of 453.1 mbsf (Core 93R), resulting in a total of 76.8 m (17%) of core material recovered. Total depth for Hole U1530A was reached at 0505 h on 19 June 2018.

After completion of coring to the target depth, another 30-barrel sweep of high-viscosity mud was pumped, followed by 30 barrels of salt water and a second 30-barrel sweep of high-viscosity mud to condition the hole for downhole measurements. The rotary shifting tool (RST) was lowered on the core line to release the bit in the bottom of the hole. The RST was then pulled back to the surface, and the reverse RST tool was run to move the releasing sleeve back into the circulating position. Because there were some conflicting indications as to whether the bit had actually released, an RCB core barrel was deployed and, after a few minutes of testing, it was verified that the bit had indeed released. Apparently, sufficient fill had accumulated underneath the end of the mechanical bit release (MBR) at the end of the drill string to give a false indication. While laying out the RCB core barrel, damage to some of the strands of the coring line were observed, so 150 m of core line was cut and slipped. The sinker bars and the oil saver were reattached. The end of the drill string was spaced out one stand of drill pipe above the bottom of Hole U1530A.

The downhole measurement plan for Hole U1530A consisted of running: (1) the ETBS tool, (2) the Kuster FTS tool, and (3) the triple combo (natural gamma ray, porosity, and density sondes). At 1030 h on 19 June, the ETBS was assembled and lowered to 429.1 mbsf where it was held stationary for 16 min before retrieval. The highest

temperature recorded was ~39.7°C. The Kuster FTS was then lowered at half the normal core line speed to just below the end of the pipe ~20 m above the bottom of the hole (i.e., depth of 436.1 mbsf). Circulation was stopped for ~20 min to allow the clock timer to activate and the sample to be taken. Upon retrieval of the tool, it was determined that a cap screw of the upper valve assembly had unscrewed, preventing the lower valve from closing to collect a sample. The tool was repaired and readied for another sampling run at the end of the logging activity.

We then raised the end of the drill string to a depth of 67.1 mbsf, rigged up the drill floor for logging, and started preparing the triple combo tool string. The average heave was estimated to be 0.75 m just prior to logging. The active heave compensator was utilized whenever the logging tools were in the open hole. A standard (low-temperature) triple combo logging tool string was made up with the following tools: HRLA (High-Resolution Laterolog Array), HLDS (Hostile Environment Litho-Density Sonde, with source), APS (Accelerator Porosity Sonde), HNGS (Hostile Environment Logging Natural Gamma Ray Spectroscopy Sonde), EDTC (Enhanced Digital Telemetry Cartridge), and LEH-MT (Logging Equipment Head-Mud Temperature Tool (model "mud temperature" [MT]).

The tool string was lowered at 1820 h on 19 June, and a downward logging pass was performed from just above seafloor to the full accessible hole depth above fill at 442 mbsf. The hole was then logged up for a 182 m calibration pass, lowered back to bottom (442 mbsf), and logged uphole with the triple combo tool string through the casing and drill string to the seafloor. The caliper was closed prior to entering the casing. The tools were pulled from the hole, cleared the seafloor at 2300 h, and were rigged down by 0030 h on 20 June.

A second tool string with the FMS was made up with the following logging tools: FMS (Formation MicroScanner), DSI (Dipole Sonic Imager), HNGS, EDTC, and LEH-MT. Deployment of the tool string commenced at 0140 h, and a downhole logging pass with the FMS calipers closed began just above the seafloor and extended to 442 mbsf where fill was encountered ~11 m above the bottom of the hole. Natural gamma ray was logged through the drill pipe to identify the seafloor to match the depth results on the first logging run. At the depth of the fill, the first upward log was started and logged from 442 to ~116 mbsf with the FMS calipers open. The tools were run back down to 442 mbsf, and the second upward log was run with the calipers open. The calipers were closed just prior to entering the drill pipe at 51.8 mbsf, and logging continued all the way to the seafloor. The FMS-Sonic tool string returned to the rig floor at 0725 h and was rigged down by 0830 h on 20 June.

Upon completion of downhole logging, the drill string was lowered back to the top of the fill at 442 mbsf, and the end of the pipe was pulled back to 428.2 mbsf. The Kuster FTS tool was lowered to ~20 m above the bottom of the hole with circulation stopped. After waiting 15 min for the mechanical clock of the Kuster FTS to trigger closure of the valves, the tool was pulled back to the rig floor, having successfully recovered a fluid sample.

At 1245 h on 20 June, the newly designed, high-temperature Petrospec spool-in TCMT was deployed for the first time on the core line. While lowering the two thermocouple joints 8 m past the end of the drill pipe to 447 mbsf, circulation was started at 20 strokes/min to cool the temperature-sensitive TCMT data logger inside the drill string. After waiting 10 min, the tool was pulled back into the pipe and returned to the surface. The TCMT recorded a maximum temperature of 20°C. With the downhole measurements complete, the drill string was pulled out of the hole and cleared the seafloor at 1540 h. While the drill pipe was being tripped, we began moving the vessel slowly in DP mode to Site U1531 at 1600 h. The end of the drill string (mechanical bit release) arrived back on the rig floor at 2005 h on 20 June 2018, ending Hole U1530A and thus Site U1530. The total time spent on Hole U1530A was 184.0 h, or 7.7 days.

Site U1531

Site U1531 (proposed alternate Site LC-1A) consists of five holes. The original plan for this site was to drill two holes: a pilot hole to core to ~50 m with the RCB system and a second hole to drill-in a reentry system to a depth based on conditions encountered in the pilot hole, followed by coring to 300 m. Actual operations proved different from the plan. Hole U1531A was RCB cored to 15.0 mbsf into the saddle between the Upper and Lower Cone. Coring was terminated when we could not retrieve the first core barrel and had to pull clear of the seafloor because of high torque and high overpull.

The second hole at Site U1531 reached 24.0 mbsf with Core 376-U1531B-3R, but hole conditions were very poor, with high torque and overpull during the entire interval in blocky, fragmented volcanic and volcaniclastic deposits. We then moved northeast, up the slope of the Lower Cone ~110 m to its summit area and attempted another pilot hole (U1531C). It was of very limited success, taking only three cores to a depth of 28.4 mbsf. Again, high torque and high overpull prevented coring further.

We then decided to try drilling-in a reentry system through the upper section of the formation. A reentry system and 13.375 inch casing for Hole U1531D was drilled-in, but after releasing from the hanger, we were unable to release from the casing, most probably because the underreamer arms failed to close completely. Forced to pull out of the seafloor with the reentry system still attached, we offset 400 m east in case the system fell during retrieval. The system did fall to the seafloor just before it was recovered. It was later located during a seafloor camera survey to record its position.

A second, similar reentry system was constructed for Hole U1531E with ~15 m of 13.375 inch casing. We experienced similar problems with releasing from the casing, but we were finally able to do so. We attempted to test the CDEX TDCS, but a stuck core barrel at the beginning of the test forced us to abandon coring with the TDCS. The RCB coring system was able to core to 39.6 mbsf, but there was high torque on the drill string throughout. Before we could abandon coring, an equipment failure on the top drive drilling system caused us to end coring slightly ahead of our planned termination time. After a short interlude, we returned to Site U1531 for a downhole temperature measurement with the ETBS memory tool in Hole U1531E. The tool recorded a value similar to bottom seawater temperatures. A total of 264.25 h, or 11.0 days, were spent while at Site U1531.

Hole U1531A

While we were recovering the drill string from Hole U1530A, we began moving the vessel to shallower water Site U1531 using the dynamic positioning system. At 1806 h on 20 June, we arrived at Site U1531, located on the saddle between the Lower and Upper Cone of Brothers volcano. The end of the drill string (mechanical bit release) arrived back on the rig floor at 2005 h on 20 June (officially ending Hole U1530A). We then reassembled the rig floor and conducted a routine cut and slip of the drilling line, before we had to stop opera-

tions due to storm-force winds and high seas. The following 35.75 h were spent waiting for the weather to improve enough to continue operations.

At 1000 h on 22 June, we made up an RCB BHA and lowered it to the seafloor at Site U1531. At 1430 h, we deployed the subsea camera system to perform a seafloor survey and verify the exact seafloor depth at three potential hole locations. After retrieving the subsea camera system and picking up the top drive, we started RCB coring in Hole U1531A at 2030 h on 22 June. Core 376-U1531A-1R penetrated from the seafloor to 15 mbsf, but we experienced excessive torque and overpull and had to pull the drill string out of the hole. After the bit cleared the seafloor (at 2330 h), we lowered the core line to retrieve Core 1R (1.5 m recovered; 7%) at 0045 h on 23 June. The time spent in Hole U1531A was 51.5 h or 2.1 days, not including the 35.75 h of waiting on weather.

Hole U1531B

We then started RCB coring in Hole U1531B, with Cores 376-U1531B-1R to 3R penetrating from the seafloor to 26 mbsf and recovering 4.0 m (15%). Drilling conditions were very poor, with high torque, overpull, and frequent stalling of the top drive; the drill string became stuck several times. These conditions forced us to start pulling the drill string out of the hole before Core 3R could be retrieved. After the bit cleared the seafloor at 1420 h on 23 June, we recovered Core 3R, ending Hole U1531B. The time recorded in Hole U1531B was 14.75 h (0.6 days).

Hole U1531C

With the drill string just above the seafloor, we deployed the subsea camera system, offset the vessel 110 m northeast to the summit of the Lower Cone, and started a seafloor survey at 1730 h on 23 June. During the survey, we tagged the seafloor in two locations to verify the exact seafloor depth. We then retrieved the subsea camera system and started coring in Hole U1531C at 1930 h on 23 June. Cores 376-U1531C-1R to 3R penetrated from the seafloor to 28.4 mbsf and recovered 2.25 m (8%). We circulated 30 barrels of high-viscosity mud at several depths to clean the hole. We experienced tight hole conditions throughout coring, facing high torque and frequent overpull, so Hole U1531C was abandoned at 28.4 mbsf. At 0815 h on 24 June, we started pulling the drill string out of the hole, and it cleared the seafloor at 0845 h. We set back the top drive, continued raising the drill string, and the bit arrived at the rig floor at 1340 h, ending Hole U1531C. Inspection of the BHA revealed massive wear on the outside diameter of the bottom three drill collars and the mechanical bit release. A total of 23.5 h, or 1.0 day, were recorded while in Hole U1531C.

Hole U1531D

After ending Hole U1531C, we decided to install a reentry system with a short casing string to establish a stable hole in the summit area of the Lower Cone for deeper coring and logging objectives. We made up a drilling BHA with a 12.25 inch tricone bit, an 11.75 inch underreamer (set to 16.5 inches), and a mud motor. At 2200 h on 24 June 2018, we assembled a reentry system with 16 m of 13.375 inch casing, a reentry funnel, and a hard rock landing frame. After the drilling BHA was lowered through and attached to the reentry system, at 0500 h on 25 June, we started lowering the entire reentry system to the seafloor. At 0800 h, we deployed the subsea camera and sonar system, continued lowering the drill-in casing assemblage, and picked up the top drive. We started drilling-in the casing in Hole U1531D at 1030 h on 25 June, reaching a total depth of 19 mbsf at 1445 h. We then deployed the go-devil to activate the HRT and release the reentry system, but we were unable to pull the drilling assembly clear of the casing string because the underreamer arms did not retract completely. We attempted to free the reentry system for 3.5 h unsuccessfully, so we decided to pull the drill string and attached reentry system out of the hole and back to the vessel. After the bit cleared the seafloor at 1835 h, we offset the vessel 400 m east. We set back the top drive, retrieved the subsea camera and sonar system, and continued raising the drill string. While we were retrieving the casing and drilling assembly to the surface, the reentry system and casing unfortunately dropped off the drilling assembly at 2310 h in sight of the moonpool with doors open while picking up the last drill collar. We began taking apart the drilling BHA, with the bit arriving back at the rig floor at 0045 h on 26 June. A total of 35.00 h, or 1.5 days, were recorded while in Hole U1531D.

Hole U1531E

On 26 June 2018, we started making up a new drilling BHA with a 12.25 inch tricone bit, an 11.75 inch underreamer (set to 16.5 inches), and a mud motor to drill-in 16 m of 13.375 inch casing into Hole U1531E, located on the saddle between the Upper and Lower Cone of Brothers volcano. After testing the mud motor and underreamer at 0530 h on 26 June, we had to stop operations for 7 h due to inclement weather. At 1545 h, we began assembling the casing string but had to stop operations again at 1900 h as the weather deteriorated. The next 24.25 h were spent waiting for the weather to improve enough to resume operations.

At 1915 h on 27 June, we continued connecting the drilling BHA (mud motor, underreamer, and drill bit) to the casing string. After welding the casing system, we attached the reentry funnel and hard rock landing skirt. We opened the moonpool doors and started lowering the casing and reentry system to the seafloor at 2350 h. Upon deployment of the subsea camera and sonar system at 0230 h on 28 June, we continued lowering the casing assembly, picked up the top drive, and positioned the vessel to start drilling. We started Hole U1531E at 0705 h and by 1545 h had drilled-in to 17.9 mbsf, working through tight spots. We then deployed the go-devil to activate the HRT to release the drilling assembly from the casing. We were initially not able to retrieve the drilling assembly from the casing string and had to work the drilling assembly to get the underreamer arms to close. After it released from the casing at 1605 h, we raised the drill string above the top of the reentry funnel and observed that the casing had been lifted 4.2 m while we were trying to release. This lifting of the casing left the base of the casing shoe at 10.7 mbsf. We then recovered the subsea camera, set back the top drive, and recovered the drill string to the rig floor. We flushed the mud motor and underreamer with freshwater and disassembled the HRT components and the BHA.

At 0030 h on 29 June, we began making up the CDEX TDCS for running a second test during this expedition. We assembled the TDCS core barrels and BHA, including a 9.875 inch PDC bit. We started lowering the TDCS BHA to the seafloor at 0530 h, deployed the subsea camera and sonar system, and picked up the top drive. We then reconfigured the TDCS core barrels and conducted a "drop test" deployment (i.e., dropped the core barrel and retrieved it prior to reentry). We reentered Hole U1531E at 1347 h on 29 June, lowered the drill string to ~8 mbsf, and flushed the interior of the casing. While recovering the subsea camera, we checked for fill below the end of the casing at 10.7 mbsf. At 1430 h, we deployed a TDCS core barrel, washed down to the bottom of the hole at 17.9 mbsf, flushed it with two back-to-back high-viscosity mud sweeps, and re-

trieved the TDCS core barrel (ghost Core 376-U1531E-2G; 0.5 m of fresh dacite pebbles). The next TDCS barrel got stuck in the BHA and could not be recovered after three attempts. We then terminated the TDCS test and started pulling the drill string out of the hole. It cleared the seafloor at 2045 h. We set back the top drive, recovered the drill string, and the bit arrived back on the rig floor at 0110 h on 30 June.

We then made up an RCB coring system BHA and started lowering it down to the seafloor. We deployed the subsea camera and sonar system to aid in reentry of Hole U1531E. We then continued lowering the drill string, picked up the top drive, and reentered Hole U1531E at 1133 h on 30 June. After recovering the subsea camera, we reassembled the rig floor, pumped 40 barrels of high-viscosity mud sweep to clean the hole, and lowered the bit until it encountered hard fill at 9 mbsf (inside the casing). At 1245 h, we dropped an RCB core barrel and washed back to bottom of the hole at 17.9 mbsf (Core 376-U1531E-4G; 0.15 m dacitic lapilli). We then cut half-length (4.8 m advances) Cores 376-U1531E-5R to 9R from 17.9 to 39.6 mbsf and recovered 0.8 m (4%). We had to pump multiple high-viscosity mud sweeps to keep the bottom of the hole clean to be able to keep coring. Hole conditions were very poor. After recovering Core 9R, the top drive blower motor seized with a bad bearing. We began repairs (4.75 h of downtime) but then evaluated the repair time versus the remaining coring time. We concluded coring activities and began other operations. We released the bit in Hole U1531E and then shifted the circulating sleeve back into the circulating position. After releasing the bit, we pulled the drill string out of the hole with the top drive installed, clearing the seafloor and ending coring operations in Hole U1531E at 1435 h on 1 July 2018.

We then left Hole U1531E and transited to Hole U1528D for fluid sampling and temperature measurements. After completing operations in Hole U1528D, we returned to Hole U1531E at 0745 h on 2 July. We lowered the drill string with the top drive installed and reentered Hole U1531E at 1015 h on 2 July. We then lowered the ETBS memory tool into the hole with the core line for a temperature profile. After completing the ETBS tool run, which yielded a stationary temperature measurement of 5°C at 20 mbsf, we pulled the drill string out of the hole and cleared the seafloor at 1135 h. The drill string was pulled back to 1149 mbsl with the top drive installed. We then began the transit back to U1528D, ending Hole U1531E at 1330 h on 2 July 2018. A total of 139.5 h, or 5.8 days, were spent on Hole U1531E.

Education and outreach

Expedition 376 had two Education and Outreach Officers on board: an education tour guide from Wellington, New Zealand, and a high school teacher from Florida, USA. The officers communicated the scientific objectives of the expedition with audiences of all ages from around the world via live video broadcasts and social media posts and also developed classroom resources and other educational products for students at all age levels.

Live ship-to-shore video broadcasts to classrooms and museums were conducted using tablets (iPads) with the videoconferencing software *Zoom* and *Google Hangouts*. Fifty-four video sessions were conducted reaching an estimated 2700 students, teachers, and museum patrons. A typical session included a brief background explanation of the location of Brothers volcano and reasons for drilling, followed by a core flow tour. Scientists and lab technicians working in the science laboratories participated in every session, which allowed participants to make questions directly to the scientists and lab technicians. Survey responses from participants indicated that they found the objectives of the expedition clearly explained; they learned about science content, process, and careers; and the programs exceeded their expectations. Respondents also indicated that the programs helped them to meet the relevant state and local education standards. In addition, GNS Science hosted a series of four broadcasts on shore at the Museum of New Zealand Te Papa Tongarewa. These events covered the key research areas of Expedition 376 and were introduced on shore with a presentation from an expert in the field. These events were attended by 150 people and received strong positive feedback from those who attended.

The Education and Outreach Officers maintained four social media sites for the duration of the expedition: a Facebook page (@JOIDES Resolution), a Twitter feed (@TheJR), an Instagram account (@joides_resolution), and a blog at **http://joidesresolution.org**. Outreach Officers created more than 62 Facebook posts, and the number of Facebook followers increased by 3.5% over the 2 months of the expedition. The team also hosted two Facebook Live video streams, with an average 400 viewers per stream. These live video sessions provided the general public with the unique ability to directly engage with the team on the ship and receive nearly instant responses to their questions. A total of 73 Twitter posts were made, with ~144 new Twitter followers added. A total of 30 Instagram posts were made on the *JOIDES Resolution* account, garnering dozens of new followers. The Outreach Officers produced 33 blog posts on the *JOIDES Resolution* website, including five guest blogs written by science party members. The team also hosted an "Ask Me Anything" session on Reddit, answering 20 questions from the public over the course of 2 h, with the help of four members of the science party.

In addition to the video broadcasts and social media, the Education and Outreach Officers created their own focused products. The USA high school teacher developed multiple lesson plans with a focus on submarine volcanoes and hydrothermal vents. These lesson plans will be hosted on the *JOIDES Resolution* website under the "For Educators" page, and though geared toward secondary school students, will be easily adaptable for many age groups. The museum educator developed a 360° tour of the *JOIDES Resolution* for YouTube, a series of microbe infographics for the *JOIDES Resolution* website, and produced a video in Te Reo Māori about IODP.

The Education and Outreach Officers each created a series of STEAM (Science, Technology, Engineering, Art, and Mathematics) based artworks. The New Zealand officer produced a set of micrographs from thin sections of hard rocks from Brothers volcano, which were shared on the *JOIDES Resolution* blog and social media. The USA officer created a set of acrylic pour paintings, utilizing the movement of the ship to distribute the paint across the canvas. The painting process and photographs of completed paintings were shared on the *JOIDES Resolution* blog page, as well as social media sites.

Education and outreach activities will continue on shore, with development of additional school curricula to be shared on the *JOIDES Resolution* website. The USA Education and Outreach Officer will participate at IODP's booth and conduct teacher outreach activities at the National Science Teachers Association annual conference in St. Louis, MO, from 11 to 14 April 2019. The New Zealand Outreach Officer has developed a card game involving extremophile microbes and environments, such as Brothers volcano, and will produce a deck and a rule-set resource for future publication on the *JOIDES Resolution* website.

Media covered Expedition 376 during both port calls, including national TV and radio as well as national/international web and newspapers (e.g., *The Sydney Morning Herald*). At the time of the publication of this report, 17 media stories have been recorded in total. Updates can be continuously retrieved from **http://iodp.tamu.edu/outreach/index.html**.

References

Baker, E.T., Embley, R.W., Walker, S.L., Resing, J.A., Lupton, J.E., Nakamura, K., de Ronde, C.E.J., and Massoth, G.J., 2008. Hydrothermal activity and volcano distribution along the Mariana arc. *Journal of Geophysical Research: Solid Earth,* 113(B8):B08S09. **https://doi.org/10.1029/2007JB005423**

Baker, E.T., Walker, S.L., Embley, R.W., and de Ronde, C.E.J., 2012. High-resolution hydrothermal mapping of Brothers Caldera, Kermadec arc. *Economic Geology,* 107(8):1583–1593. **https://doi.org/10.2113/econgeo.107.8.1583**

Barriga, F.J.A.S., Binns, R.A., Miller, D.J., and Herzig, P.M. (Eds.), 2007. *Proceedings of the Ocean Drilling Program, Scientific Results,* 193: College Station, TX (Ocean Drilling Program). **https://doi.org/10.2973/odp.proc.sr.193.2007**

Bischoff, J.L., 1991. Densities of liquids and vapors in boiling NaCl-H_2O solutions: a PTVX summary from 300° to 500°C. *American Journal of Science,* 291:309–338.

Bischoff, J.L., and Rosenbauer, R.J., 1985. An empirical equation of state for hydrothermal seawater (3.2 percent NaCl). *American Journal of Science,* 285:725–763.

Caratori Tontini, F., Davy, B., de Ronde, C.E.J., Embley, R.W., Leybourne, M., and Tivey, M.A., 2012a. Crustal magnetization of Brothers Volcano, New Zealand, measured by autonomous underwater vehicles: geophysical expression of a submarine hydrothermal system. *Economic Geology,* 107(8):1571–1581. **https://doi.org/10.2113/econgeo.107.8.1571**

Caratori Tontini, F., de Ronde, C.E.J., Yoerger, D., Kinsey, J.C., and Tivey, M., 2012b. 3-D focused inversion of near-seafloor magnetic data with application to the Brothers Volcano hydrothermal system, southern Pacific Ocean, New Zealand. *Journal of Geophysical Research: Solid Earth,* 117(B10):B10102. **https://doi.org/10.1029/2012JB009349**

Clark, M.R., and O'Shea, S., 2001. Hydrothermal vent and seamount fauna from the southern Kermadec Ridge, New Zealand. *InterRidge News,* 10b:. **https://www.interridge.org/files/interridge/IR_News_10b.pdf**

de Ronde, C.E.J., Baker, E.T., Massoth, G.J., Lupton, J.E., Wright, I.C., Sparks, R.J., Bannister, S.C., Reyners, M.E., Walker, S.L., Greene, R.R., Ishibashi, J., Faure, K., Resing, J.A., and Lebon, G.T., 2007. Submarine hydrothermal activity along the mid-Kermadec arc, New Zealand: large-scale effects on venting. *Geochemistry, Geophysics, Geosystems,* 8(7):Q07007. **https://doi.org/10.1029/2006GC001495**

de Ronde, C.E.J., Butterfield, D.A., and Leybourne, M.I., 2012. Metallogenesis and mineralization of intraoceanic arcs I: Kermadec arc—introduction. *Economic Geology,* 107(8):1521–1525. **https://doi.org/10.2113/econgeo.107.8.1521**

de Ronde, C.E.J., Chadwick, W.W., Jr., Ditchburn, R.G., Embley, R.W., Tunnicliffe, V., Baker, E.T., Walker, S.L., Ferrini, V.L., and Merle, S.M., 2015. Molten sulfur lakes of intraoceanic arc volcanoes. *In* Rouwet, D., Christenson, B., Tassi, F., and Vandemeulebrouck, J. (Eds.), *Advances in Volcanology: Volcanic Lakes*. Nemeth, K. (Series Ed.): Berlin (Springer-Verlag), 261–288. **https://doi.org/10.1007/978-3-642-36833-2_11**

de Ronde, C.E.J., Hannington, M.D., Stoffers, P., Wright, I.C., Ditchburn, R.G., Reyes, A.G., Baker, E.T., Massoth, G.J., Lupton, J.E., Walker, S.L., Greene, R.R., Soong, C.W.R., Ishibashi, J., Lebon, G.T., Bray, C.J., and Resing, J.A., 2005. Evolution of a submarine magmatic-hydrothermal system: Brothers Volcano, southern Kermadec arc, New Zealand. *Economic Geology,* 100(6):1097–1133. **https://doi.org/10.2113/gsecongeo.100.6.1097**

de Ronde, C.E.J., Humphris, S.E., and Höfig, T.W., 2017. *Expedition 376 Scientific Prospectus: Brothers Arc Flux.* International Ocean Discovery Program. **https://doi.org/10.14379/iodp.sp.376.2017**

de Ronde, C.E.J., Massoth, G.J., Baker, E.T., and Lupton, J.E., 2003. Submarine hydrothermal venting related to volcanic arcs. *In* Simmons, S.F., and Graham, I.G. (Eds.), *Volcanic, Geothermal, and Ore-Forming Fluids: Rulers and Witnesses of Processes Within the Earth.* Society of Economic Geologists - Special Publication. 10:91–109.

de Ronde, C.E.J., Massoth, G.J., Butterfield, D.A., Christenson, B.W., Ishibashi, J., Ditchburn, R.G., Hannington, M.D., Brathwaite, R.L., Lupton, J.E., Kamenetsky, V.S., Graham, I.J., Zellmer, G.F., Dziak, R.P., Embley, R.W., Dekov, V.M., Munnik, F., Lahr, J., Evans, L.J., and Takai, K., 2011. Submarine hydrothermal activity and gold-rich mineralization at Brothers Volcano, Kermadec arc, New Zealand. *Mineralium Deposita,* 46(5–6):541–584. **https://doi.org/10.1007/s00126-011-0345-8**

Delteil, J., Ruellan, E., Wright, I., and Matsumoto, T., 2002. Structure and structural development of the Havre Trough (SW Pacific). *Journal of Geophysical Research: Solid Earth,* 107(B7):1–17. **https://doi.org/10.1029/2001JB000494**

Driesner, T. and Heinrich, C. (2007) The system H_2O–NaCl. Part I: Correlation formulae for phase relations in temperature–pressure–composition space from 0 to 1000°C, 0 to 5000 bar, and 0 to 1 X_{NaCl}. Geochim Cosmochim Acta, V 71, 4880–4901.

Embley, R.W., de Ronde, C.E.J., Merle, S.G., Davy, B., and Catatoni Tontini, F., 2012. Detailed morphology and structure of an active submarine arc caldera: Brothers Volcano, Kermadec arc. *Economic Geology,*107(8):1557–1570. **https://doi.org/10.2113/econgeo.107.8.1557**

Flores, G.E., Wagner, I.D., Liu, Y., and Reysenbach, A.-L., 2012. Distribution, abundance, and diversity patterns of the thermoacidophilic "deep-sea hydrothermal vent euryarchaeota 2." *Frontiers in Microbiology,* 3:47. **https://doi.org/10.3389/fmicb.2012.00047**

Freudenthal, T., and Wefer, G., 2007. Scientific drilling with the seafloor drill rig MeBo. *Scientific Drilling,* 5:63–66. **https://doi.org/10.5194/sd-5-63-2007**

Gamble, J.A., Woodhead, J.D., Wright, I.C., and Smith, I.E.M., 1996. Basalt and sediment geochemistry and magma petrogenesis in a transect from oceanic island arc to rifted continental margin arc: the Kermadec–Hikurangi margin, SW Pacific. *Journal of Petrology,* 37(6):1523–1546. **https://doi.org/10.1093/petrology/37.6.1523**

Gamble, J.A., and Wright, I.C., 1995. The southern Havre Trough geological structure and magma petrogenesis of an active backarc rift complex. *In* Taylor, B. (Ed.), *Backarc Basins: Tectonics and Magmatism:* New York (Plenum Press), 29–62. **https://doi.org/10.1007/978-1-4615-1843-3_2**

Gruen, G., Weis, P., Driesner, T., de Ronde, C.E.J., and Heinrich, C.A., 2012. Fluid-flow patterns at Brothers Volcano, southern Kermadec arc: insights from geologically constrained numerical simulations. *Economic Geology,* 107(8):1595–1611. **https://doi.org/10.2113/econgeo.107.8.1595**

Gruen, G., Weis, P., Driesner, T., Heinrich, C.A., and de Ronde, C.E.J., 2014. Hydrodynamic modeling of magmatic-hydrothermal activity at submarine arc volcanoes, with implications for ore formation. *Earth and Planetary Science Letters,* 404:307–318. **https://doi.org/10.1016/j.epsl.2014.07.041**

Haase, K.M., Stroncik, N., Garbe-Schönberg, D., and Stoffers, P., 2006. Formation of island arc dacite magmas by extreme crystal fractionation: an example from Brothers Seamount, Kermadec island arc (SW Pacific). *Journal of Volcanology and Geothermal Research,* 152(3–4):316–330. **https://doi.org/10.1016/j.jvolgeores.2005.10.010**

Haase, K.M., Worthington, T.J., Stoffers, P., Garbe-Schönberg, D., and Wright, I., 2002. Mantle dynamics, element recycling, and magma genesis beneath the Kermadec arc-Harve Trough. *Geochemistry, Geophysics, Geosystems,* 3(11):1071. **https://doi.org/10.1029/2002GC000335**

Herzig, P.M., Humphris, S.E., Miller, D.J., and Zierenberg, R.A. (Eds.), 1998. *Proceedings of the Ocean Drilling Program, Scientific Results,* 158: College Station, TX (Ocean Drilling Program). **https://doi.org/10.2973/odp.proc.sr.158.1998**

Humphris, S.E., Reysenbach, A.-L., Tivey, M., de Ronde, C.E.J., and Caratori Tontini, F., 2018. Brothers volcano, March 6-26, 2018. R/V *Thomas G. Thompson*, ROV *Jason* TN350 Cruise Report.

Lupton, J., Butterfield, D., Lilley, M., Evans, L., Nakamura, K., Chadwick, W., Jr., Resing, J., Embley, R., Olson, E., Proskurowski, G., Baker, E., de Ronde,

C., Roe, K., Greene, R., Lebon, G., and Young, C., 2006. Submarine venting of liquid carbon dioxide on a Mariana arc volcano. *Geochemistry, Geophysics, Geosystems,* 7(8):Q08007. **https://doi.org/10.1029/2005GC001152**

Merle, S., Embley, B., de Ronde, C. and Davy, B., 2007. New Zealand American Submarine Ring of Fire 2007 (NZASRoF'07/ROVARK), Brothers volcano, Kermadec arc, Ngatoro Rift and Havre Trough, R/V *Sonne* Cruise Report. **https://www.pmel.noaa.gov/eoi/pdfs/cruisereport-kermadec07-final.pdf**

Nakamura, K., and Takai, K., 2014. Theoretical constraints of physical and chemical properties of hydrothermal fluids on variations in chemolithotrophic microbial communities in seafloor hydrothermal systems. *Progress in Earth and Planetary Science,* 1(1):5. **https://doi.org/10.1186/2197-4284-1-5**

Plank, T., Kelley, K.A., Zimmer, M.M., Hauri, E.H., and Wallace, P.J., 2013. Why do mafic arc magmas contain ~4 wt% water on average? *Earth and Planetary Science Letters,* 364:168–179. **https://doi.org/10.1016/j.epsl.2012.11.044**

Reyes, A.G., 1990. Petrology of Philippine geothermal systems and the application of alteration mineralogy to their assessment. *Journal of Volcanology and Geothermal Research,* 43(1–4):279–309. **https://doi.org/10.1016/0377-0273(90)90057-M**

Ruellan, E., Delteil, J., Wright, I., and Matsumoto, T., 2003. From rifting to active spreading in the Lau Basin—Havre Trough backarc system (SW Pacific): locking/unlocking induced by seamount chain subduction. *Geochemistry, Geophysics, Geosystems,* 4(5):8909. **https://doi.org/10.1029/2001GC000261**

Stott, M.B., Saito, J.A., Crowe, M.A., Dunfield, P.F., Hou, S., Nakasone, E., Daughney, C.J., Smirnova, A.V., Mountain, B.W., Takai, K., and Alam, M., 2008. Culture-independent characterization of a novel microbial community at a hydrothermal vent at Brothers Volcano, Kermadec arc, New Zealand. *Journal of Geophysical Research: Solid Earth,* 113(B8):B08S06. **https://doi.org/10.1029/2007JB005477**

Takai, K., and Nakamura, K., 2011. Archaeal diversity and community development in deep-sea hydrothermal vents. *Current Opinion in Microbiology,* 14(3):282–291. **https://doi.org/10.1016/j.mib.2011.04.013**

Takai, K., Nunoura, T., Horikoshi, K., Shibuya, T., Nakamura, K., Suzuki, Y., Stott, M., Massoth, G.J., Christenson, B.W., de Ronde, C.E.J., Butterfield, D.A., Ishibashi, J., Lupton, J.E., and Evans, L.J., 2009. Variability in microbial communities in black smoker chimneys at the NW caldera vent field, Brothers Volcano, Kermadec arc. *Geomicrobiology Journal,* 26(8):552–569. **https://doi.org/10.1080/01490450903304949**

Timm, C., Bassett, D., Graham, I.J., Leybourne, M.I., de Ronde, C.E.J., Woodhead, J., Layton-Matthews, D., and Watts, A.B., 2013. Louisville seamount subduction and its implication on mantle flow beneath the central Tonga-Kermadec arc. *Nature Communications,* 4:1720, **https://doi.org/10.1038/ncomms2702**

Timm, C., Davy, B., Haase, K., Hoernle, K.A., Graham, I.J., de Ronde, C.E.J., Woodhead, J., Bassett, D., Hauff, F., Mortimer, N., Seebeck, H.C., Wysoczanski, R.J., Caratori Tontini, F., and Gamble, J., 2014. Subduction of the oceanic Hikurangi Plateau and its impact on the Kermadec arc. *Nature Communications,* 5:4923. **https://doi.org/10.1038/ncomms5923**

Timm, C., de Ronde, C.E.J., Leybourne, M.I., Layton-Matthews, D., and Graham, I.J., 2012. Sources of chalcophile and siderophile elements in Kermadec arc lavas. *Economic Geology,* 107(8):1527–1538. **https://doi.org/10.2113/econgeo.107.8.1527**

Wallace, P.J., 2005. Volatiles in subduction zone magmas: concentrations and fluxes based on melt inclusion and volcanic gas data. *Journal of Volcanology and Geothermal Research*, 140(1–3):217–240. **https://dx.doi.org/10.1016/j.jvolgeores.2004.07.023**

Wright, I.C., 1997. Morphology and evolution of the remnant Colville and active Kermadec arc ridges south of 33°30′S. *Marine Geophysical Research,* 19(2):177–193. **https://doi.org/10.1023/A:1004266932113**

Wright, I.C., and Gamble, J.A., 1999. Southern Kermadec submarine caldera arc volcanoes (SW Pacific): caldera formation by effusive and pyroclastic eruption. *Marine Geology,* 161(2–4):207–227. **https://doi.org/10.1016/S0025-3227(99)00040-7**

Wright, I.C., Parson, L.M., and Gamble, J.A., 1996. Evolution and interaction of migrating cross-arc volcanism and backarc rifting: an example from the southern Havre Trough (35°20′–37°S). *Journal of Geophysical Research: Solid Earth,* 101(B10):22071–22086. **https://doi.org/10.1029/96JB01761**

Table T1. Microbiological whole-round samples collected and preserved during Expedition 376.

Location	Hole	Samples (*N*)
NW Caldera (rim)	U1527C	5
Upper Cone	U1528A	3
Upper Cone	U1528C	1
Upper Cone	U1528D	13
NW Caldera (wall)	U1530A	18
Lower Cone	U1531C	1

Table T2. Site summary, Expedition 376. NA = not applicable.

Hole	Latitude	Longitude	Water depth (mbsl)	Cores (*N*)	Interval cored (m)	Core recovered (m)	Recovery (%)	Drilled interval (m)	Total penetration (m)	Time on hole (h)	Time at site (days)	Comments
U1527A	34°51.6528′S	179°03.2397′E	1464.23	15	101.4	1.27	1.25	0	101.4	51.3		
U1527B	34°51.6519′S	179°03.2526′E	1464.19	NA	NA	NA	NA	105.5	105.5	76.3		
U1527C	34°51.6625′S	179°03.2534′E	1464.12	19	138.1	25.9	18.75	99.9	238.0	122.0		
			Site U1527 totals:	34	239.5	27.17	11.34	205.4	444.9		10.4	
U1528A	34°52.9177′S	179°04.1070′E	1228.36	15	84.4	17.09	20.25	0	84.4	50.3		
U1528B	34°52.9222′S	179°04.1077′E	1240.30	NA	NA	NA	NA	25.6	25.6	79.3		
U1528C	34°52.9215′S	179°04.1128′E	1229.01	7	31.5	3.63	11.52	22	53.5	47.8		Includes return at end of expedition for downhole measurements
U1528D	34°52.9219′S	179°04.1164′E	1228.04	62	298.0	87.23	29.27	61.3	359.3	391.5		
			Site U1528 totals:	84	413.9	107.95	26.08	108.9	522.8		23.7	
U1529A	34°52.5161′S	179°03.5139′E	1734.99	1	12.0	1.86	15.5	0	12.0	15.0		
U1529B	34°52.5217′S	179°03.5207′E	1732.99	4	34.4	0.6	1.74	0	34.4	29.0		
			Site U1529 totals:	5	46.4	2.46	5.30	0	46.4		1.8	
U1530A	34°51.6588′S	179°03.4572′E	1594.86	93	453.1	76.77	16.94	0	453.1	184.1		
			Site U1530 totals:	93	453.1	76.77	16.94	0	453.1		7.7	
U1531A	34°52.7767′S	179°04.2241′E	1354.87	1	15.0	1.0	6.67	0	15.0	51.5		
U1531B	34°52.7721′S	179°04.2111′E	1351.87	3	26.0	3.98	15.31	0	26.0	14.8		
U1531C	34°52.7239′S	179°04.2586′E	1306.87	3	28.4	2.25	7.92	0	28.4	23.5		
U1531D	34°52.7228′S	179°04.2606′E	1306.85	NA	NA	NA	NA	19.0	19.0	35.0		
U1531E	34°52.7591′S	179°04.2344′E	1355.01	8	21.7	0.79	3.64	17.9	39.6	139.5		
			Site U1531 totals:	15	91.1	8.02	8.80	36.9	128.0		11.0	
			Expedition 376 totals:	231	1244.0	222.37	17.88	351.2	1595.2		54.6	

Figure F1. Bathymetric map of the Kermadec arc, trench, and major tectonic elements. Brothers volcano is located on the active volcanic front in the southern half of the arc. From de Ronde et al., 2012.

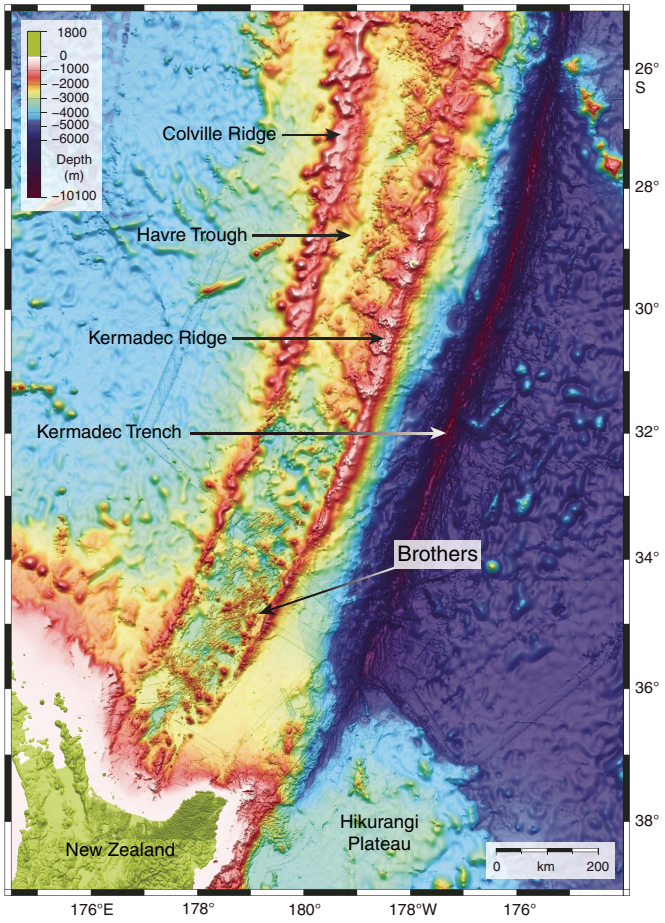

Figure F2. Detailed bathymetry of Brothers volcano and surrounding area. Dashed lines = structural ridges. NF = North fault, SF = South fault, NRZ = North rift zone, UC = Upper Cone, LC = Lower Cone, UCald = Upper Caldera, NWC = NW Caldera, WC = W Caldera, SEC = SE Caldera, RTR = regional tectonic ridge. A-B and C-D are endpoints for the bathymetric cross sections shown in the top panels. The topographic cross section "A-B" is coincident with the seismic section Line Bro-3. Contour interval = 200 m. Modified from Embley et al., 2012.

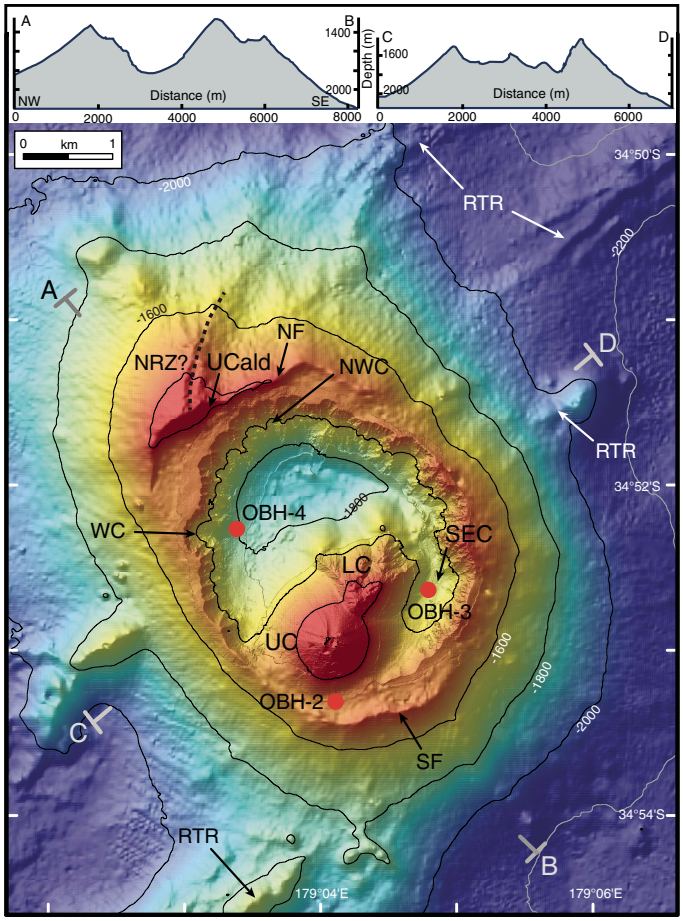

Figure F3. A. Autonomous underwater vehicle (AUV) tracks from the 2007 *ABE* dives (colored tracks) and the 2011 AUV *Sentry* dive (white tracks). Figure from Baker et al. (2012). B. Results of the high-resolution (~2 m) mapping of the caldera walls and cones from the *ABE* survey overlain on EM300 bathymetric survey (~25 m resolution) data for the caldera floor, Upper Caldera walls in the northwest, and the outside flanks of the volcano. From Merle et al. (2007) and reproduced with some modification in Embley et al. (2012).

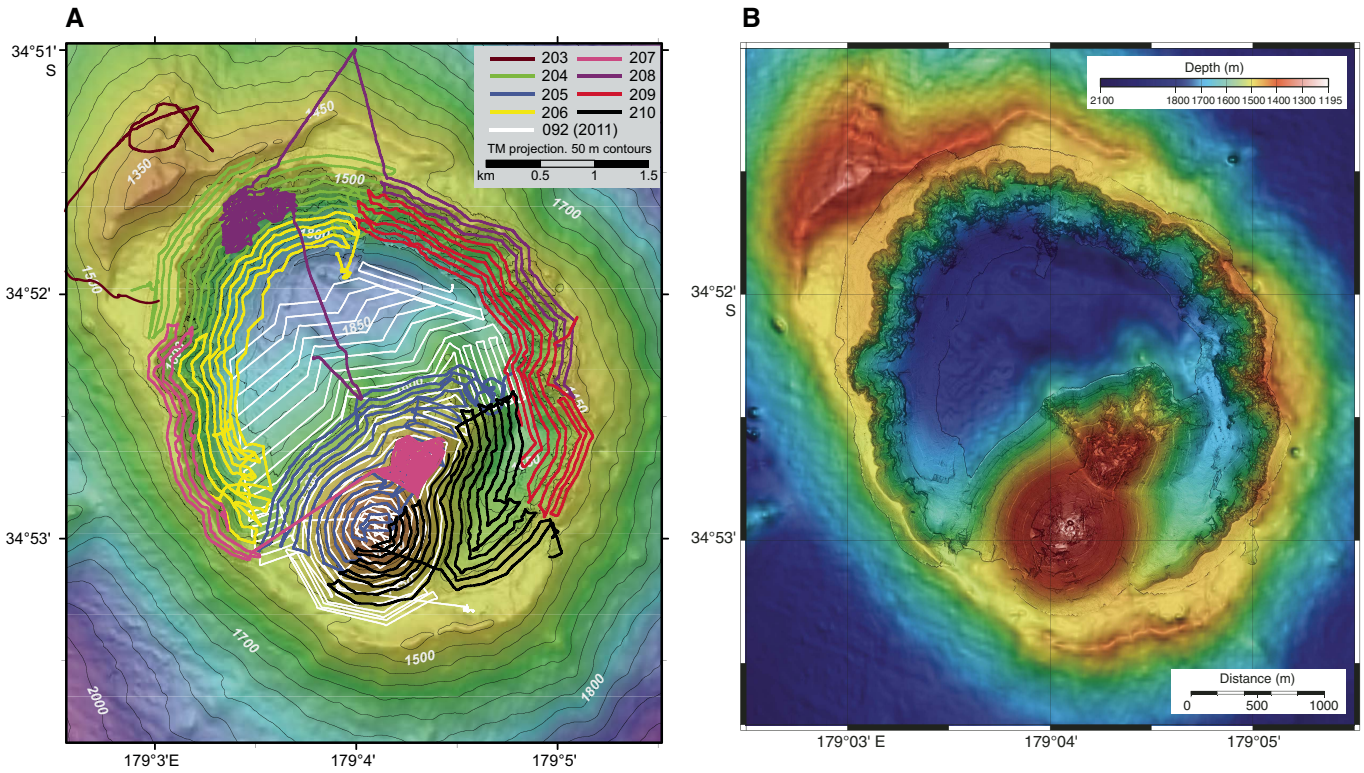

Figure F4. Distribution of plume tracers in 2007 using the *ABE* survey (A–D) and in 2011 using the *Sentry* survey (E, F) overlain on bathymetry from Figure F3B. Light blue shaded area in some panels marks area of Dive #205 survey (see Figure F3A) where no ΔNTU or dE/dt data were recorded. A. ΔΘ (°C) anomalies. B. ΔNTU anomalies. C. dE/dt (mV/s) anomalies. D. Fluid discharge types inferred from ΔNTU/ΔΘ ratios. E. ΔNTU anomalies. F. dE/dt (mV/s) anomalies. Plots from Baker et al. (2012).

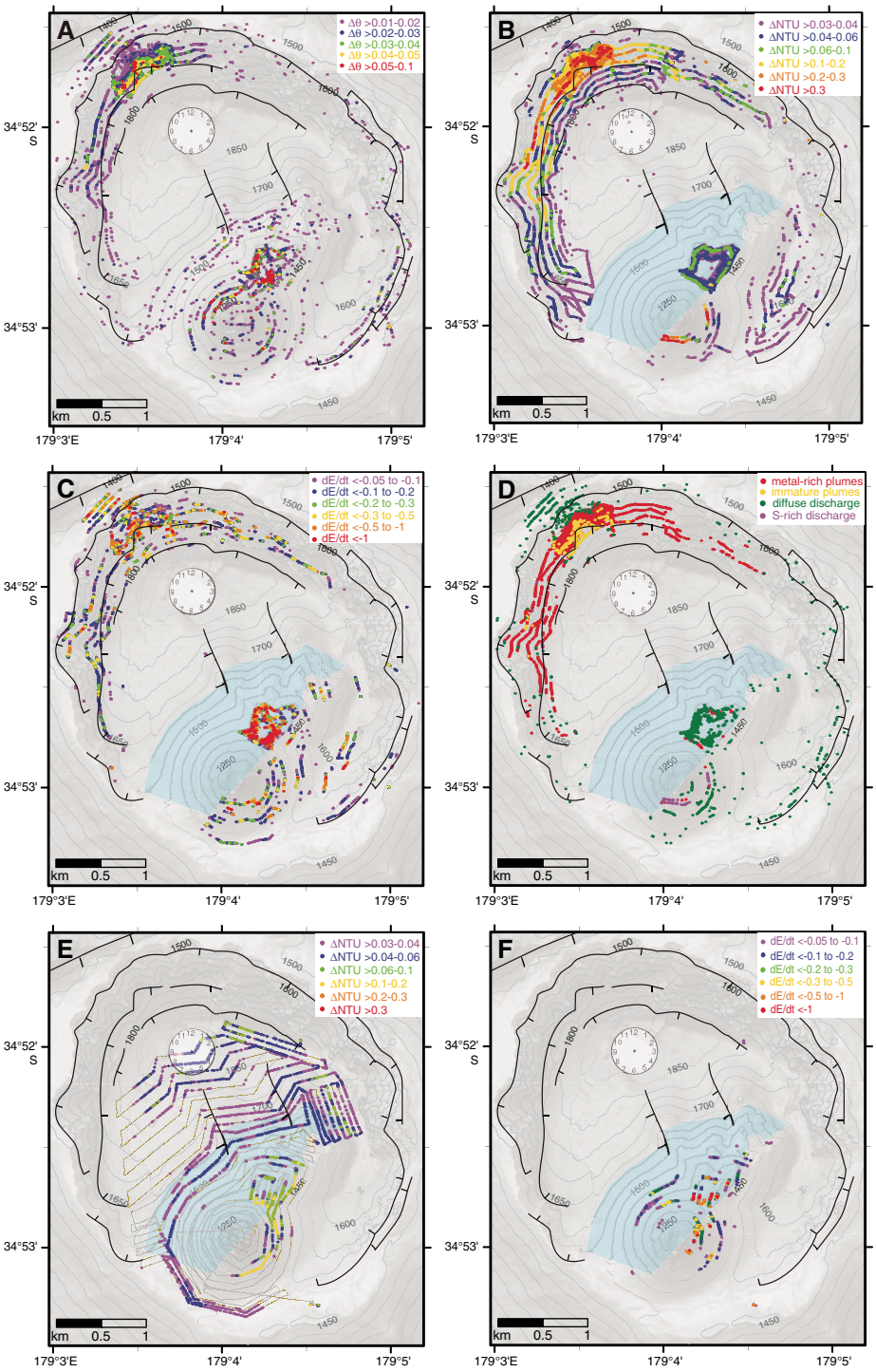

Figure F5. Apparent magnetization map of Brothers volcano showing reduced crustal magnetization over four areas that include five hydrothermal vent sites. A = Upper Caldera and NW Caldera, B = Upper Cone, C = SE Caldera, D = W Caldera. Outlined areas have either very low (<2.5 A/m; Zones A and D) or moderate (<3.5 A/m; Zones B and C) magnetization, which is in general agreement with the location of the various vent fields. The Lower Cone hydrothermal vent site is situated immediately northeast of Zone B and does not have an associated reduced crustal magnetization signature. Zone C is largely an extinct vent site. Structural lineaments (white lines) and ring faults (white lines with hash marks) are shown for reference. Figure from Caratori Tontini et al. (2012a).

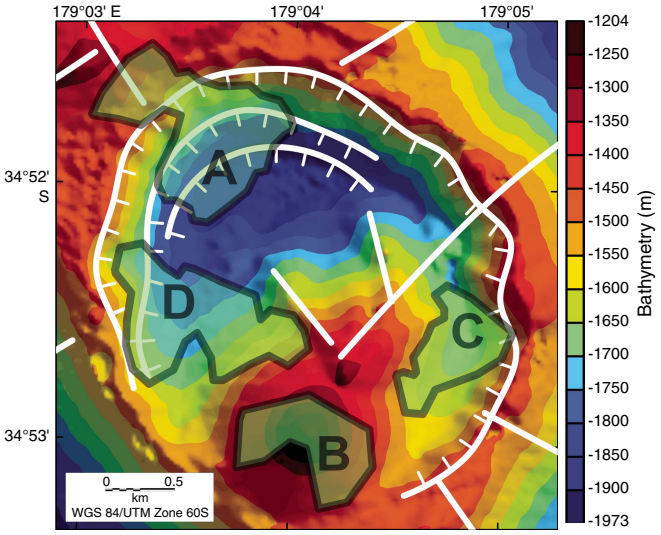

Figure F6. Detailed bathymetry showing the location of sites drilled during Expedition 376. Contour interval is 200 m of Brothers volcano and surrounding area. Modified from Embley et al., 2012.

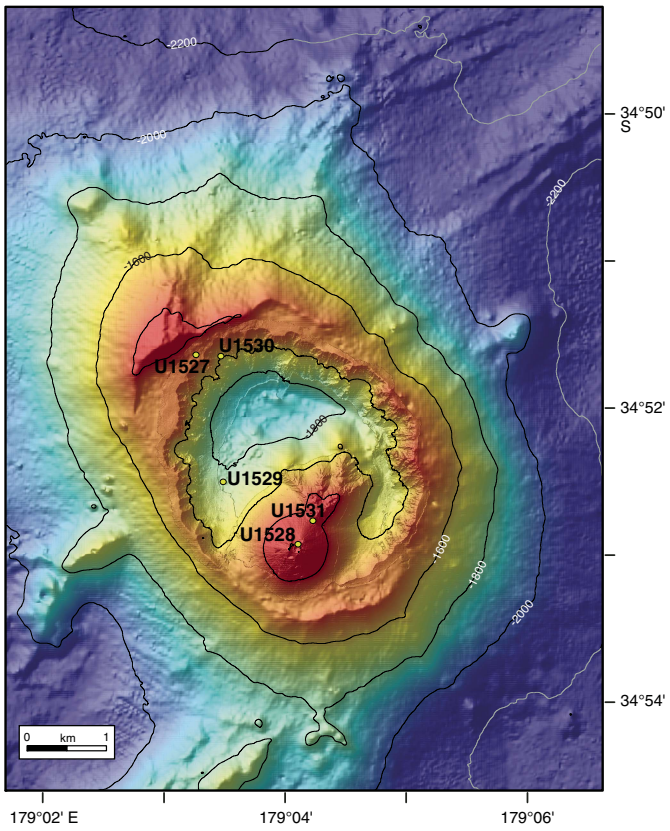

Figure F7. Lithostratigraphic summary, Holes U1527A and U1527C on the rim of the caldera at the NW Caldera hydrothermal field.

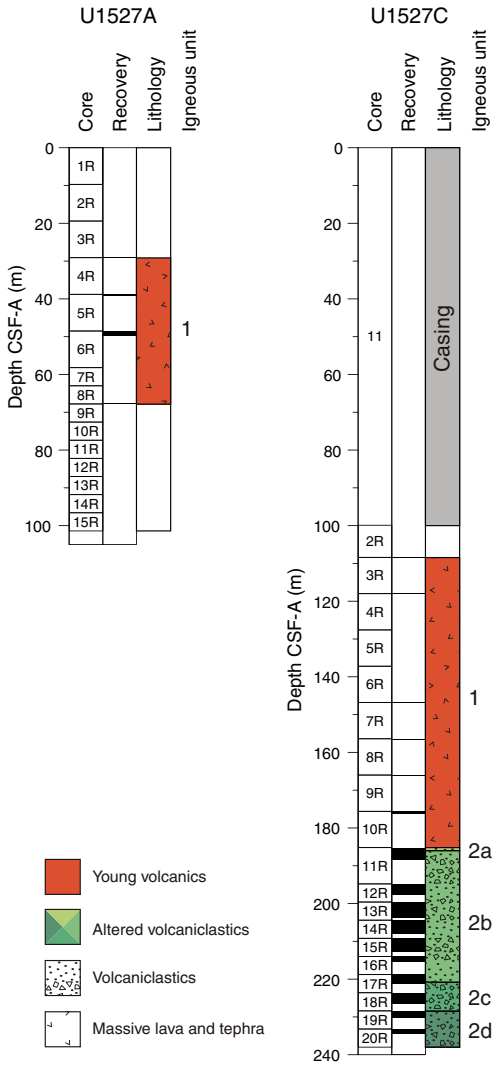

Figure F8. Distribution of alteration types and abundance of key minerals, Site U1527. CSF-A = core depth below seafloor (m).

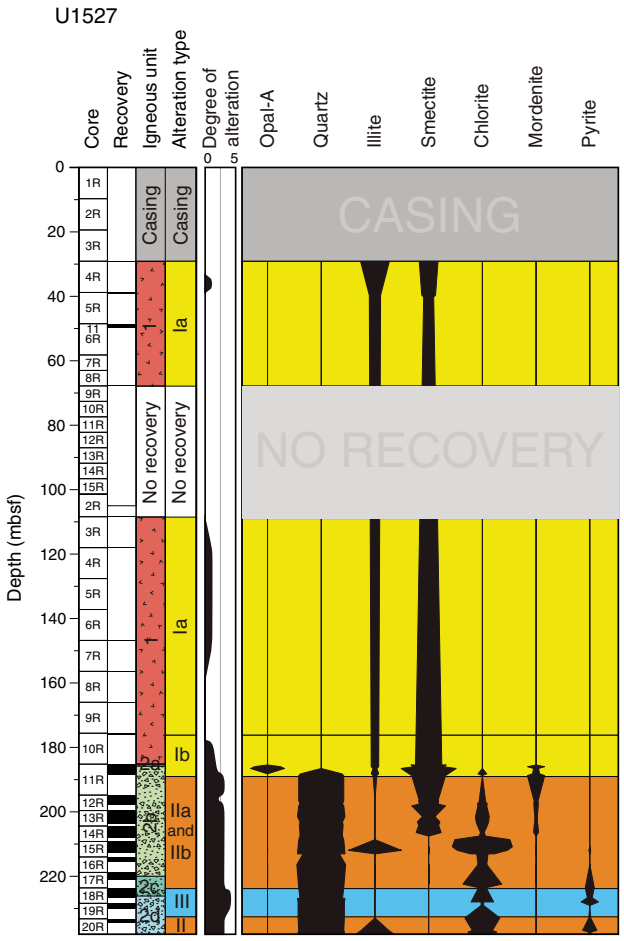

Figure F9. Representative intervals of alteration types, Hole U1527C. Type Ia: unaltered to slightly altered clast of dacite (376-U1527C-6R-1, 94–101 cm). Type Ib: dark unaltered clasts of dacite with well-defined boundaries surrounded by altered yellow-brown matrix (376-U1527C-11R-1, 0–6 cm). Type IIa: pervasively altered clasts surrounded by chlorite-altered matrix (376-U1527C-14R-2, 120–138 cm). Type IIb: overprint of Type IIb onto Type IIa (14R-2, 4–20 cm). Type III: pervasively altered clasts with resorbed, gradational boundaries (376-U1527C-18R-1, 30–39 cm).

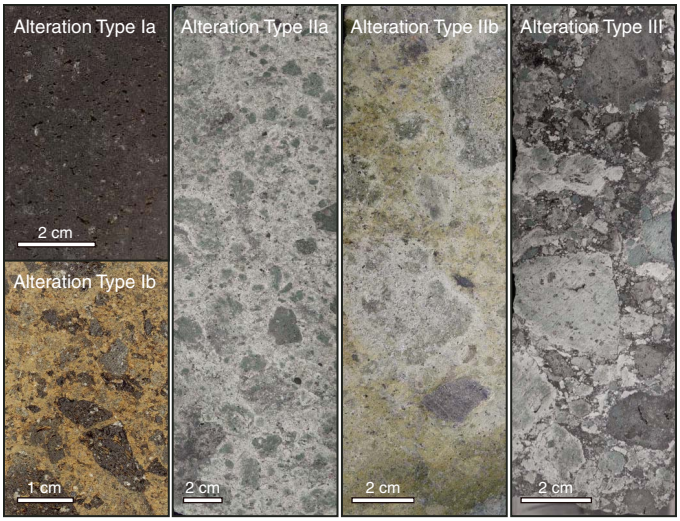

Figure F10. Variations of K_2O, MgO, and SiO_2 compared with macroscopic estimate of alteration intensity, Holes U1527A and U1527C. Vertical lines = average values of shallower unaltered igneous Unit 1 in Hole U1527A. Dashed lines = 1σ from average values. The two shallowest samples correspond to relatively unaltered volcanic material recovered from the bottom-hole assembly (BHA) in Hole U1527C.

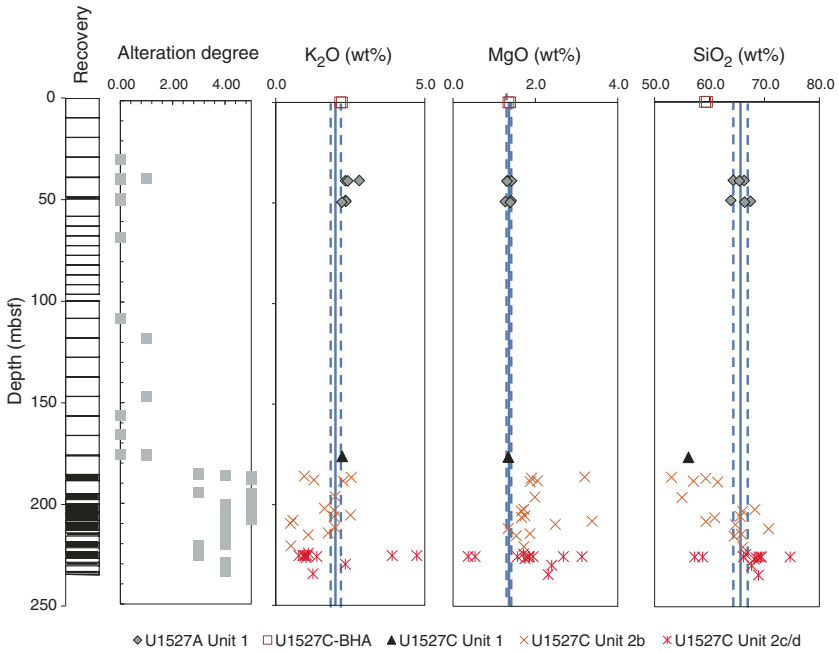

Figure F11. Lithostratigraphic summary, Holes U1528A, U1528B, and U1528D in the pit crater of the Upper Cone. CSF-A = core depth below seafloor (m).

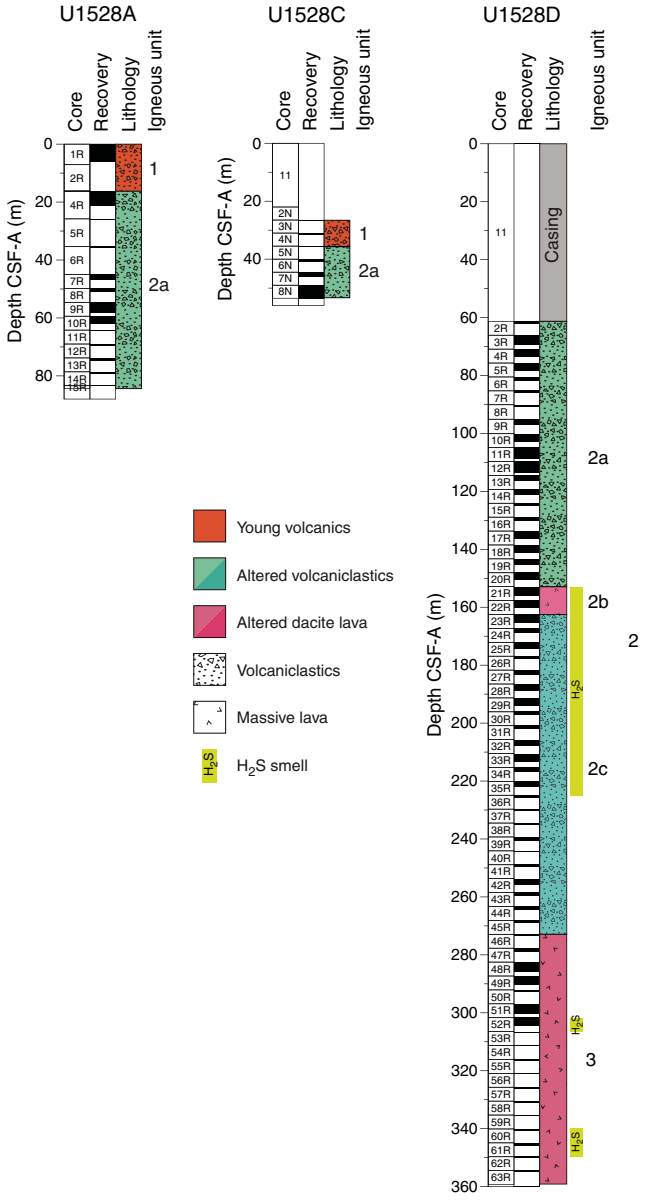

Figure F12. Distribution of alteration types and abundance of key minerals, Site U1528.

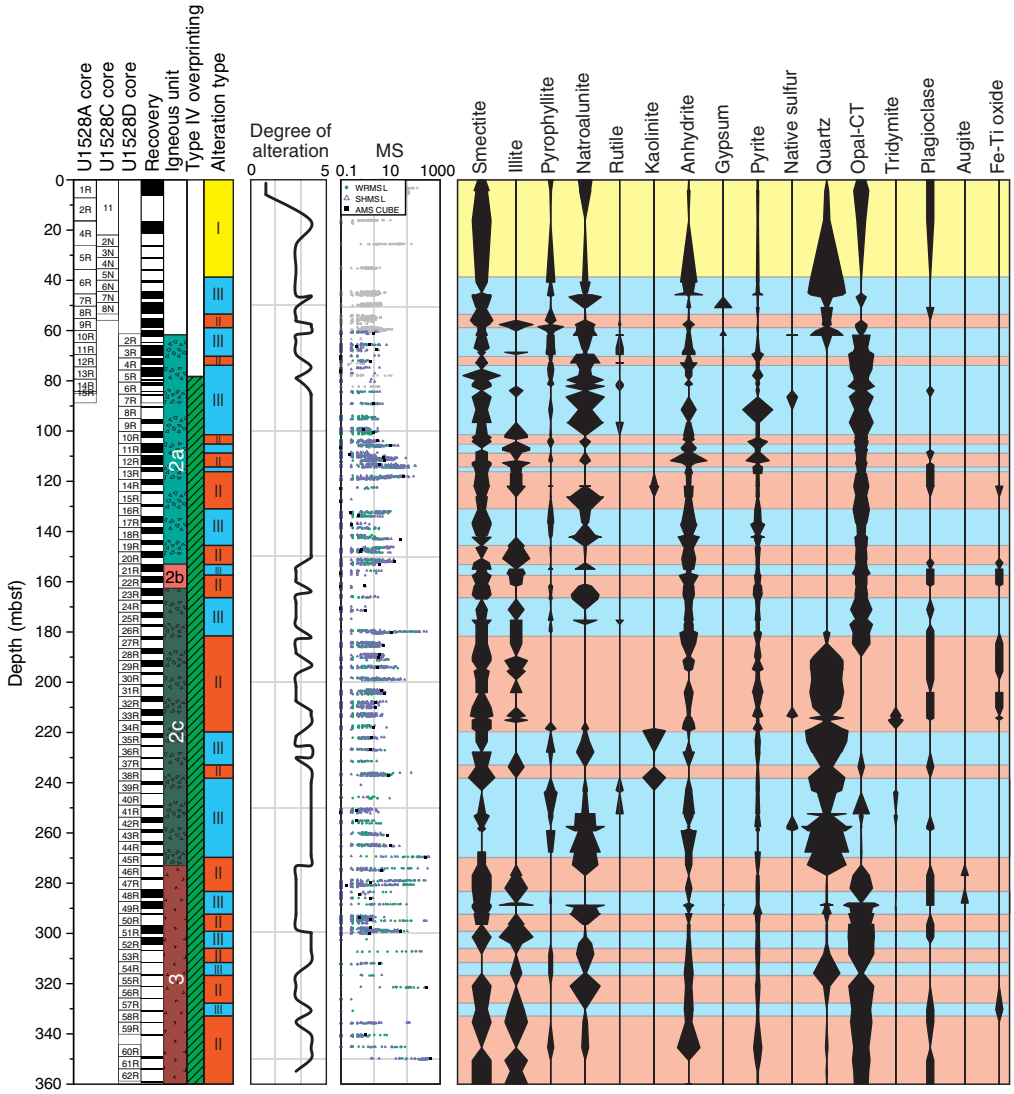

Figure F13. Representative intervals of alteration types, Site U1528. A. Type I (376-U1528A-1R-3, 25–38 cm). B. Type II (376-U1528D-22R-1, 91–103 cm). C. Type III (376-U1528D-4R-2, 94–102 cm). D. Type IV. Top: Type IV crosscutting Type II (376-U1528D-10R-1, 71–76 cm). Bottom: Type IV crosscutting Type III (376-U1528D-18R-2, 71–77 cm).

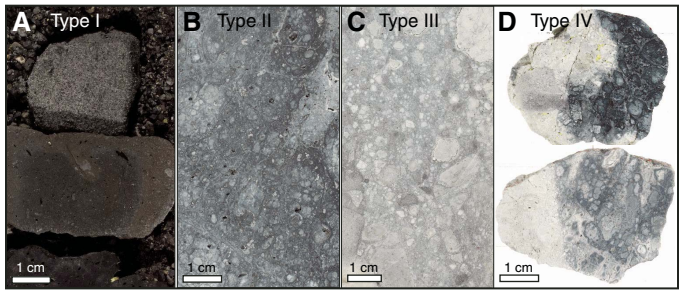

Figure F14. Salinity (NaCl equivalent wt%) versus homogenization temperature and corresponding enthalpy of NaCl-H_2O (Bischoff and Rosenbauer, 1985) for fluid inclusions from anhydrite, gypsum, and alunite recovered from Site U1528. The critical line divides the diagram into the supercritical and subcritical zones. The NaCl saturation curve was calculated from Driesner and Heinrich (2007) and the NaCl vapor conjugate curve from Bischoff (1991). Phase separation (boiling) curves are calculated for seawater (bc1), seawater (sw) + 0.22 m CO_2 (bc2), 33 wt% NaCl equivalent hypersaline brine (bc3) and 33 wt% NaCl equivalent hypersaline brine + 0.22m CO_2. Also shown is a broken line with arrow indicative of salinities caused by vapor condensation under subcritical conditions.

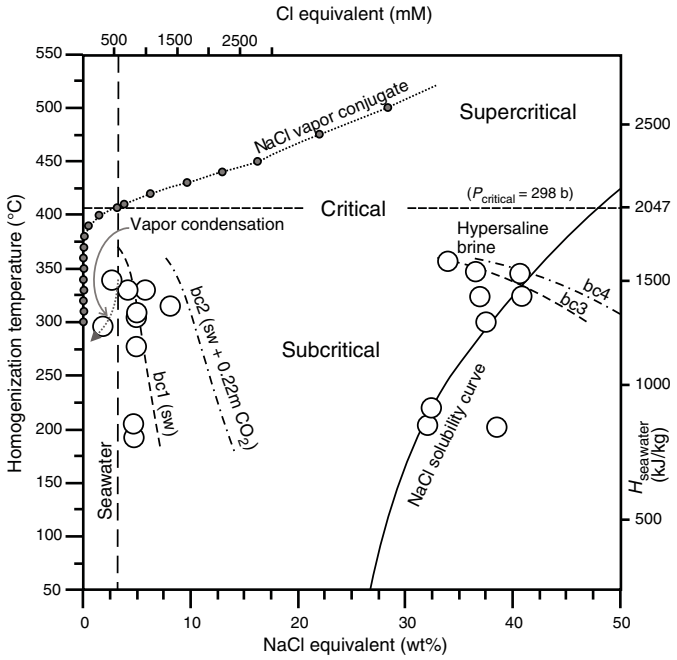

Figure F15. Variations in major element oxides CaO, K_2O, MgO, Fe_2O_3, and SiO_2 at Site U1528. Horizontal dashed lines = depth intervals marked by major geochemical changes and alteration types. Vertical gray shaded area = compositional range (and 2σ from the average) for unaltered dacites from Igneous Unit 1 in Hole U1527A and at Site U1529. Data are from ICP-OES analyses, except those with plus symbols, which are pXRF-generated data.

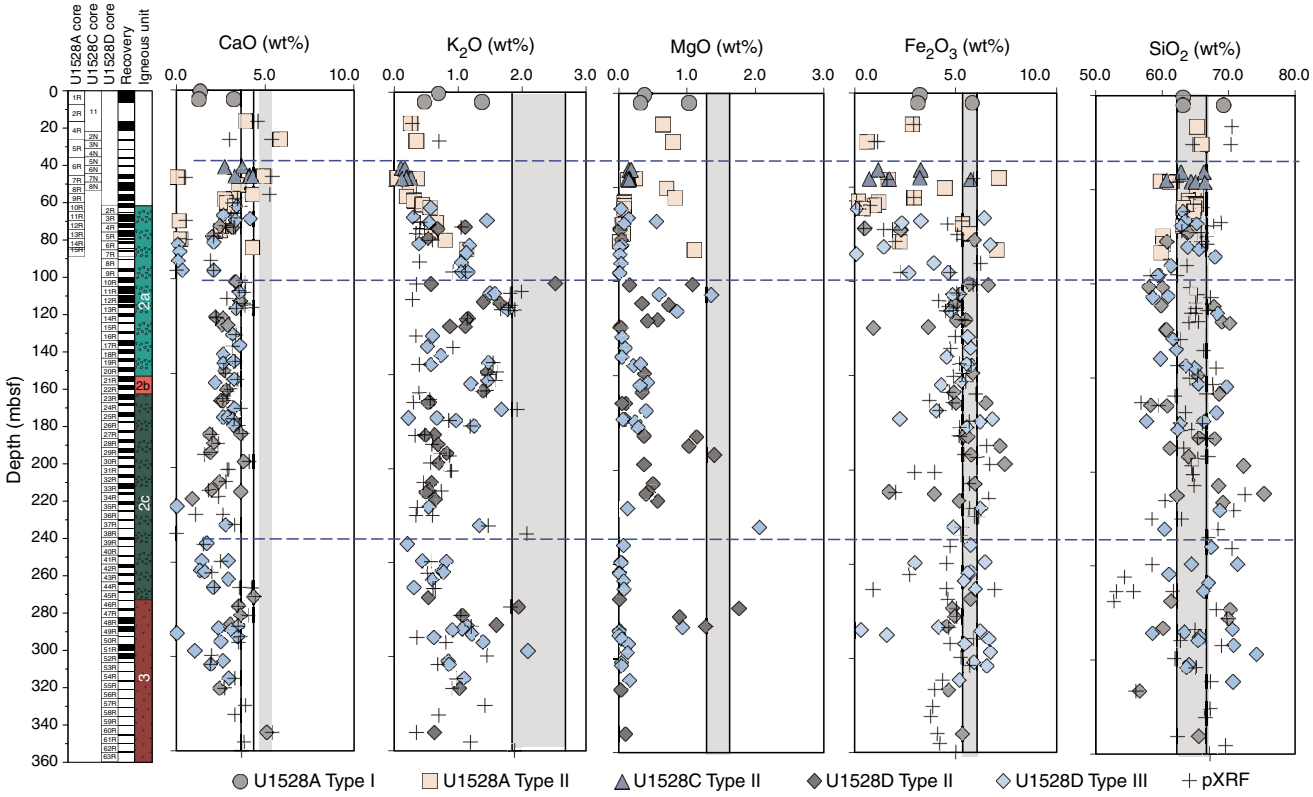

Figure F16. Representative macroscopic samples from the single igneous unit at Site U1529. A. Volcaniclastic xenocryst included in dacite lava (376-U1529B-4G-4, 98–101 cm). B. Dacite with fractures accentuated by white halite (376-U1529B-4G-CC, 25–41 cm). C. Another example of dacite with fractures accentuated by white halite (376-U1529B-2R-1, 6–11 cm). D. Lapilli-sized fragments of dacite lava (376-U1529A-1R-2, 89–97 cm).

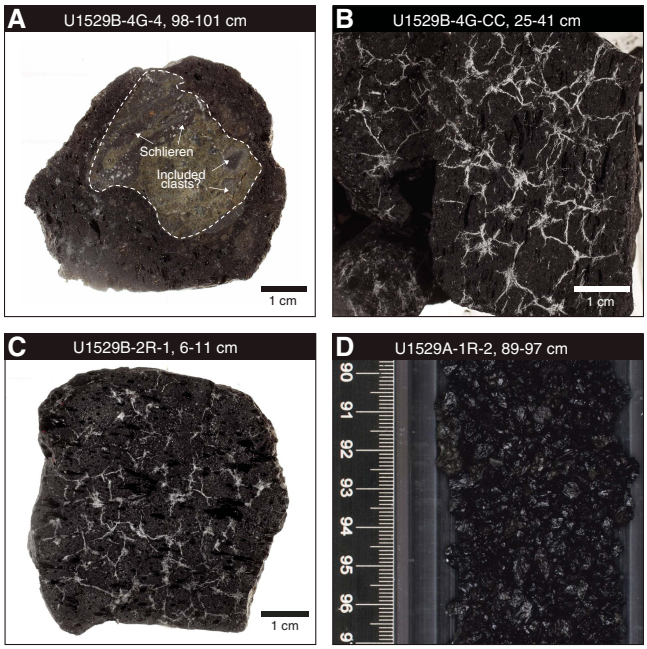

Figure F17. Lithostratigraphic column, Hole U1530A on the caldera wall of the NW Caldera hydrothermal field. CSF-A = core depth below seafloor (m).

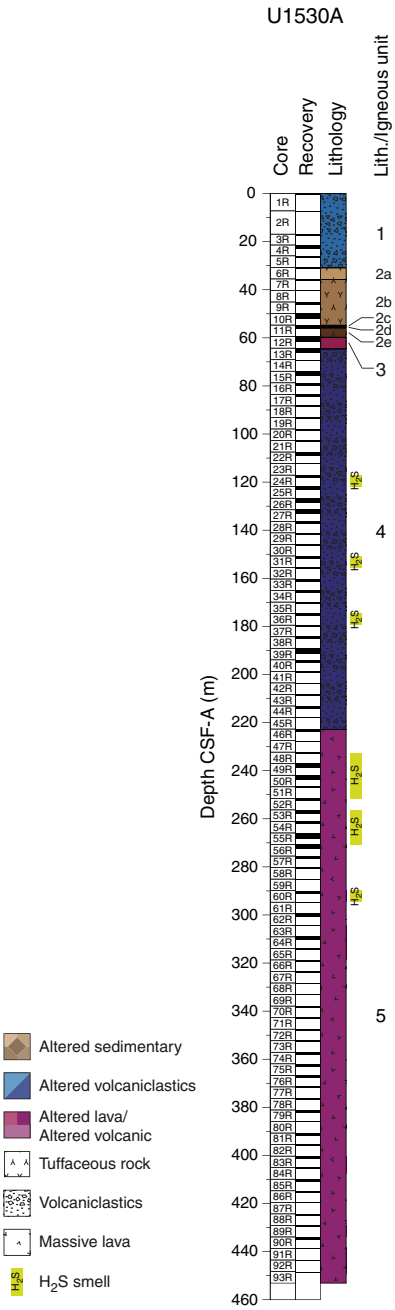

Figure F18. Distribution of alteration types and abundance of key minerals, Site U1530. Abundance is based on the mineral assemblages determined by XRD and thin section observations. Core recovery and igneous units for Hole U1530A are shown.

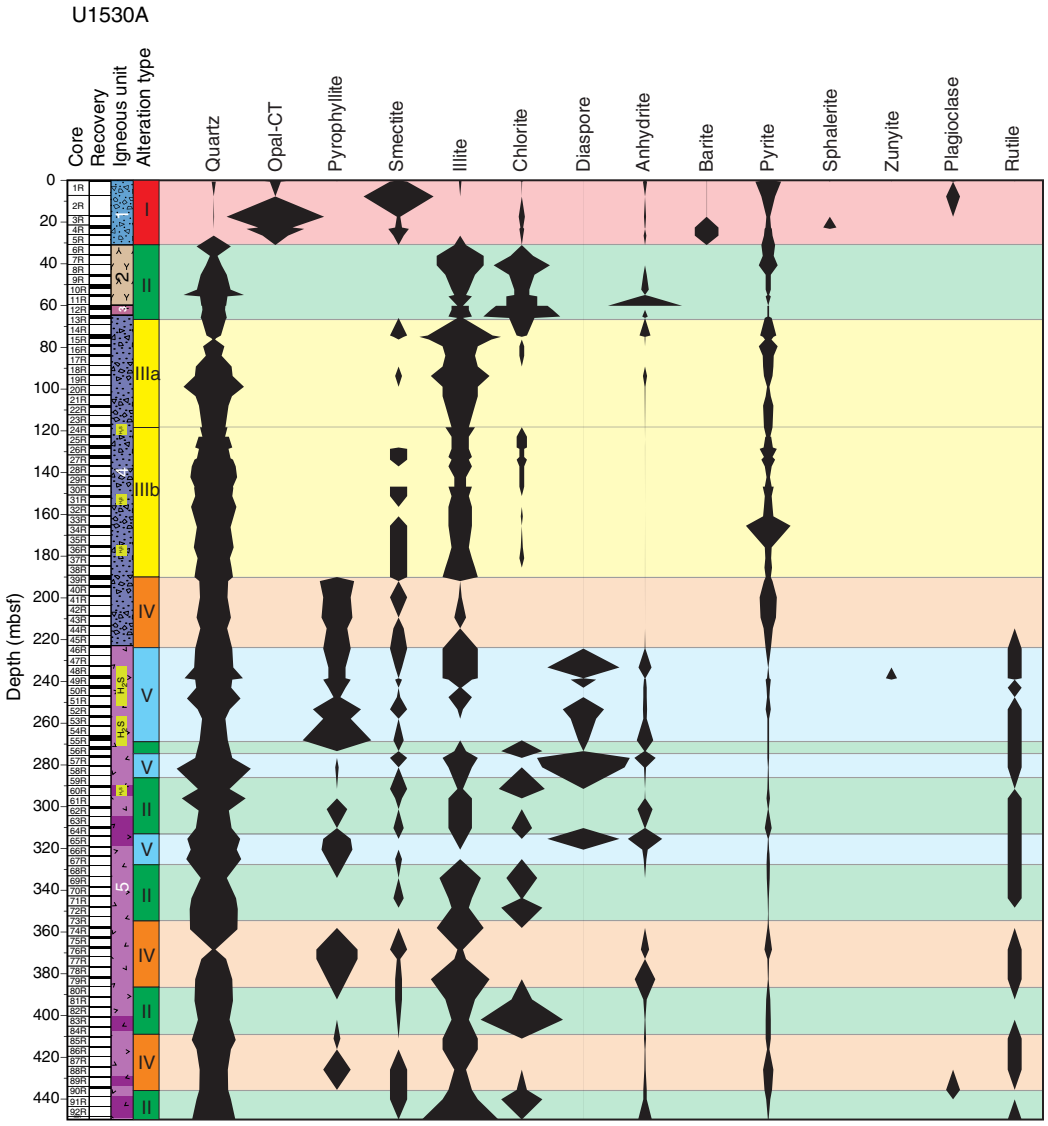

Figure F19. Representative hand specimens of alteration types, Hole U1530A. A. Type I: blue-gray illite-rich clasts crosscut by a network of pyrite-anhydrite-silica veins with a mesh texture (376-U1530A-4R-1, 47–56 cm). B. Type II: sediment with fine-grained, subhorizontal laminations that are subsequently cut by a vuggy anhydrite vein (376-U1530A-10R-2, 18–31 cm). C. Type IIIa: subrounded to subangular light gray clasts in a gray silicified matrix (376-U1530A-16R-1, 65–71 cm). D. Type IIIb: variably silicified blue-gray clasts exhibiting extensive resorption in a matrix of pyrite intergrown with quartz, along with the occasional vug infilled with anhydrite (376-U1530A-25R-1, 38–46 cm). E. Type IV: homogeneous gray matrix with poorly distinguishable clasts containing patchy pyrophyllite and abundant vugs infilled with quartz and anhydrite (376-U1530A-40R-1, 6–15 cm). F. Type V: mottled equigranular rock with a clear distinction between light gray quartz-dominated and dark gray diaspore-pyrophyllite–rich areas (376-U1530A-57R-1, 17–26 cm).

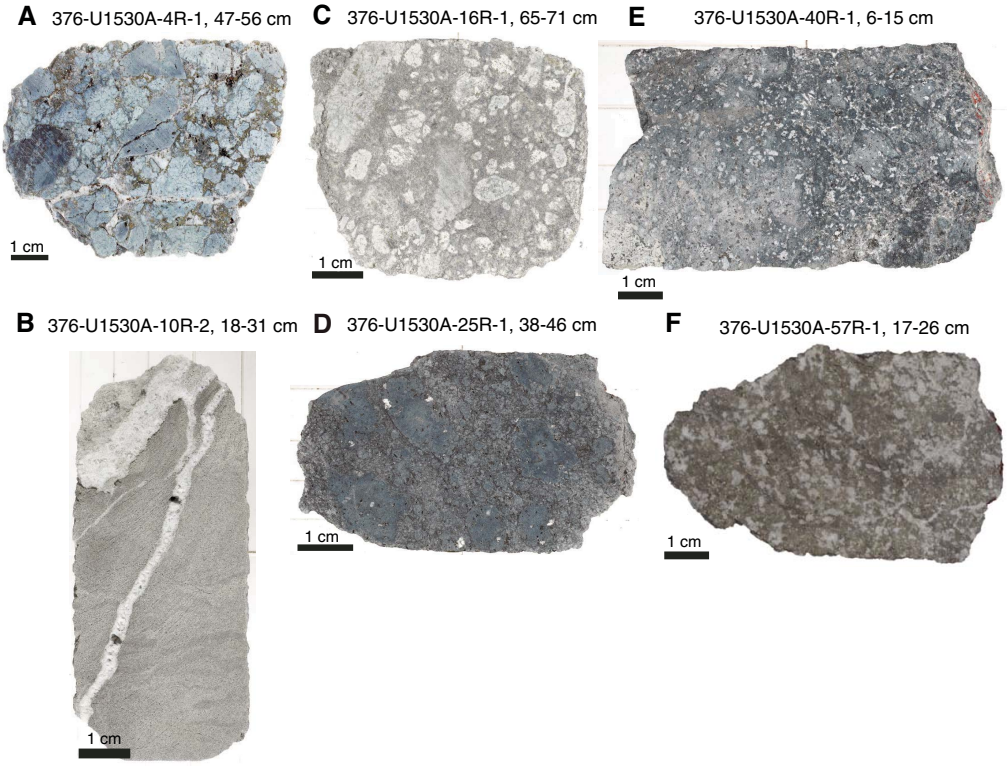

Figure F20. Salinity (NaCl equivalent wt%) versus homogenization temperature and corresponding enthalpy of NaCl-H_2O (Bischoff and Rosenbauer, 1985) for fluid inclusions from anhydrite, Site U1530. The critical line divides the diagram into the supercritical and subcritical zones. The NaCl saturation curve was calculated from Driesner and Heinrich (2007) and the NaCl vapor conjugate curve from Bischoff (1991). Phase separation (boiling) curves are calculated for seawater and for 41 wt% NaCl equivalent hypersaline brine (bc1). Salinities measured near the seawater line may be due to condensation from a supercritical NaCl vapor. Hypersaline brine salinities above the NaCl saturation curve may be caused by boiling (bc1) or a NaCl brine with additional major cations such as K (line NK).

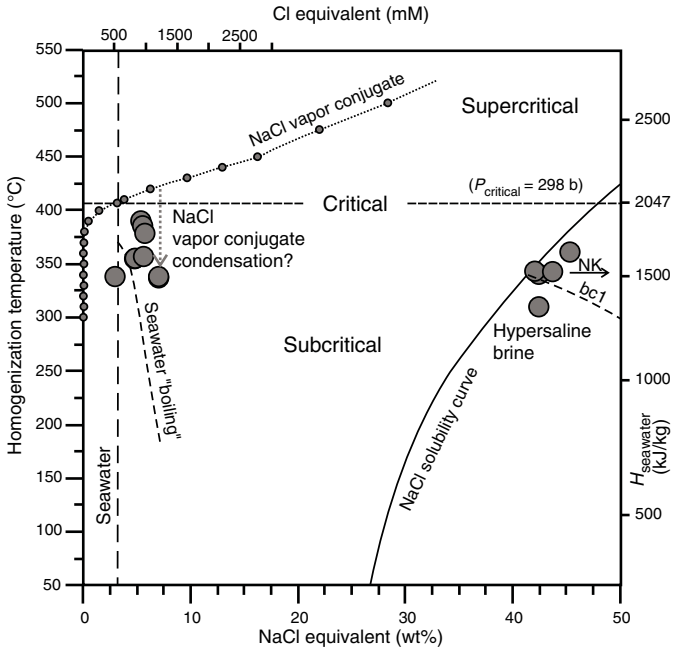

Figure F21. K_2O, MgO, Na_2O, and CaO concentrations in altered volcaniclastic rocks and lavas, Hole U1530A. Average values for unaltered dacites recovered in Hole U1527A and at Site U1529 are shown with dashed vertical lines representing 2σ from average values.